UNCERTAINTIES IN GLOBAL AND REGIONAL CLIMATE CHANGE PROJECTION OF SUMMER MONSOON TEMPERATURE AND PRECIPITATION OVER WEST AFRICA

NIKIEMA, PINGHOUINDE MICHEL

(MSc)

MET/12/2037

A THESIS

IN THE DEPARTMENT OF METEOROLOGY AND CLIMATE SCIENCE IN PARTNERSHIP WITH THE WEST AFRICAN SCIENCE SERVICE CENTRE ON CLIMATE CHANGE AND ADAPTED LAND USE (WASCAL) SUBMITTED TO THE SCHOOL OF POSTGRADUATE STUDIES,
IN PARTIAL FULFILLMENT OF THE REQUIREMENT FOR THE AWARD OF THE DEGREE OF DOCTOR OF PHILOSOPHY IN METEOROLOGY AND CLIMATE SCIENCE OF THE FEDERAL UNIVERSITY OF TECHNOLOGY, AKURE, ONDO STATE IN NIGERIA

JUNE, 2016

CERTIFICATION

a) By the student:

This work has not been presented elsewhere for award of degree, or any other purpose.

Candidate's Name: NIKIEMA, Pinghouinde Michel

Signature:. . . . . Date:. . . . . .

b) By the Supervisor(s):

I certify that this research work was carried out by Mr. NIKIEMA, Pinghouinde Michel under my supervision and that to the best of my knowledge, it has not been submitted elsewhere for the award of a degree.

Supervisor's Name:

Major supervisor's Name**:** Dr. M. B. Sylla

Signature:. . . . . Date:. . . . . .

Co-supervisor's Name: Prof. K. O. Ogunjobi

Signature:. . . . . Date:. . . . . .

ACKNOWLEDGMENTS

I want to acknowledge the full scholarship and financial support from the German Federal Ministry of Higher Education and Research (BMBF) and WASCAL for my doctoral program.

My gratitude goes to FUTA department of Meteorology and Climate Science, the GRP-WACS team in Akure and WASCAL Competence Center in Ouagadougou for their efforts in making this program a success.

Special mention goes to my supervisor, Dr. Mouhamadou Bamba Sylla from WASCAL Competence Center. I do not have enough words to express my sincere appreciation.

I thank Prof. K.O Ogunjobi , current Director of GRP-WACS, who accepted to co-supervise this work .

I specially thank the General Director of Meteorology for offering the study leave and encouragement for my PhD work.

Furthermore, I would like to thank my classmates and friends Kebe Ibourahima, Gibba Peter, Coulibaly Amadou, Kouakou Kouadio, Nabil Edward,Odulami Roamric Ojeh Vicent, Talabi Christie, Waongo Moussa, Diasso Jacques and Zablone Owitti for the nice talks and time we had during the process.

Lastly, I would like to thank my family for all their love and encouragement. I must express my very profound gratitude to my parents JULES O. NIKIEMA and Sampoko SIMPORE and to my wife Bernadette NIKIEMA for providing me with support and continuous encouragement. This accomplishment would not have been possible without them.

DEDICATION

This research study is dedicated to my wife, Bernadette NIKIEMA, to my mother, Sampoko SIMPORE, and in the memory of , Jules O. NIKIEMA, Boukary NIKIEMA and Therese SAMA

ABSTRACT

This study aims at investigating climate change scenarios over West Africa with the associated uncertainties to improve the value of climate information to end-users for informed decision making. For the present day (1982-2005), the mean climatology, intermodel variability and spatio-temporal patterns of temperature and precipitation over West Africa from CMIP5, CMIP5_SUBSET (ensemble of GCMs driving CORDEX) and CORDEX multimodel ensembles (MMEs) were first evaluated and intercompared for the monsoon season (June-September). While CORDEX failed to outperform the simulated mean climatology of temperature by the CMIP5 ensembles, it substantially improved precipitation and provided more realistic fine-scale features tied to local topography and landuse. This improved performance over the region depend more on the internal models physics than the driving boundary conditions and results from a more consistent and realistic simulation of monsoon precipitation across the various Regional Climate Models (RCMs). Rotated Empirical Orthogonal Function (REOF) analysis indicated that the CORDEX ensemble captures better the spatio-temporal variability of both temperature and precipitation (first REOF mode), in particular depicting the warming and Sahel precipitation recovery in recent decades over West Africa. On the other hand, the spatial patterns and associated time series of the last two REOF modes in CORDEX mostly follow the CMIP5_SUBSET pointing towards a strong role of the boundary forcing in the RCM simulation of precipitation variability. For the future climate 2070-2099 relative to 1976-2005, a Bayesian model was applied to the three sets of models (CMIP5, CMIP5_Subset and CORDEX) and PDFs of Temperature and precipitation change for two sub region (Sahel and Guinea Coast) were derived. For temperature change over the Guinean Coast, CMIP5_S models under RCP8.5 has a lot of uncertainties showing more bias and less agreement among models but the

CORDEX seems to reduce those uncertainties. Over the Sahel, only CORDEX under RCP4.5 scenario shows more agreement and less bias. CMIP5 and CMIP_S show multi modal PDF pointing out some uncertainties and less agreement among models. For precipitation change over the Guinean Coast under RCP8.5 and RCP4.5 uncertainties still remain in CORDEX model with an increasing precipitation trend for the late century. There is no significant difference on precipitation change between RCP4.5 and RCP8.5. CORDEX has a wide PDF curve under RCP4.5 and RCP8.5 scenario showing the persistence of uncertainties. Two sources of uncertainty in climate projection from CMIP5, CMIP5_Subset and CORDEX were also examined for temperature and precipitation. An ordinary least square was used to fit each decadal anomalies prediction of CMIP5, CMIP5_Subset and CORDEX with a fourth-order polynomial over the years of 2006-2099 for the two scenarios RCP45 and RCP85. The anomalies were computed with the reference period of 1976-2005. The new generation of models had an added value compare to the driving GCMs (CMIP_S) and CMIP5 MMEs by reducing the Internal and Inter Model Variability over the West African region. Inter Model Variability was the dominant source of uncertainties and is explaining up to 90 % of total uncertainty. The study conclude that for temperature under the two scenarios, the change is robust (Signal to Noise ratio greater than one) over most of West African countries with more spatial details and improved signal to noise ratio with CORDEX MMEs compare to CMIP5 and CMIP5_S MMEs. Over West Africa, CORDEX under RCP4.5 has a signal to noise ratio greater than one with an increasing trend of precipitation while the noise dominates the signal under RCP8.5, in CMIP5, CMIP5_S and CORDEX. An assessment of climate change information over West African region needs to rely on the careful evaluation and compounded information deriving from multiple sources.

TABLE OF CONTENTS

LIST OF TABLES

LIST OF FIGURES

Title **Page**

ACRONYMS

AEJ African Easterly Jet

AEW African Easterly Wave

AMMA African Monsoon Multidisciplinary Analysis

AOGCM Atmosphere-ocean general circulation model

BCC Beijing Climate Center, China Meteorological Administration

BNU-ESM Beijing Normal University Earth System Model

CANESM2 Canadian Earth System Modelling version 2

CCLM COSMO model in CLimate Model

CDD Consecutive Dry Days index

CDF Cumulative Distribution Function

CES Central-Eastern Saharan

CMAP Climate Prediction Center Merged Analysis of Precipitation

CMIP5 Coupled Model Intercomparison Projects 5

CNRM Centre National de Research en Meteorologie model

CRCM5 5^{th} generation of Canadian Regional Climate Model

CRU Climate Research Unit

CORDEX COrdinated Regional Dawnscaling EXperiment

ECHAM5 European Centre/Hamburg Model version 5

ECMWF European Centre for Medium-range Weather Forecast

ENSO El-Nıno Southern Oscillation

EOF Empirical Orthogonal Functions

ERAINT ECMWF Reanalyses Interim

ESM Earth System Model

GC Guinean Coast

GCM Global Climate Model

GFDL-ESM-2M Geophysical Fluid Dynamics Laboratory Earth System Model version 2M

GPCP Global Precipitation Climatology Project

GHG Green House Gases

GISS Goddard Institute for Space Studies

HadGEM2-ES Hadley center Global Environment Model 2 - Earth System

HWD Heat Wave Day index

HYINT Hydroclimatic Intensity index

IMV Inter Model Variability

IPCC Intergovernmental Panel on Climate Change

ITCP International Centre for Theoretical Physics

ITCZ Intertropical Convergence Zone

IV Internal Variability

IQR Inter Quantile Range

JJA June-July-August

JJAS June-July-August-September

LR Low Resolution

MAR Model Atmospherique Regional

MCMC Markov Chain Monte Carlo Simulation

MME Multi Model Ensemble

MPI Max Planck Institute for Meteorology

MPI-ESM MPI Earth System Model

MPI-ESM-MR Max-Planck Institute Earth System Model – Medium Resolution

MR Medium Resolution

NASA National Aeronautics and Space Administration

NCAR National Centre for Atmospheric Research

NCEP National Center for Environmental Prediction

P Pattern Correlation Coefficient

PC	Principal Components
PRECIS	Providing REgional Climates for Impacts Studies model
PDF	Probability Density Function
R	Pearson Correlation Coefficient
RACMO	Regional Atmospheric Climate Model
RCA	Rossby Centre regional Atmospheric model
RCM	Regional Climate Model
RCP	Representative Concentration Pathways
REA	Reliability Ensemble Average
REGCM	ICTP Regional Climate Model
RegCM3	ICTP Regional Climate Model version 3
RegCM4	ICTP Regional Climate Model version 4
REMO	REgional Model
REOF	Rotated Empirical Orthogonal Functions
SA	Sahel
SHL	Sahel Heat Low
SNR	Signal to Noise Ratio
SST	Sea Surface Temperature
TEJ	Tropical Easterly Jet

TRMM	Tropical Rain Measurement Mission
UDEL	University of DELaware
UKMO	United Kingdom Met Office
WA	West Africa
WAM	West African Monsoon
WAMME	West African Monsoon Modelling and Evaluation
WS	Western Saharan

CHAPTER ONE

INTRODUCTION

1.0 Research background

Coupled Global Climate Models (or simply GCMs) forced by greenhouse gas (GHG), aerosols and/or land use change are the primary tools to derive future climate change scenarios (Hulme *et al.*, 2001; Jenkins *et al.*, 2002; Kamga and Buscarlet, 2006). In this regards, many phases of the Coupled Model Intercomparison Project (e.g. CMIP2; CMIP3; Meehl *et al*., 2000; 2007) have been carried out during the last few decades by the World Climate Research Programme (WCRP). The implementation of these different stages of CMIP has led to substantial progress in climate modeling. For example, the latest phase (i.e. CMIP5 ; Taylor *et al*., 2012) includes the development of Earth System Models (ESMs) which better describe the interactions of atmosphere, ocean, land, ice, and biosphere but also incorporate biogeochemical processes and their feedbacks (Taylor *et al.*, 2012).

Despite this significant progress, there are still substantial shortcomings preventing the GCMs from accurately estimating the state of West African regional climate under a range of conditions. Among these limitations are the presence of persistent biases across different versions of the GCMs (Li *et al.*, 2013; Roehrig *et al.*, 2013**;** Bellenger *et al*., 2014) and the existence of large uncertainties in the projections in many parts of West Africa (Biasutti, 2013; James *et al*., 2014; Rodriguez-Fonseca *et al*., 2015). In addition, the horizontal grid spacing of the GCMs is still coarse making them unable to capture the local forcing such as complex topography and land surface heterogeneity (Giorgi *et al.*, 2009; Sylla *et al*., 2012).

Regional Climate Models (RCMs) are now extensively used to dynamically downscale GCMs in order to produce fine-scale and improved regional climate information (Giorgi and Means, 1999). In this regards, various regional climate change studies have been carried out over West Africa using RCMs (Paeth *et al.,* 2005; Sylla *et al.,* 2010a; Mariotti *et al.*, 2011; Diallo *et al*., 2012 ; Abiodun *et al*., 2013; Sylla *et al*., 2015).However uncertainties associated with those projection have not been quantified. In order to adequately design long-term adaptation policies and decision making that are climate-proof, it is important that decision makers are informed about the reliability of future climate projections. This will support planners in making informed decisions on future investments aimed at optimizing the use of scarce resources available and promote climate-resilient development.

There are three main sources of uncertainty: the first is the internal variability of the climate system, which describe the natural fluctuation arising in the absence of any radiative forcing. The second is the model uncertainty which explain how climate models produce different responses to the same Green House Gases (GHG) forcing due to varying dynamics and physics parameterizations. The third is scenario uncertainty results from unknown future greenhouse gases emissions (Hawkins and Sutton, (2009)).

1.1 Motivation for the study

Climate change is undeniably occurring and poses significant risks to a wide range of societies and natural systems (IPCC, 2007). The latest report by the Intergovernmental Panel on Climate Change (IPCC,2014) states that global average surface air and ocean temperatures are increasing at rates unequivocal to any other period on record, including paleo records.

In the last few decades, droughts have become more common, especially in the tropics and subtropics and increases have occurred in the number of heavy precipitation events. These extreme conditions, expected to be exacerbated in the future, have already caused substantial flooding and food shortage, and constitute significant threats to water resource and public health management (Parry *et al.*, 2007). For Africa, based on climate model results', warming is very likely (90 to 99% probability) to be larger than the globally average in all seasons by the end of the 21st century, particularly in drier subtropical regions. Africa is thus one of the most vulnerable continents to such changes, a situation aggravated by different interactions between population and ecosystems and low adaptive capacity.

This is particularly true for West Africa where agriculture is the prominent instrument for spurring growth, enhancing food security and overcoming poverty (Boko, 2007). Due to the predominance of rain-fed agriculture, the dependence of local population to natural resources and increasing drought episodes and flooding events, it therefore becomes critical to provide reliable climate change scenarios for the end-users community of West Africa. Such scenarios require quantification of uncertainties and thus the use of multiple regional climate models.

1.2 Statement of research problem

Reliable climate change scenario with associated uncertainties over West Africa is still lacking. To overcome this gap and provide climate change scenarios useful for impact studies and for the development of adaptation and mitigation strategies, we highlight a number of scientific questions to be answered:

- Do dynamical downscaling of RCMs always performs better than GCMs?
- What is the state-of-the-science regional climate change projection in term of mean change over West Africa?

- What is the associated uncertainty range and how can it be quantified?

The answers to such questions will help to deliver climate change information at the local/regional useful for end-users, quantify and minimise the range of uncertainty and provide relevant information for future modelling work.

1.3 Aim and objectives

1.3.1 Aim

This research aims at investigating climate change scenarios over West Africa with the associated uncertainties to improve the value of climate information to end-users for informed decision making.

1.3.2 Specific objectives

The specific objectives of this study are to:

i. determine the ability of RCMs and GCMs to simulate the present day climate in terms of capturing spatial patterns and inter annual variability
ii. identify methods to extract reliable climate change scenarios for West Africa from the Multi Models Ensemble
iii. determine the range of uncertainty in global and regional climate change projections for precipitation and temperature over West Africa for the late 21^{st} century(2070-2099) under RCP45 and RCP85 scenario
iv. identify the signal to noise ratio patterns over West African region for precipitation and temperature under RCP45 and RCP85 scenario.

CHAPTER TWO

LITERATURE REVIEW

2.1 Introduction

Translating climate projections into credible climate information services for decision-makers is complicated by uncertainty and lack of understanding of the physical processes responsible for the changes. In the absence of understanding of the nature of climate projections, policy-makers may expect high resolution impacts-centred projections, yet uncertainty about the detail of future climate change impacts remains high. It is therefore fundamental to characterize and quantify uncertainty in climate change projection over West Africa as a contribution to resolve a critical knowledge gaps in the understanding of the regional climate for strategic approaches to adaptation and mitigation. Giorgi *et al.* (2009) highlight the vulnerability of Africa to the impacts of climate change due to relatively low adaptive capacity of its economy. Temperature and precipitation patterns may change significantly and interact with other environmental stressor such as land use change, desertification and aerosols emissions. Future climate change has three main sources of uncertainties (Hawkins and Sutton, (2009) and Tebaldi and Knutti, (2007)): (i) the internal variability which is the natural variability of the climate system without an external forcing, (ii) the model uncertainty which characterized different model response to the same external forcing and (iii) forcing uncertainty because of the incomplete knowledge of the external factors such as GHGs, land use change among others. According to Kang *et al.* (2013) internal variability is the most challenging source of uncertainty since it will persist even if the models become more accurate with known forcing.

2.2 Climate downscaling over West Africa

In order to address the sources of uncertainties and understand the dynamics behind the West African climate, a lot of studies using RCMs have been carried out. Gallee *et al. (*2004) used a high resolution model (Model Atmospherique Regional (MAR)) of 40 km resolution over West Africa to simulate the intra seasonal variations of rainfall. The model captured the spatial variability of monthly mean rainfall with some overestimation over some area from the beginning of August. European Center for Medium range Weather Forecasting (ECMWF) reanalysis were used to compare with temperature and wind and cold bias were identified where the simulated hydrological cycle was strong. The regional climate model REMO at 0.5^{o} resolution from Max Planck Institute for Meteorology (Paeth *et al.*, 2005) was used to investigate the cause of West African rainfall inter annual variability during the period of 1979-2003. Atlantic Sea Surface Temperature (SST) and some external atmospheric forcing were playing a key role in inter annual variability. A warm tropical Atlantic is accompanied by a surface wind convergence near the Guinean coast and a change in the strength of the TEJ.

Jenkins *et al.* (2005) used RegCM3 with NCEP (National Center for Environmental Prediction) reanalysis as boundary condition for the period of 1960–2002 to also investigate inter annual variability of precipitation and found that the model was able to reproduce the wetter conditions in the 1960s to the very dry conditions in the 1980s. Dry conditions were linked to a weaker TEJ related to a warmer Indian Ocean temperature during past decade. Afiesimmama *et al.* (2006) investigated the West African monsoon inter annual variability with REGM 3 and NCPEP as boundary condition during the period 1979 to 1990 and found that there is an overestimation of rainfall amounts along the Guinean coast (complex topography area) and underestimation over the Soudano- Sahel. The increased rainfalls along the coast were explained by an enhanced low-

level convergence of the moist southwesterly winds along the coast leading to a reduction of the moisture content in the atmosphere. The decrease over the Soudano- Sahel could be associated with the weakening of the land– sea temperature gradient and hence the decrease in the low level southerly flows.

Sylla *et al. (*2009) used RegCM3 with different lateral boundary condition to downscale AOGCM and reanalysis data as a first step in future climate change scenario during 1981-2000 period. Output of precipitation and temperature from both simulations were compared and Climate Research Unit observations data were used as reference data. Beyond the fact that RCMs perform better than the driving field , evaluation of seasonal precipitation biases were made, which shows that RCM dry biases are highest on June–August around and cold biases in temperature are connected to wet biases in precipitation outside orographic zones. Biases brought by the driving GCM were negligible.

Hernández-Díaz *et al. (2012)* followed the CORDEX protocol with a new fifth-generation Regional Climate Model (CRCM5) driven by ERA-interim reanalysis for the period 1984–2008 over the African continent to investigate African climate. The model succeeded in reproducing the main features of African climate and the West African monsoon. Biases in surface temperature and precipitation were linked to some circulation defects noted in the simulation. For the Sahel region, CRCM5 captures the timing of the monsoon onset. In boreal summer the CRCM5 simulation exhibits a weak cold bias over the Sahara and the maximum temperature is located too far south, resulting in a southward bias in the position of the Saharan Heat Low. Panitz *et al. (*2013) applied COSMO-CLM Regional Climate Model (CCLM) over the CORDEX-Africa domain and performed two simulations at different resolution one of 0.44 and another one of 0.22. The model was driven by the ERA-Interim reanalysis (1989–2008). CCLM

is able to reproduce the features of the African climate with some weakness like the presence of an excessive pressure gradient between the Gulf of Guinea and the Sahara. The excessive pressure gradient related to a bias distribution marked with a warm bias over the Sahara and a cold bias over southern Sahel. The model had dry bias explained by the misplacement of the monsoon center (link to the northern shift of the Heat low) and weakening of the monsoon intensity (link with the surface energy budget). The study also show also that the higher resolution (0.22) didn't performed better than the coarse one (0.44) at the monthly means time scale. Hadley Centre Global Environmental Model version 3 regional climate model (HadGEM3-RA) was used (Diallo *et al*., 2014) to investigate the onset of West African monsoon and rainfalls totals over the June-July-August (JJA) season and the underlying dynamical processes. CORDEX experimental protocol was followed and the model was driven by ERA-Interim reanalysis. A realistic monsoon onset timing was found with an error on the mean date of two pentads. Dry bias (15-20%) was found over the Sahel. The dry bias was explained by the model error in simulating the position of the Saharan heat low (too far south), lower position of the ITCZ and weaker moisture convergence of the Sahel. HadGEM3-RA's representation of the general rainfall distribution during the WAM appears superior to that of ERA-Interim when using Global Precipitation Climatology (GPCP) Project or Tropical Rain Measurement Mission data as reference (TRMM). Akinsanola *et al.* (2015) used Three Regional Climate Models over CORDEX Africa in Simulating West African Summer Monsoon Precipitation (RCMs) to investigate the characteristics of rainfall pattern during the West Africa Summer Monsoon from 1998 to 2008. The validation was made using precipitation data from eighty-one (81) ground observation stations and TRMM satellite data. Beyond assessing the ability of RCMs to capture the seasonal climatology, annual rainfall cycles, and wind fields

of the RCMs over three homogenous sub regions, low frequencies variability (El Nino and La Nina) were also assessed. Two models were able to capture the main features and the monsoon dynamics over the region and can therefore be used for the assessment of West African Summer Monsoon and future climate projections. Druyan *et al.* (2010) use five (RCMs) from (WAMME) during May-October (2000-2005) with National Center for Environmental Prediction reanalysis II (NCEP) data as boundary conditions. Four of the five models generate positive precipitation biases and all simulate cold biases from surface air temperature. Over the Sahel RCMs spatial patterns of June–September mean precipitation with observational analyses is about 0.90 while the correlation over West Africa of surface air temperature and observation is 0.88. Over West Africa RCMs is capturing the seasonal zonal wind and meridional moisture advection and two overestimate moisture convergence. Diallo *et al. (*2012) shows the importance of local processes and the use of different driving GCMs to construct a MME since there is systematic errors compensation from both the nested and the driving GCMs and it give more robustness to climate change projection. The western Sahel will go under substantial drying in future climate projections (early 21st century A1B 2031-2050 with 1981-2000 as reference period) due to a decrease in peak monsoon. Four regional climate models (RCMs) were driven by two global climate models (GCMs) for the present and future climate over West Africa. Models precipitation is compared to the observational datasets: GPCP (Global Precipitation Climatology Project; 2.5 ×2.5 resolution, CRU (Climate Research Unit, land only, 0.5× 0.5 resolution, CMAP (Climate Prediction Center Merged Analysis of Precipitation, 2.5×2.5 and GPCC (Global Precipitation Climatology Centre, 1×1 resolution]). The GISS (NASA/Goddard Institute for Space Studies (GISS)) RM3 regional climate model (Druyan *et al.*, 2015) was used to investigate the added value of downscaling atmosphere–ocean global climate model

(NASA/Goddard Institute for Space Studies (GISS) coupled ModelE) simulations over Africa and adjacent oceans during June– September 1998–2002 period.The coarse ModelE resolution is 2° latitude by 2.5° longitude and the RM3 grid spacing is 0.44°. Results show an important added value in onset simulation produced by downscaling with RM3. It eliminated the ModelE double ITCZ over the Atlantic with a more realistic orographic precipitation maxima. Downscaling improvements of the meridional movement of the rain band over West Africa and the configuration of orographic precipitation maxima were realized irrespective of the SST biases noted in ModelIE (Coarse resolution).

Paxian *et al.* (2016) found that the ability of RCMs and improved boundary conditions to reduce rainfall biases for climate impact research depends on the considered West African region. Hypothesis that global prediction biases can be reduced by dynamical downscaling with an MME ensemble of three regional climate models were made. Previous Global predictions reveal typical positive and negative biases over the Guinea Coast and the Sahel were respectively related to a southward shifted Intertropical Convergence Zone (ITCZ) and a positive tropical Atlantic SST bias. By using RCMs, rainfall biases were reduced by some regional predictions in the Sahel but aggravated by all RCMs over the Guinea Coast, resulting from the inherited SST bias from GMCs thus increased westerlies and evaporation over the tropical Atlantic and shifted African easterly waves. The coupled regional predictions simulate high-resolution atmosphere-ocean interactions strongly improving the SST bias, the ITCZ shift and the Guinea Coast and Central Sahel precipitation biases. Kim *et al.* (2013) investigate in the 10 CORDEX regional hindcast experiment the skill in simulating the monthly-mean precipitation, minimum and maximum surface air temperature and cloudiness. The period 1990-2007 was used as a baseline of the evaluation with CRU as observation. All RCMs capture the basic climatological features

with some systematic biases across models. A better skill in simulating precipitation and temperature over West Africa and lower skill in simulating cloudiness were shown. MME outperforms individual models for all variables. Cretat *et al.* (2013) investigate extreme (daily intense rainfall) with two RCMs simulations at two different resolution (90 and 30 km) by downscaling four GCMs from CMIP5 during the 1998-2008 period. A daily intense rainfall event with the 95^{th} percentile threshold at each grid point during a rainy day was defined. Both RCMs capture the spatial and temporal features but underestimate their intensity. The added value of downscaling to investigate the physics behind the intense event and their change under global warming is highlighted. Gbobaniyi *et al.(*2014) also examine the seasonal climatology and inter annual variability with an ensemble of 10 Regional Climate Models (RCMs), driven by ERA-Interim reanalysis during the period of 1990-2008. RCMs show acceptable performance in simulating the spatial distribution of the main precipitation and temperature features with some biases across model. However the interannual variability of seasonal anomalies is well captured in temperature compared to the one of precipitation. The ensemble means considerably outperform individual RCMs. This highlights the importance of performing multi-model assessment.

Dosio *et al.* (2015) use the same models to investigate whether RCMs are effectively able to add value and outperform GCMs at regional scale for the present day. According to their study, the boundary condition is affecting the spatial distribution of surface temperature and seasonal precipitation, and seasonal statistics are not always improved by the downscaling. Klutse *et al. (*2015) analyze and intercompare the performance of a set of ten regional climate models (RCMs) from CORDEX outputs along with the ensemble mean of their statistics in simulating daily precipitation characteristics during the West African monsoon (WAM) period (June–July–

August–September). The ensemble mean of the indices substantially improves the RCMs' simulated frequency and intensity of precipitation events, moderately outperforms that of the 95th percentile, and provides mixed benefits for the dry and wet spells. Paeth *et al.* (2007) investigate the future African climate north of 15^{o}S under greenhouse warming and land use changes (land degradation) with a Regional model. At the near future (2025) the model shows a considerable drying over the Sahel (20–40% of the annual sum) during the boreal summer. A warming up to 7^{o}C due to the change in the surface energy fluxes is found. This has implication (temperature gradient modified) on the circulation of the West African monsoon with a drying tendency over the region. Abiodum *et al.* (2008) used RegCM3 to investigate the feedback mechanisms between land cover and the monsoon in West African using reanalysis as boundary conditions under three idealized vegetation states (potential, desertified and deforested). The study shows that both desertification and deforestation tend to increase the monsoon flow over the Guinean region, although the mechanisms for change are different in each case. Desertification increases the flow mainly by increasing the meridional temperature gradient. While this reduces rainfall over the desertification region, it increases rainfall to the south. On the other hand, deforestation increases the monsoon flow mainly due to the reduced surface friction experienced by the flow over the Guinean region. This reduces rainfall over the entire West African region. Overall, this study suggests that the state of the biosphere in West Africa may play an important role in determining the characteristics of the monsoon and rainfall pattern. Sylla *et al.* (2010b) used RegCM3 to investigate the relationship between rainfall changes and the monsoon dynamics under increased greenhouse gas forcing with ECHAM5 as a driving GCM. They found a drying condition over Sahel and wetter conditions over orographic area. The drying condition is associated with a weaker monsoon flow, a strengthening of the AEJ, a

weaker TEJ and wave activity is reduced. Mariotti *et al.* (2011) used the same model RegCM3 to simulate over a large African domain a transient climate change for the 21st century (1980–2100) with ECHAM5 as a driving GCM. For present climate, the two models have different spatial patterns for temperature and precipitation with similar biases in terms of magnitude .For the future climate, a significant difference between the coarse and fine resolution precipitation change pattern where noticed while the temperature changes patterns depend on the driven GCM over the West Africa and Sahel regions. The two model have different response in simulating the forcing of El Niño – Southern Oscillation and of local soil moisture/precipitation feedbacks.The Met Office Hadley Centre's PRECIS regional climate modelling system (Buetenmpo *et al.,* 2014) has been used to generate a five member ensemble of climate projections for Africa over the 50 km resolution for 1949-2100 period (CORDEX-Africa domain). From Hadley Centre's perturbed physics global climate model (GCM) ensemble, a subset has been created by discarding ensemble members which are not able to reproduce some basics features of African climate. The RCM ensemble substantially improve the patterns and magnitude of precipitation compared to their driving GCM which is particularly noticeable in the Sahel for both the magnitude and timing of the wet season. Present-day simulations indicate that the climatology is influenced significantly by the RCM internal physics and less by their driving GCMs. Giorgi et *al* . (2014), used three CMIP5 GCMs to drive ICTP regional model RegCM4 new version over five CORDEX domains (Africa, Central America, South America, South Asia, Mediterranean) under RCP8.5. Four extreme indices (HeatWave Day Index (HWD), Maximum Consecutive Dry Day index (CDD), fraction of precipitation above the 95th intensity percentile (R95) and Hydroclimatic Intensity index (HYINT)) were analyzed. Coarse (GPCP) and high (TRMM) resolution daily precipitation data for the present day conditions shows that the

precipitation intensity distributions from the GCMs are close to the GPCP data, while the RegCM4 ones are closer to TRMM, which show the added value of the increased resolution of the regional model. All global and regional model simulations project a regime shift towards more intense, less frequent rain events and increasing risk of heat wave, drought and flood with global warming. RegCM4 was used to dynamically downscale at 25 km (Sylla *et al.*, 2015) horizontal grid spacing three CMIP5 ESMs: MPI-ESM-MR (Max-Planck Institute Earth System Model – Medium Resolution), HADGEM2-ES (Hadley Centre Global Environment Model version 2 – Earth System configuration) and GFDL-ESM-2M (Geophysical Fluid Dynamics Laboratory Earth System Model version 2M). These ESMs were selected because they provide a relatively good representation of the monsoon climate of West Africa. The response of the annual cycle of high-intensity daily precipitation events over West Africa to anthropogenic greenhouse gas for the late twenty-first century was investigated using the ensemble of high-resolution regional climate model experiments. For the present day, the RCM ensemble improved the simulation of the annual cycle compared to the driving Earth system models. For the late-twenty-first-century projected changes in mean precipitation, a delay of the monsoon season, a prevailing decrease in frequency but increase in intensity of very wet events were found. Sylla et *al. (*2016a) found that the projected climate change indicates continuous and stronger warming (1.5–6.5 °C) and a wider range of precipitation uncertainty (roughly between −30 and 30 %) larger in the Sahel and increasing in the farther future. However, the spatial distribution unveils significant precipitation decrease confined to the westernmost Sahel and becoming greater and more extensive in the high level GHG forcing scenario by the end of the 21st century. This coexists with a substantial increase in both dry spell length and extreme precipitation intensity. West Sahel is thus the most sensitive region to anthropogenic climate

change. The rest of West Africa also experiences more intense extremes in future climate but to a lesser extent. It is also reported from other previous studies that the projected rainy season and the growing season will become shorter while the torrid, arid and semi-arid climate conditions will substantially extend. It is thus evident that in a "business as usual" World, most countries in West Africa will have to cope with shorter rainy seasons, generalized torrid, arid and semi-arid conditions, longer dry spells and more intense extreme precipitations. Dosio *et al.* (2016) created an ensemble of climate change projection for Africa from the downscaling of four Global Climate model (MPI-ESM-LR, HadGEM2-ES, CNRM-CM5, and EC-Earth) in the framework of CORDEX with CCLM (COSMO RCM), the projected increase of seasonal temperature is relatively similar between GCMs and RCM with some local differences. Larger uncertainties in the future precipitation changes due to inter-model (GCMs) variability over some areas (e.g.Sahel) were found.

These studies above mainly found that RCMs were able to capture the general feature of West African climate although some differences and biases still persist in some regions and seasons.

2.3 Multi Model Ensemble techniques

Based on the availability of GCMs and RCMs simulation data through CMIP5 and CORDEX program, Multi Model Ensemble have been used to investigate the future climate over the region. These data have been used for seasonal prediction (Palmer *et al*, 2004, Stephenson *et al.*, 2005). Annan *et al.* (2011) found that Multi Model Mean tends to have a lower Root Mean Square Error compared to most individual models. Paeth *et al.* (2011) shows that MME have clearly an added value in WAM rainfall with respect to the European Reanalysis-Interim driving field. While Diallo *et al.* (2012) suggested that for improved performance, the multi-model RCM ensembles

should be based on different driving GCMs. Multi Model Ensemble were used in their simplest form. There are more complex methods combining the models.

Giorgi and Mearns (2002) proposed Reliability Ensemble Averaging method based on a weighted mean of the different GCM/RCM that account for reliability of each model that produces a weighted average of an ensemble of climate change results, taking into account the ability of a particular model to simulate the observed climate, and its degree of convergence in the predicted climate change with respect to the other models. The method was applied to calculate average, uncertainty range, and a measure of reliability of simulated climate changes (mean seasonal temperature and precipitation changes for the late decades of the twenty-first century) over 22 land regions of the world from nine Atmospheric Ocean GCM (AOGCM) experiments for two anthropogenic emission scenarios (the A2 and B2 scenarios of the Intergovernmental Panel for Climate Change). Some of the findings indicate that in the simulations for the A2 scenario the REA average regional temperature changes varied between about 2 and 7 ^{o}C across regions and they were all outside the estimated natural variability. The uncertainty range around the REA average changes varied between 1 and 4 ^{o}C across regions. A noticeable exception was found in the Sahel region in June-July-August season, where a large difference is found between the ensemble average and the REA average. The main reason was that most of the model simulations exhibit a large precipitation bias over this region, in excess of 200% with the exception of 3 simulations that have a bias of less than 100% (only 1 model has a bias lower than 10%). As a result, since the REA average is dominated by three simulations only, it can be substantially different from the ensemble average.

Furthermore, the method also allows the derivation of PDFs for climate variables under climate change conditions (Giorgi and Mearns, 2003). Compared to simpler approaches, the REA method allows a reduction of the uncertainty range in the simulated changes by minimizing the influence of outlier or poorly performing models. The method also produces a quantitative measure of reliability that shows that both criteria need to be met by the simulations in order to increase the overall reliability of the simulated changes.

Xu *et al.* (2010) upgrades the REA method mainly for the calculations of model weight. In the original REA method the model weight is given by the multiplication of two reliability factors which are measures of the model performance and convergence criteria. In the upgrade one, the use of the convergence criterion by eliminating the convergence-based reliability factor from the definition of the overall weight was abandoned. Then multiple variables (temperature, precipitation, pressure) and multiple statistics (mean, interannual variability) were added in the definition of the reliability weight. The augmented REA was first applied for illustrative purpose to calculate temperature and precipitation changes based on ensembles of global model simulations for the East Asia region. The dataset employed is the ensemble of coupled Atmosphere-Ocean General Circulation Model (AOGCM) simulations conducted in the Phase 3 of the Coupled Model Inter-comparison Project (CMIP3) in support of the fourth assessment report of the Intergovernmental Panel on Climate Change (IPCC AR4). Cumulative Density Functions (CDFs) of changes in temperature and precipitation for 2081-2100 with respect to 1961-1980 over 6 Chinese sub-regions as well as the entire China territory were calculated. This exercise was repeated for the eight European regions used in the PRUDENCE project (Christensen and Christensen, (2007)).

REA approach from multi-model ensemble was extended by Tebaldi *et al.* (2004, 2005) with a formal statistical framework using Bayesian methods. Their Bayesian inference treats the unknown quantities as random variables (present and future climate signal) with reference prior distributions. The likelihood function is determined through the assumption made from observation and model output. Bayes theorem is then used to derive the posterior distribution through Markov Chain Monte Carlo simulations. Applying the model to precipitation from AOGCMs (CCC, CCSR, CSIRO, GFDL, MPI, MRI, NCAR, NCARDOE and UKMO) over 22 land regions for A2 and B2 scenarios. They found a high degree of uncertainty for precipitation projection change (in percentage) over the Sahel region (SAH) with a wide PDFs explained by large model bias (up to 600% for June July August (JJA) season. The future period was 2070-2099 relative to the present day period 1961-1990.

2.4 Separating sources of uncertainties

Hawkins and Sutton (2009) separate and quantify the sources of uncertainties in decadal global mean air temperature change projection using CMIP3 archive for 21st Century. The residual from a 4th order polynomial fit to the global mean time series for each model is defined as the internal variability. The contribution of each source of uncertainty to the total uncertainty was estimated. Internal variability and model uncertainty is found to be dominant for few decades ahead. The scenario uncertainty is dominant at the end of the 21st century. Another important finding is the fact that, for temperature, the signal to noise ratio is greater than one for all the regions highlighting certainty of global warming. With The progress of climate science, model uncertainty and internal variability can be potentially reduced. A follow-up study by Hawkins and Sutton (2011) was applied using precipitation projection in global and regional scale. Their main findings are that internal variability is the most important uncertainty for precipitation for

all the regions up to mid-21st century. Over the Sahel region scenario uncertainty for precipitation during the JJA season is negligible. The signal to noise ratio over the tropics for precipitation is lower (close to zero) than for the temperature meaning that precipitation projection over West Africa is still uncertain. Time of emergence defined by Giorgi and Bi (2009) as the time of 21st century when the magnitude of the ensemble mean precipitation change signal becomes greater than the total uncertainties identified early decade of 21st century(northern high latitude, Mediterranean and East Africa), the mid decades (East and South Asia, Caribbean) and late decades (South Africa, western United States, Amazone Basin, Southern Australia and Central America). Knutti *et al*. (2013) investigate the robustness and uncertainties in CMIP5 climate model projections. Despite model development (new generation of more complex model) and increase in computational capacity, representation of more process in details and internal variability remain a challenge. In fact, projected global temperature change is still similar to those from IPCC AR4 under the same scenarios, with little change in the model spread.

CHAPTER THREE

DATA AND METHODOLOGY

3.1 Presentation of the study area

The study area of this research is West Africa located between the latitudes 0 N and 20N and the longitudes 20E and 20W (Fig3.1). Sixteen counties constitutes the WA region: Benin, Burkina Faso, Cape Verde, Gambia, Ghana, Guinea, Guinea Bissau, Cote d'Ivoire, Liberia, Mali, Mauritania, Niger, Nigeria, Senegal, Sierra Leonne and Togo. West Africa has several climatic zones from humid (southern coast) to arid (toward the North). The major water resources are the Niger river, lake Chad, the Senegal river, the Gambia river and the Volta basin covering Burkina Faso and Ghana.

Following Sylla *et al.* (2012) from April to September the region is driven by the West African Monsoon (WAM) system which is a large scale circulation characterise at the low level of the atmosphere by the wind direction reversal transporting moisture to land from the Atlantic Ocean and triggering the monsoonal rainfall up to the Sahelian belt. During the boreal summer(July-August-September) the WAM monsoon is fully develop with South-westerlies moisture flux converging onto the Sahel and retreat in early autumn (Gaetani *et al.*,2013). The monsoon sub-seasonal, seasonal and inter annual variability are controlled by various factors such as Sea Surface Temperature (SST), the continental-land surface condition and the atmospheric circulation (configuration of Tropical Easterly Jet (TEJ), African Easterly Jet (AEJ)

,Intertropical Convergence Zone (ITCZ) and African Easterly waves(AEW) (Sylla *et al.*, 2012 ; Nicholson, 2009).

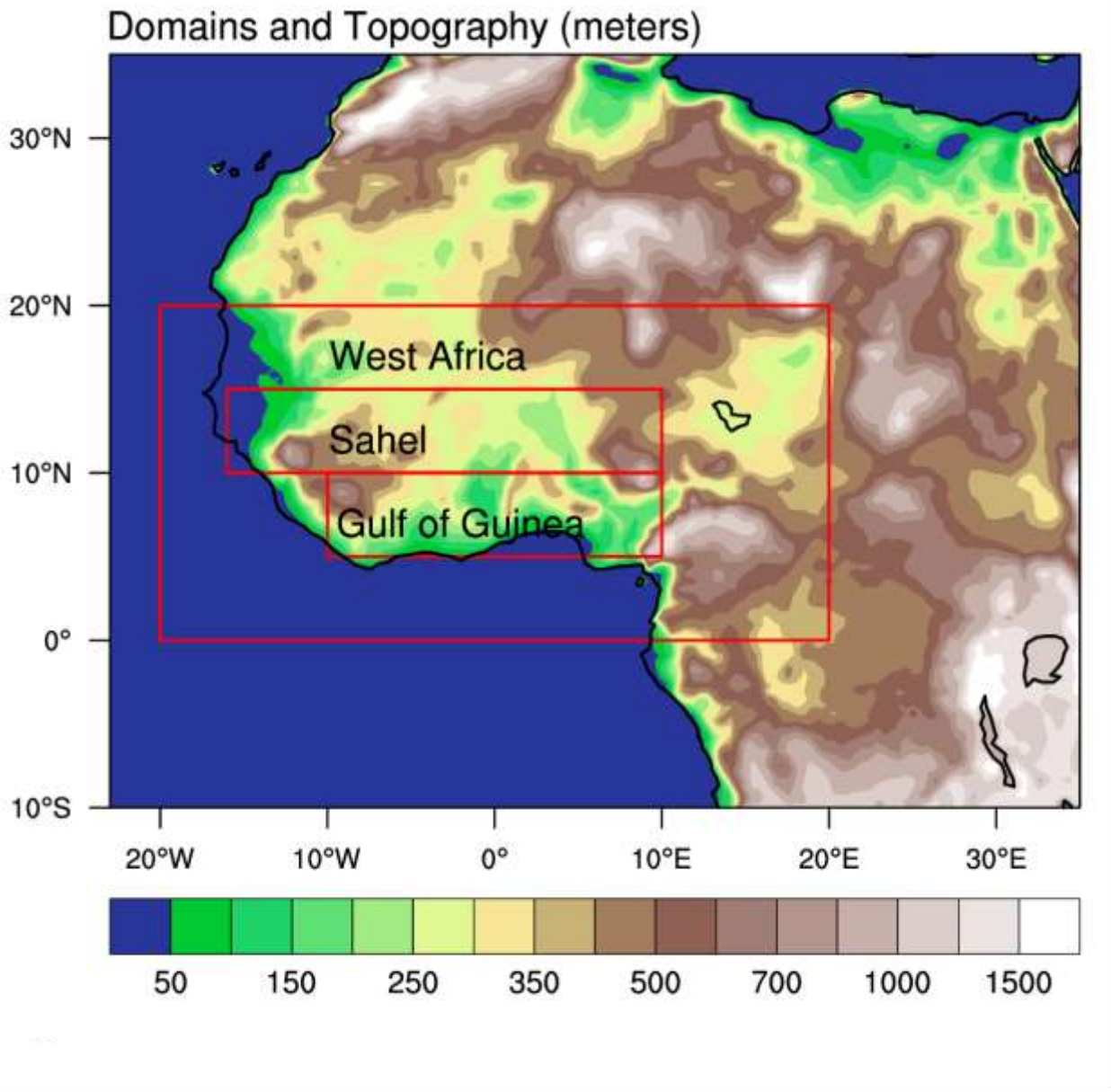

Figure 3.1: CORDEX experiment domain and topography including 3 three key sub regions of interest (i.e. rectangle) Gulf of Guinea, Sahel and West Africa used for the descriptive statistics

3.2 Data

Ensembles of 29 CMIP5 GCMs (CMIP5) and 16 CORDEX RCMs (CORDEX) experiments (Table 3.1) for the historical (1982-2000) and future period (2070-2099) under the two scenarios RCP45 and RCP85 are analyzed and inter-compared over West Africa. To identify the origin of the bias in the downscaling experiments, the ensemble of the eight CMIP5 GCMs that forced the CORDEX experiments (CMIP5_SUBSET) is also considered. While the CMIP5 GCMs cover the whole globe at 100-200 km resolution, CORDEX RCMs are integrated over the Africa CORDEX domain with a grid interval of ~50 km. However our domain of interest (Figure 1) is limited to West Africa, along with two small subregions (Sahel and Gulf of Guinea) in which the statistics are calculated. More detailed information on the CMIP5 and CORDEX experimental set-ups can be found in Taylor *et al*. (2012) and Jones *et al.* (2011), respectively.

Observations used to evaluate the different ensembles for the historical conditions are the Global Precipitation Climatology Project (GPCP 1DD 1^{O} x 1^{O} resolution; Huffman *et al.*, 2001), the Climatic Research Unit of the University of East Anglia (CRU 0.5^{O} x 0.5^{O} resolution; Harris *et al.*, 2014) and the University of Delaware (UDEL 0.5^{O} x 0.5^{O} resolution; Legates and Willmott (1990)). Although the various precipitation and temperature products available for Africa are characterized by substantial differences, the use of these multiple observed data sources can help to account for observational uncertainties (Nikulin *et al.*, 2012; Sylla *et al.*, 2013). All the datasets are re-gridded onto a common 50 km resolution grid.

Table 3.1: CMIP5 ESMs and CORDEX RCMs with downscaled GCMs (blue colors)

Model	RCA4	CCLM4	HIRHAM5	RACMOT2	CanRCM4	RegCM4
BCC-CSM1.1						
BCC-CSM1.1(m)						
CanESM2	**α**				**α**	
CNRM-CM5	**α**	**α**				
ACCESS1.0						
CSIRO-Mk3-6-0						
EC-EARTH	**α**	**α**	**α**	**α**		
FIO-ESM						
INM-CM4						
BNU-ESM						
IPSL-CM5A-MR						
IPSL-CM5A-LR						
IPSL-CM5B-LR						
MIROC-5	**α**					
MIROC-ESM						
HADGEM2-CC						
HADGEM2-ES	**α**	**α**				**α**
MPI-ESM-LR	**α**					
MPI-ESM-MR						**α**
MRI-CGCM3						
GISS-E2-R						
CCSM4						
NORESM1-M	**α**					
NORESM1-ME						
HADGEM2-AO						
GFDL-ESM2G						
GFDL-ESM2M	**α**					
CESM1-BGC						
CESM1-CAM5						

3.3 Methodology

3.3.1. Validation of CMIP5 and CORDEX data for the present day using simple MME

The MME approach is applied to the CMIP5 and CORDEX ensembles. Precipitation and temperature mean climatology from the different MMEs as well as their spatio-temporal variability are considered only for the summer monsoon season (June-September, or JJAS).

We first compare the simulations with the multiple observation products mentioned above through a simple bias operation (simulation minus observation) for the whole West Africa analysis domain. The ability of the RCM MME to improve upon the forcing GCM MME is quantified using an Added Value (AV) metric defined by Di Luca *et al.* (2012) with the normalization introduced by Dosio *et al.* (2015). The AV is given by the formula:

$$AV = \frac{((X_{CMIP5} - X_{OBS})^2 - (X_{CORDEX} - X_{OBS})^2)}{Max((X_{CMIP5} - X_{OBS})^2, (X_{CORDEX} - X_{OBS})^2)} \quad (3.1)$$

where X_{OBS}, X_{CMIP5} and X_{CORDEX} are the mean values for observations (i.e. UDEL), CMIP5 (or CMIP5_SUBSET) and CORDEX. This formula is applied at each grid point. A positive AV means that the CORDEX mean square error is smaller than the CMIP5 one and therefore indicates the existence of added value. This is depicted by an open circle or a sign + in Figures 4.1 and 4.2. In addition, to characterize the intermodel spread we use box plots including the ensemble median, upper (25%) and lower (75%) quartiles as well as the maximum and minimum of the different data sources. These are computed for the Gulf of Guinea, the Sahel and the West Africa domain shown in Figure 3.1.

Finally for the spatio-temporal variability, a Rotated Empirical Orthogonal Function (REOF) analysis is applied to the time series of the seasonal (JJAS) temperature and precipitation derived from UDEL observations and each MME at each grid point and for the whole period of interest

(1982-2005). The EOF analysis is often used to study spatial modes (i.e. patterns) of variability and how they change with time (Lorenz, 1956). In this study, REOF is chosen instead of the simple EOF analysis because the latter has a tendency to produce unphysical modes (Hannachi, 2007). Such shortcoming is partly alleviated by the REOF analysis, thus facilitating the interpretation of the results (Lian and Chen (2012)). As a measure of model performance in capturing this spatio-temporal variability, we use the Pattern Correlation Coefficients (P) and Pearson Correlation Coefficients (R) with respect to observations. P measures similarities between two spatial patterns (here observed and simulated REOFs) while R measures the strength of the linear relationship between two variables as they vary in time (here observed and simulated PCs). We emphasize, however, that since the models do not include any assimilation of observed data, significant temporal correlations can be expected only in so far as they are attributable to the greenhouse gas and aerosol forcing and not to natural climate variability.

3.3.2 Validation of CMIP5 and CORDEX data for the present day using bayesian inference

3.3.2.1 Definition of Bayesian inference

The process of fitting a set of data with probability model which summarize the results in the form of probability distribution on the parameter of the model is defined as Bayesian inference. Via Bayes rule, it provides a rational method to update our beliefs in the light of new information. The method has an advantage of providing a computational framework for model selection, validation and uncertainty quantification and reduction. Parameters are random variable with distribution attached to them. Due to some lack of knowledge on some processes in the atmosphere and imperfect parameterization in climate modeling, uncertainty remain in our GCMs/RCMs present and future climate projection and need to be quantified. Bayesian inference is one option to address above issues. The method has three components: the prior, the

likelihood and the posterior distribution. The prior is representing the current state of knowledge prior to the data being observed. The likelihood function is constructed once the data has been observed. Assuming that the data values $y = y_1,...,y_n$ are obtained independently and the vector of the unknown parameter is θ, the likelihood function is given by

$$L(\theta \mid y) = p(y_1,...,y_n \mid \theta) = \prod_{i=1}^{n} p(y_i \mid \theta) \tag{3.2}$$

To obtain the posterior distribution $p(\theta \mid y)$, the probability distribution of the parameter θ, once the data have been observed, Bayes theorem is applied

$$p(\theta \mid y) = \frac{p(\theta)L(\theta \mid y)}{p(y)} \propto p(\theta)L(\theta \mid y) \tag{3.3}$$

Markov Chain Monte Carlo (MCMC) algorithm is then used after an initial burn-in period (which is discarded) to simulate an equilibrium distribution of sample in parameter space such that the density of sample is proportional to the joint posterior Probability Density Function (PDF). The Bayesian inference has been applied on present climate for validation purpose and on future climate projection.

3.3.2.2 Bayesian inference on CMIP5 and CORDEX present day climate simulation

A Bayesian model adapted from Mesquita *et al. (*2012) is applied on precipitation data over Guinea coast and Sahel region. The joint prior distribution $p(\theta, \sigma^2)$ where θ is mean precipitation and (σ^2) the variance, the posterior inference will use Bayes' rule,

where $y_1,...,y_n$ represent the data. Since the joint distribution for the two quantities can be expressed as the product of a conditional probability and a marginal probability, the posterior distribution can be decomposed

$$p(\theta,\sigma^2 \mid y_1,...,y_n) = p(\theta \mid \sigma^2, y_1,...,y_n)\, p(\sigma^2 \mid y_1,...,y_n) \tag{3.4}$$

Where the first part of the equation is the conditional probability of θ on the variance and the the second part is the marginal distribution of σ^2 . The conditional probability part was assumed to have a normal distribution: $\{\theta \mid y_1,...,y_n,\sigma^2\} \sim normal(\mu_n, \sigma^2 / k_n)$ (3.5)

where $k_n = k_0 + n$ representing the degrees of freedom (df) as the sum of the prior df (k_0) and that from the data (n). μ_n is given by $\mu_n = \dfrac{(k_0/\sigma^2)\mu_0 + (n/\sigma^2)\bar{y}}{k_0/\sigma^2 + n/\sigma^2} = \dfrac{(k_0\mu_0 + n\bar{y})}{k_n}$ (3.6)

where $\bar{y}$ represent the sample mean taken from the model simulation and μ_0 is the prior mean from UDEL observation over the considered region (Guinean Coast or the Sahel). The second part of the equation 2, the marginal distribution of σ^2 has a gamma distribution $\{1/\sigma^2 \mid y_1,...,y_n\} \sim gamma(\nu_n/2, \nu_n{\sigma_n}^2/2)$ (3.7)

with $\nu_n = \nu_0 + n$ sum of the degree of freedom of the prior (ν_0) and the data (n).

$${\sigma_n}^2 = \frac{1}{\nu_n}[\nu_0{\sigma_0}^2 + (n-1)s^2 + \frac{k_0 n}{k_n}(\bar{y} - \mu_0)^2] \tag{3.8}$$

where $\bar{y}$ is the sample mean and s^2 is the sample variance taken from the model simulations. σ_0^2 is the prior variance. Posterior mean and variance is derived through an averaging of MCMC large sample size (10000) and 95% central posterior interval probability limit is drawn.

3.3.3 Bayesian inference on CMIP5 and CORDEX future climate projection

Bayesian approach is applied to CMIP5 GCMS and CORDEX RCMS data in order to quantify the probability associate with precipitation and temperature change over Guinean Coast and Sahel region. This statistical framework had been proposed by Tebaldi *et al.* (2005) to find out how projections from different models contribute to a final PDF (Probability Distribution Function) of climate change. The method is summarized as follows. For each region, X_i and Y_i denoted respectively the present (1976-2005) and future (2070-2099) simulated temperature by the i^{th} model, for JJAS season and averaged over the region of interest. For each region μ and ν represent respectively the true present and future temperature average over 30 years. They made an assumption that X_i and Y_i have normal distribution $X_i \sim N(\mu, \lambda_i^{-1})$ $Y_i \sim N(\nu, \theta_i\lambda^{-1})$ where the parameter λ_i is called the precision of the model i and for Y_i the precision of the model i is $\theta\lambda_i$. θ is a multiplication factor for the model precisions in future climate simulations. It constitutes the likelihoods function. The observation likelihood is $X_o \sim N(\mu, \lambda_0)$. λ_0 is a function of the natural variability derived from the observation and is specific to a region. $\Delta T = \mu - \nu$ is the expected temperature change. A gamma prior densities were chosen for the parameters $\lambda_i, i = 1,...,n$ and θ. Bayes' Theorem was applied to the likelihood and priors specified above to derive the joint posterior density for the parameters μ, ν

$,\theta,\lambda_1.....\lambda_n$ through Markov Chain Monte Carlo (MCMC) simulation (details about the methods, the MCMC and Gibbs sampler can be found in Tebaldi *et al.* (2005).

Inference cannot be drawn from this equation since its distribution is not a member of any known parametric family. Therefore Markov Chain Monte Carlo simulation was used to generate a large number of sample values through the implementation of a Gibbs sampler. The details about the methods, the MCMC and Gibbs sampler can be found in Tebaldi *et al.* (2005).

The posterior distribution of μ is Gaussian with mean $\mu \approx (\sum_{i=0}^{n} \lambda_i X_i) / (\sum_{i=0}^{n} \lambda_i)$ (3.9)

which is a weight average of observation and model present day output with weights $\lambda_0, \lambda_1.....\lambda_n$ and the posterior distribution of ν is Gaussian with mean

$$\nu \approx (\sum_{i=0}^{n} \lambda_i Y_i) / (\sum_{i=0}^{n} \lambda_i) \quad (3.10)$$

a weight average of the n model forcing response with weight $\lambda_1.....\lambda_n$. The mean of the posterior distribution of the λ_i's, for i=1,….,n, is $\lambda_i \approx \frac{1}{|X_i - \mu|^2 + \theta |Y_i - \nu|^2}$ (3.11)

The equation shows that if both $|X_i - \mu|$ and $|Y_i - \nu|$ are small the weight λ_i is large. These two quantities correspond to the bias and convergence criteria respectively in Giorgi and Mearns (2002). $|Y_i - \nu|$ measures the distance of the i^{th} model future response from the overall average response while $|X_i - \mu|$ measure the distance of the i^{th} model to the present.

3.3.4 Partitioning and quantifying uncertainties in climate projection over West Africa

The method used to separate the different component of uncertainties was based on Hawkins and Sutton (2009) methods. An ordinary least square was used to fit each decadal anomalies prediction of CMIP5, CMIP5_Subset and CORDEX with a fourth-order polynomial over the years of 2006-2099 for the two scenarios RCP45 and RCP85. The anomalies were computed with the reference period of 1976-2005. The raw predictions (X) for each model (m) and period (t) are written as, $X(m,t) = z(m,t) + \mu_{ref}(m) + \varepsilon(m,t)$ (3.12)

where $\mu_{ref}(m)$ is the reference temperature for each model, $z(m,t)$ is the polynomial fit of the projected change of the parameter and the regression error is $\varepsilon(m,t)$.

The internal variability is defined as the multi-model mean of the variance of the regression error $\varepsilon(m,t)$

$$V_{HS} = \frac{1}{N_m T}\sum_{m=1}^{N_m}\sum_{t=1}^{T}(\varepsilon(m,t))^2 \quad (3.13)$$

The internal variability is assumed to have a constant variance in time.

The model uncertainty is the mean of inter-model variance of $z(m,t)$.

$$M_{HS}(t) = \frac{1}{N_m}\sum_{m=1}^{N_m}[z(m,t) - z(.,t)]^2 \quad (3.14)$$

The total uncertainty ($T_{HS}(t)$) is defined to be the sum of V_{HS} and $M_{HS}(t)$

$$T_{HS}(t) = V_{HS} + M_{HS}(t) \quad (3.15)$$

The signal to noise ratio (S/R) at the period (t) (based on Cox and Stephenson, (2007)) is defined as $S/N = \frac{Z(.,t)}{1.65\sqrt{T_{HS}(t)}}$ (3.16)

The fraction of variance of internal variability and model uncertainty are defined respectively by $V_{HS}/T_{HS}(t)$ and $M_{HS}(t)/T_{HS}(t)$.

CHAPTER FOUR

. RESULTS AND DISCUSSION

4.1 Multimodel CMIP5 and CORDEX simulations of historical summer temperature and precipitation variabilities over West Africa

4.1.1 Multimodel ensemble mean climatology

Before evaluating the simulated spatio-temporal variability of temperature and precipitation during the boreal summer season (July-September) for the different MMEs, in this section we first analyze the spatial patterns of their mean climatology.

The temperature distribution from observations (UDEL and CRU) and the MMEs of CMIP5, CMIP5_SUBSET and CORDEX as well as their respective bias distributions are presented in Figure 4.1. Observations indicate that in general the Sahara desert experiences the highest temperatures (more than 36^{o}C) and the Gulf of Guinea the lowest ones (between 24^{o}C and 26^{o}C). The Sahel, which is the transition zone between the two regions, exhibits intermediate values ranging from 26^{o}C to 32^{o}C. The temperature maxima and minima are found in the area of the Saharan Heat Low (SHL) and at the peak of orographic zones (Guinea Highlands, Cameroon Mountains and Jos Plateau), respectively.

The MMEs reproduce the general observed pattern of summer temperature, however with notable discrepancies among them. The spatial distribution is smoothed in the CMIP5 and CMIP5_SUBSET compared to the observations, while CORDEX shows more spatial details and lower temperature values around orographic zones as a result of its higher resolution. As a

consequence, a negative bias of about 2^{o}C more extended in CORDEX compared to CMIP5 and CMIP5_SUBSET prevails over the Gulf of Guinea.

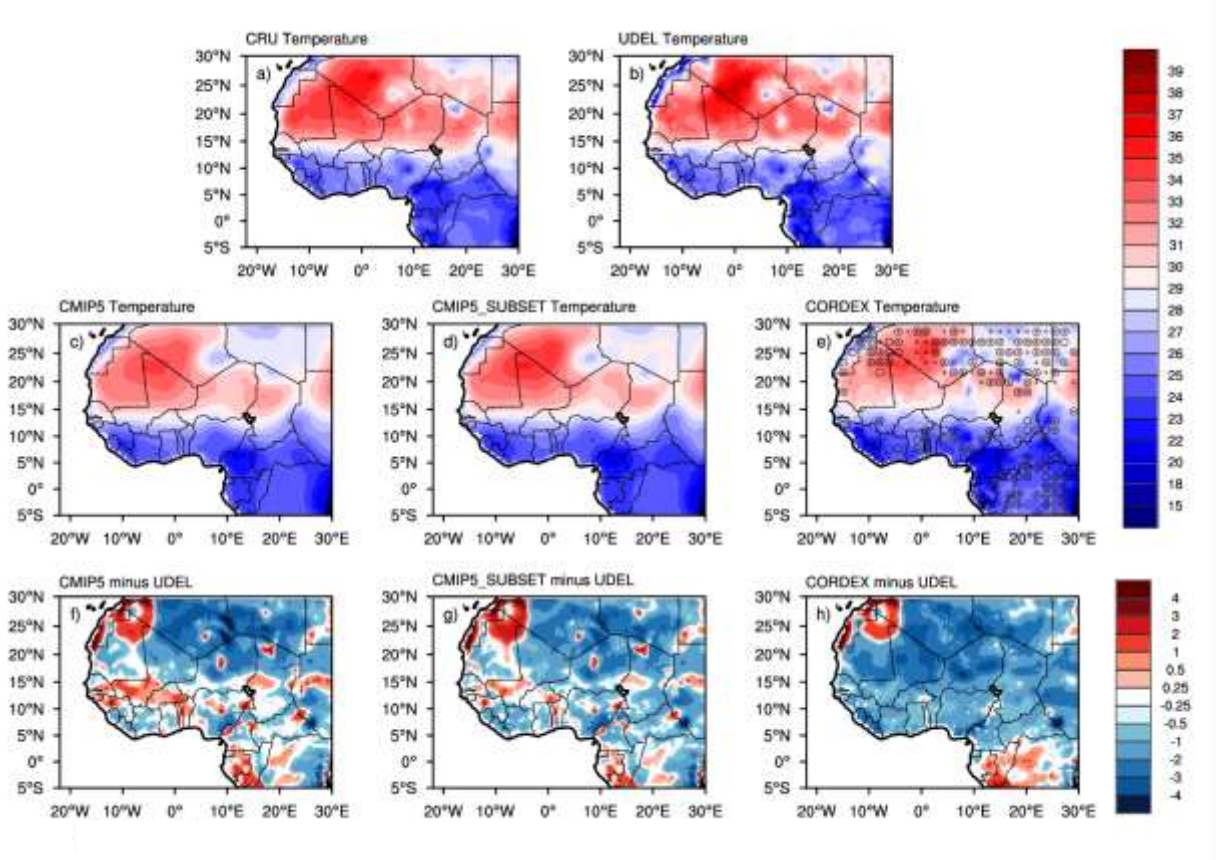

Figure 4.1: 1982-2005 JJAS mean temperature (^{o}C) for a) CRU observation, b) UDEL observation, c) CMIP5, d) CMIP5_SUBSET, e) CORDEX and respectively their corresponding bias with respect to UDEL in f), g), h). For CORDEX i.e. in e), the open circles mean improvement compare to CMIP5_SUBSET while the sign plus is for improvement compared to CMIP5

In addition, a cold bias of more than 3^{o}C widely spread over the Sahara desert develops in all MMEs. Finally, over the Sahel band, a predominant warm bias is simulated by CMIP5 and to lesser extent by CMIP5_SUBSET. Therefore, in general CORDEX fails to outperform the simulated mean temperature by CMIP5 and CMIP5_SUBSET over the Gulf of Guinea, over the Sahel and over the southern Sahara desert. However, we note some improvements with respect to both CMIP5 MMEs over the area of the SHL, western Sahara and Central Africa.

Considering the corresponding spatial patterns of precipitation shown in Figure 4.2, the Intertropical Convergence Zone (ITCZ) is observed in a zonal and tilted band between 8N and 12N in GPCP, CRU and UDEL with a sharp decreasing precipitation gradient south and north of this band. The minima are located north of 18N while maxima are found in topographically complex terrains of the Guinea highlands, Jos plateau and Cameroon mountains. As noted by Nikulin *et al.* (2012) and Sylla *et al.* (2013b), there are discrepancies among the various observed precipitation products over West Africa.

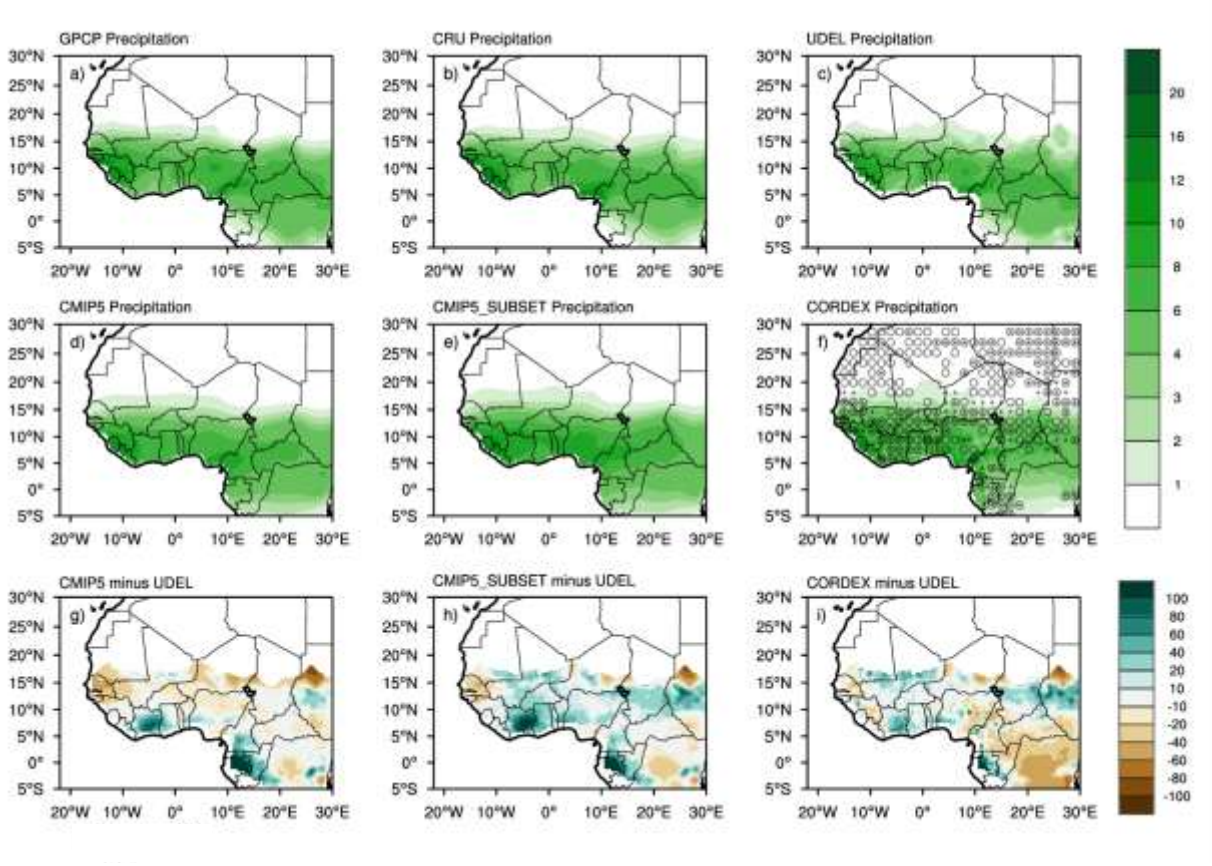

Figure 4.2: 1982-2005 JJAS mean precipitation (mm/day) for a) CRU observation, b) UDEL observation, c) CMIP5, d) CMIP5_SUBSET, e) CORDEX and respectively their corresponding bias with respect to UDEL in f), g), h). For CORDEX i.e. in e), the open circles mean improvements compared to CMIP5_SUBSET while the sign plus is for improvement compared to CMIP5

In this case, these differences include a missing maximum in CRU over the Jos Plateau and a much better defined ITCZ in GPCP (e.g. GPCP does not show any break in the ITCZ). Note that the observational uncertainty is relatively low for the JJAS climatology in temperature and rainfall compared to higher uncertainties at finer temporal scales (i.e. Cretat *et al.,* 2014).

The MMEs show close agreement with observations in simulating the spatial patterns of the summer monsoon precipitation features, including the ITCZ position, the northward and southward decreasing gradients and the large precipitation amount around orographic zones. However, a notable wet bias (40% to 80%) along the Gulf of Guinea and dry bias (mostly 10% to 20%, but up to 60%) over the Sahel are dominant in CMIP5. In CMIP5_SUBSET the wet bias is more extended to cover almost the whole West Africa, with overestimations of 10% to 80%. This originates from a broader representation of the ITCZ in the CMIP5 ensembles, especially in the CMIP5_SUBSET used for driving the RCM simulations. Conversely, in CORDEX both the wet and dry biases are reduced, resulting in a substantial improvement compared to both CMIP5 ensembles, and an added value in many areas of the Gulf of Guinea, the Sahel and most of West Africa. In addition to these significant improvements, it can be noted that the spatial pattern of rainfall biases simulated by the RCM MME resembles that of the CMIP5_SUBSET MME. This suggests a stronger control by the driving GCMs on the spatial distribution of precipitation than on the intensity of RCM-simulated rainfall. It should be emphasized that around peaks of mountainous areas, CORDEX does not show any added value because of more fine-scale details simulated in the presence of complex topography than found in the observations.

Overall the MMEs exhibit different levels of performance in their simulations of temperature and precipitation compared to observations, with CMIP5 and CMIP5_SUBSET showing a smoothed spatial pattern and CORDEX providing more fine-scale features tied to local complex

topography and coastlines. In addition, although CORDEX underestimates temperature with a greater cold bias compared to the CMIP5 ensembles, it substantially improves both the magnitude and spatial extent of simulated summer monsoon precipitation. To examine whether this results from a more consistent simulation of the West African summer monsoon precipitation among RCMs or from cancellation of errors of opposite signs, we assess in the next section the ensemble spread.

4.1.2 Multimodel Ensemble Spread

The spatial patterns of the inter-model standard deviation (i.e. Figure 4.3a,b,c) highlights a good consistency among the models of the same ensemble in their simulation of the temperature field over the Gulf of Guinea (standard deviation less than 1°C).

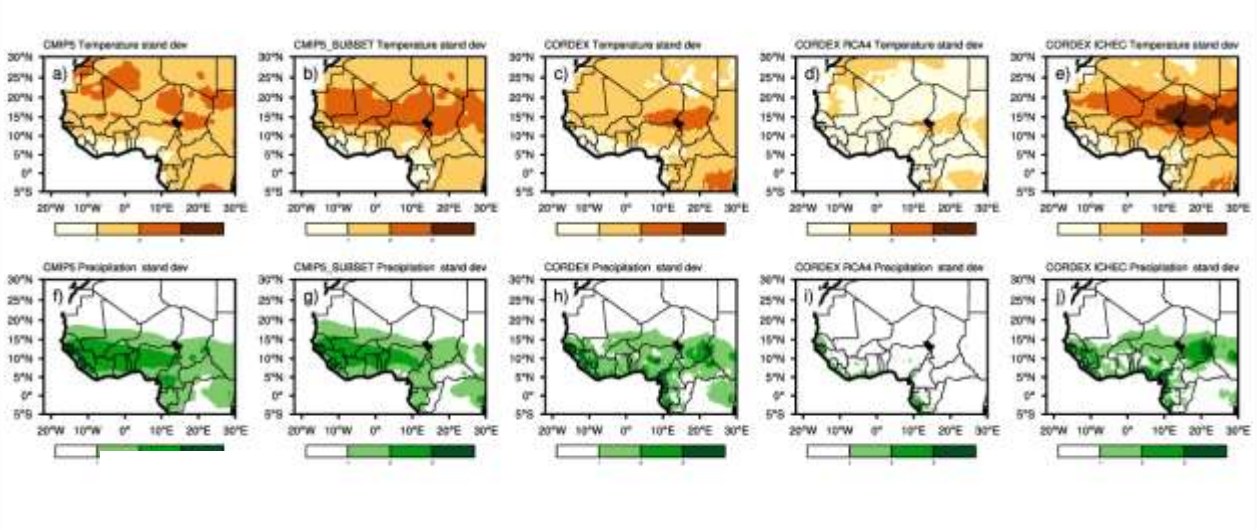

Figure 4.3: 1982-2005 JJAS mean temperature (a, c, e, g, i) and precipitation (b, d, f, h, j) ensemble standard deviation for respectively CMIP5, CMIP5_SUBSET, CORDEX, CORDEX RCA4 and CORDEX ICHEC-EC-EARTH. Units are degrees C for temperature and mm/day for precipitation

However, substantial differences are present over the Sahel and the Sahara desert across the various ensembles. For instance, CMIP5 exhibits a standard deviation of more than 2°C in the area of the SHL, part of northeastern Sahel and in some regions of the western Sahara desert. Conversely, CMIP5_SUBSET simulates a wide zonal band of more than 2°C standard deviations stretching from the west to the east and extended from 12N to 23N. For CORDEX, such a standard deviation occurs only over a small portion of the northeastern Sahel, indicating that the CORDEX RCMs provide a greater inter-model agreement in simulating surface air temperature.

To address the spread induced by the use of different lateral boundary forcings and the one due to the use of different RCMs for the same boundary forcing, two CORDEX subsets are introduced: the MME derived from the eight (8) RCA4 experiments driven by different GCMs (i.e. Figure 4.3d) and the MME of the four (4) CORDEX RCMs driven by the EC-EARTH GCM (i.e. Figure 4.3e). The RCA4 ensemble exhibits a standard deviation smaller than 1°C throughout the region, suggesting that the boundary forcing does not have a strong impact on the temperature simulation by a single model compared to its internal physics. This evidently also contributes to reducing the inter-model spread for the full CORDEX ensemble (Figure 4.3g). Conversely, the ensemble of RCMs driven by EC-EARTH shows greater standard deviations (up to more than 3°C) compared to all MMEs, especially over the Sahel, confirming that the internal model physics of the four RCMs produce substantially different simulations of temperature even with the use of the same boundary forcing.

For precipitation (i.e. Figure 4.3f,g,h), both CMIP5 and CMIP5_SUBSET show larger standard deviations (between 2 and 3 mm/day) along the ITCZ, relatively smaller one (between 1 and 2 mm/day) north and south of it and a good consistency among models above 20N. CORDEX generally produces lower standard deviations (less than 2 mm/day) over the whole West Africa

except over orographic zones. The separation of the CORDEX standard deviation into the contribution from different boundary conditions (Figure 4.3h) and that from different RCM physics (Figure 4.3j) indicates that, similar to what was found for temperature, the latter dominates, and in fact that different boundary forcing only provides a minor contribution to the RCM ensemble spread. Overall, Figure 4.3 clearly points to the prominent role of model physics in determining the intermodel spread in surface climate simulation, both for the GCM and the RCM ensembles.

To further assess and compare the performances of the MMEs, better highlight their ensemble spread and quantify the added value at the regional scale, we analyze in Figure 4.4 the box-plots for temperature and precipitation from the various ensembles over the different subregions of West Africa defined in Figure 3.1. Comparing the areal average of CRU, UDEL and the GCMs and RCMs experiments presented in Figure 5a, the results first confirm the cold bias simulated by the MMEs over West Africa in general and the relatively warm bias along the Sahel band in CMIP5. The cold bias is also seen in the RCA4 ensemble and the ensemble of the 4 RCMs driven by EC-EARTH. CORDEX produces the largest bias (also seen in the median) as a result of lower temperature values simulated by the RCMs in the presence of more realistic complex topography compared to CMIP5 GCMs. In addition, the interquartile range (IQR) is similar for all MMEs (except for the ensemble of RCA4, in which it is smaller) over the Sahel and West Africa but greater in CORDEX over the Gulf of Guinea, indicating a larger dispersion among most of the RCMs in their responses to the topographical forcing in this region. Furthermore, we note that for all subregions and all MMEs the bottom whisker, i.e. the colder model, is more extended than the top one, corresponding to the warmest model (except for the ensemble of RCA4 and the one built from the RCMs driven by EC-EARTH). Finally, CORDEX appears to

be negatively skewed compared to CMIP5 and CMIP5_SUBSET. As a consequence, a shift of the median occurs towards the upper quartile of the box with a broader range of simulated temperature values in the lower quartile. Consistent with Figure 4.3, this confirms the largest cold bias present in CORDEX but also the more consistent simulations of temperature values among the RCMs. As already mentioned, this is due to the large number of RCA4 simulations in the CORDEX ensemble, which are characterized by a small spread.

For precipitation, Figure 4.3b confirms the improved performance of CORDEX over CMIP5 and CMIP5_SUBSET in the Gulf of Guinea and the Sahel as discussed in Figure 4.3a. Over the whole West Africa, such an improvement is only achieved with respect to the CMIP5_SUBSET driving models. In fact, while the observations lie outside the IQR in the CMIP5_SUBSET, they are within the IQR in the CORDEX MMEs, except for the RCA4 ensemble in the Guinea Coast region. An interesting feature in Figure 4.4b is the presence of more extended upper whiskers and symmetrical boxes in all MMEs and subregions, except for RCA4 ensemble in the Sahel. This highlights a similar dispersion of models about their respective ensemble median and the existence in each MME of outliers that are substantially different than the rest of the ensemble. It should be emphasized that, consistently with Figure 4.3a, the CORDEX IQR is similar to that of CMIP5 and CMIP5_SUBSET in the Gulf of Guinea, but smaller in the Sahel. We finally note that the CORDEX subsets show results in line with the temperature box plots (i.e. Figure 4.4a) with regards to the spread induced by the use of different boundary conditions and RCMs.

Therefore, although the ensemble mean rainfall bias and the ensemble standard deviation are systematically lower in the CORDEX than the CMIP5 ensemble, the IQR is not necessarily smaller in CORDEX, suggesting that the spread induced by the model physics is greater in the RCMs than the GCMs. Overall, it is evident that the improved performance of CORDEX is more

likely a consequence of a better and more consistent simulation of monsoon precipitation than greater error cancellations, and depends more on the internal model physics than the driving boundary conditions.

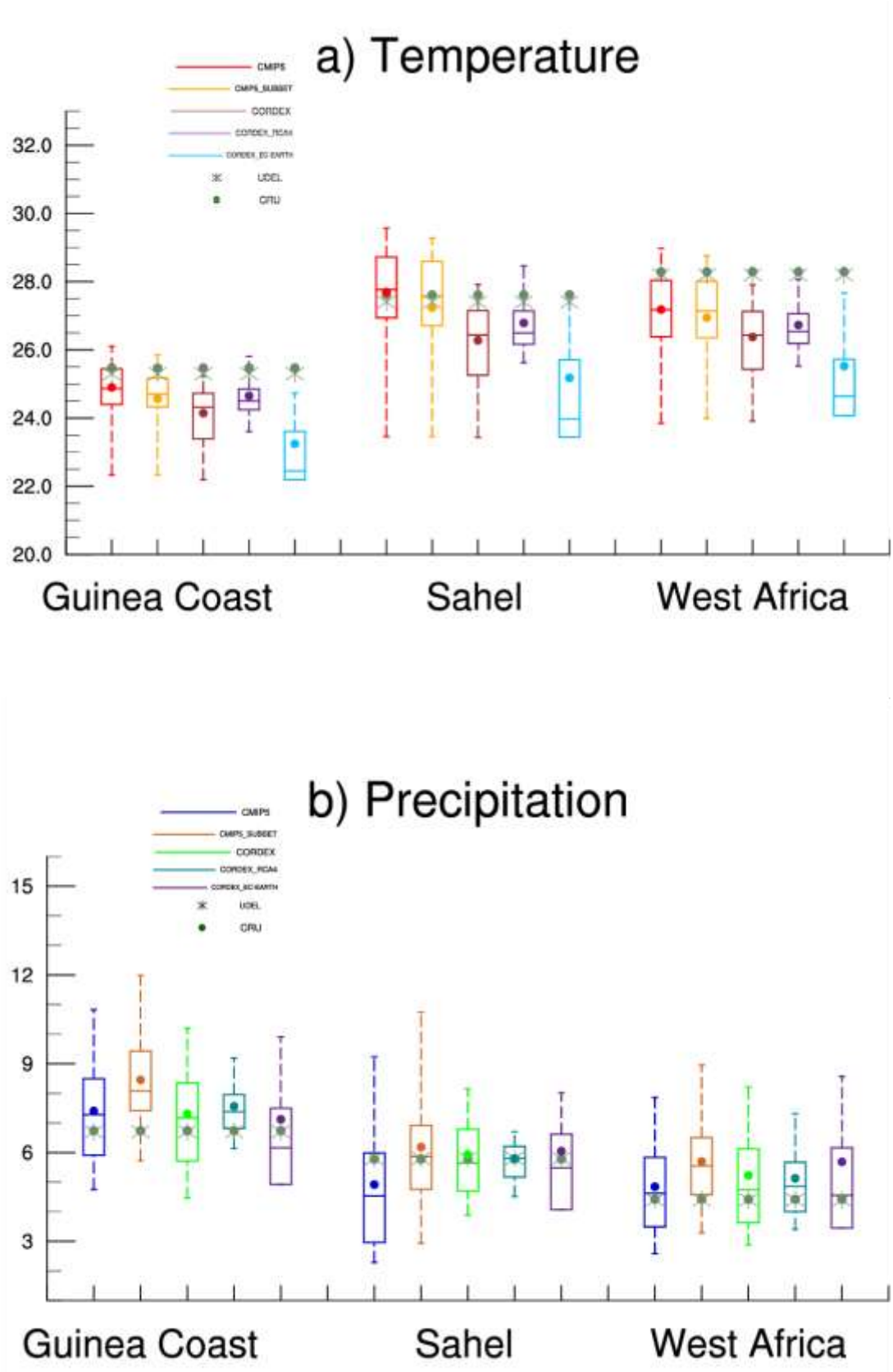

Figure 4.4 : Box plots for JJAS mean a) temperature and b) precipitation for CMIP5, CMIP5_SUBSET, CORDEX, CORDEX RCA4 and CORDEX ICHEC-EC-EARTH over the 3 key subregions of Gulf of Guinea, Sahel and West Africa. Units are degrees C for temperature and mm/day for precipitation

4.1.3 Spatio-Temporal Variability

The first three principal component loading patterns along with their time series generated from the REOF analysis applied to the temperature (Figures 4.5 and 4.6 respectively) and precipitation (Figures 4.7 and 4.8 respectively) fields are intercompared here for UDEL observations and the CMIP5, CMIP5_SUBSET and CORDEX MMEs. Hereafter, the loading patterns are referred to as REOFs and the time series as Principal Components (PCs).

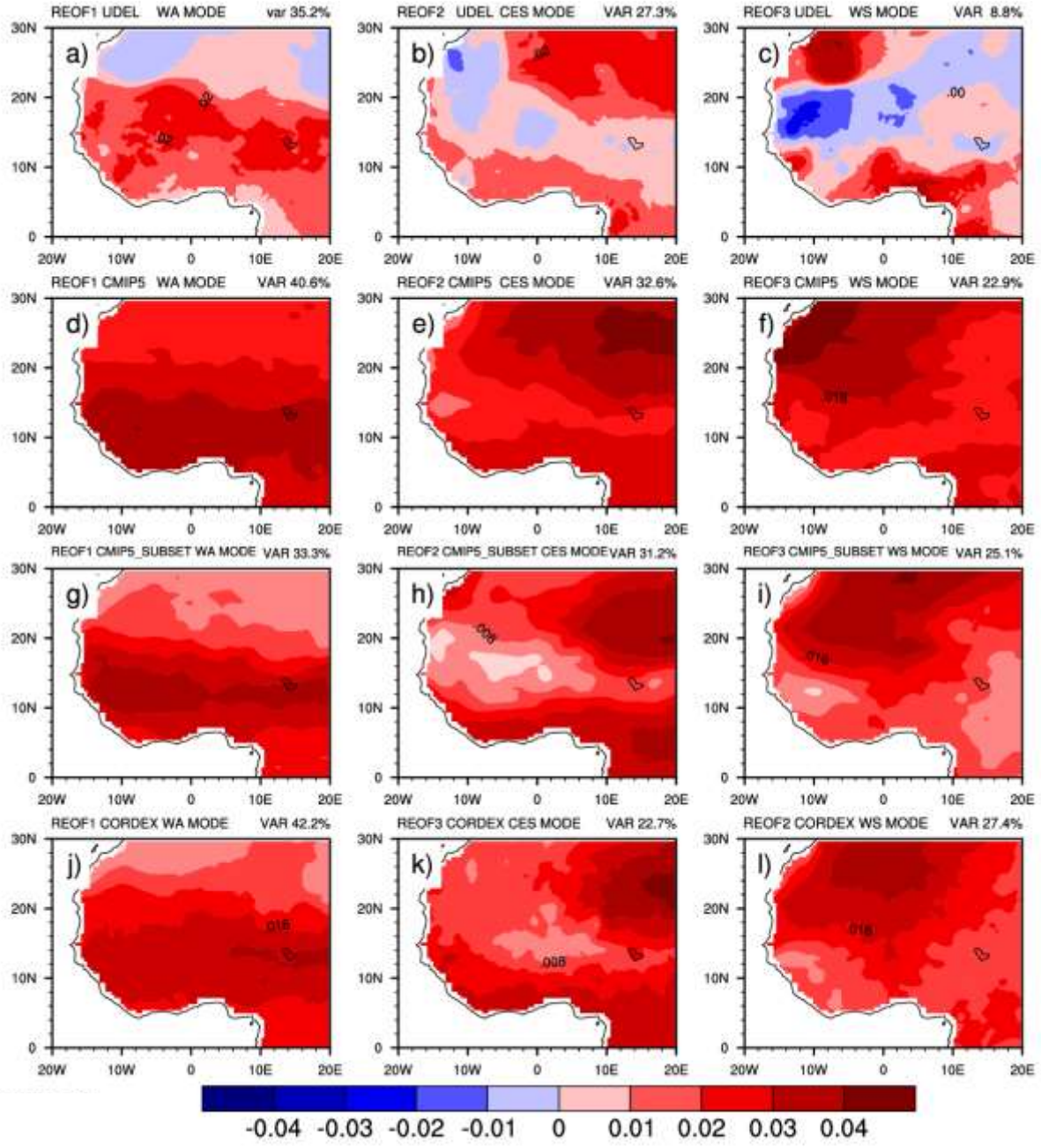

Figure 4.5: REOFs of the first three modes for JJAS mean temperature from UDEL (a, b, c), CMIP5 (d, e, f), CMIP5_SUBSET(g, h, i) and CORDEX (j, k, l). The percentage of variance explained by each mode is labeled

The first three observed REOFs explain more than 70% of the total variance, i.e. most of the spatio-temporal variability in summer surface temperature can be synthesized in three main modes of variability. The first mode accounts for 35% of the total variance and corresponds to a widespread surface warming (cooling) locked over West Africa during its positive (negative) phase, while surface temperature anomalies remain systematically weak in the northern Sahara. The second and third modes represent 27% and 9% of the total variance, respectively. They describe a tripole in surface temperature variability with anomalies that are positive along the coast of the Gulf of Guinea and parts of Sahara, and negative or weakly positive in the Sahel during their positive phase. This is reversed during their negative phase. The main spatial differences between these two modes are found north of ~10°N. During their positive phase, warm anomalies spread over the central and eastern Sahara for REOF2, while they are confined in the north-western regions for REOF3. Similarly, negative to weak positive anomalies are embedded in a northwest-southeast band for REOF2, and in a southwest-northeast band for REOF3. For simplicity, these three observed modes are referred as the West African mode (REOF1), the Central-Eastern Saharan mode (REOF2), and the Western Saharan mode (REOF3), respectively.

The MMEs (Figure 4.5d-l) roughly capture the spatial patterns of these modes of variability but with different variance and occurrences of the modes, and different magnitudes and signs of the anomalies. In fact, the spatial patterns explain nearly or more than 90% of the total variance, thus overestimating the corresponding observed values. This demonstrates that the CMIP5 GCMs struggle in simulating fine-scale patterns of surface temperature variability and that the

CORDEX RCMs do not substantially correct this bias. In addition, all the MMEs exhibit persistent warm biases throughout the domain and fail to reproduce the observed negative anomalies located over the western (REOF1 and REOF2) and eastern Sahara (REOF2) and the northern Sahel (REOF3). Furthermore, REOF2 and REOF3 are shifted in the CORDEX patterns compared to observations, suggesting that the CORDEX MME simulates the main modes of variability but fails to capture their frequency of occurrence. The Pattern Correlation Coefficient (P, i.e. Table 4.1) between the MMEs and UDEL modes is higher in CORDEX (P=0.86) compared to CMIP5 (P=0.73) and CMIP5_SUBSET (P=0.77) for REOF1 while for REOF2 and REOF3, they are close to each other.

Table 4.1: Temperature Rotated EOFs pattern correlation coefficients between UDEL and CMIP5, CMIP5_SUBSET and CORDEX. Bold values show the modelled REOFs to compare with each observed REOF, and the red color shows the MME that performs best. Note that to enable direct comparison, CORDEX REOF2 and REOF3 have been switched.

UDEL	CMIP5/CMIP5_SUBSET			CORDEX		
	REOF1	REOF2	REOF3	REOF1	REOF2	REOF3
REOF1	**0.73/0.77**	-0.52/-0.41	-0.37/-0.41	**0.85**	-0.27	-0.42
REOF2	-0.31/-0.48	**0.73/0.63**	-0.29/0.11	-0.41	**0.67**	0.11
REOF3	-0.00/-0.03	-0.02/0.26	**0.13/0.13**	-0.16	0.03	**0.09**

For the corresponding PC1 (i.e. Figure 4.6a), the observations show a strong temporal variability and there is no evidence that the observed West African mode exhibits a positive trend. However, the Central-Eastern (PC2; i.e. Figure 4.6b) and Western Saharan (PC3; i.e. Figure 4.6c) modes exhibit a slow positive trend prior to 1990, an abrupt rupture in the early 1990s followed by a rapid recovery and a strong positive trend persisting afterward. This is likely an indication towards an amplification of desert surface warming as discussed by Cook and Vizy (2016). The MMEs simulate lower variability than observed but also show an abrupt shift and rapid recovery, along with an emergent positive trend, highlighting the greenhouse gas forcing on the recent increase of temperature over West Africa. Finally, all the three MMEs generate comparable Pearson Correlation Coefficients (R; i.e. Table 4.2) which are higher in PC2 (more than 0.6) and PC3 (more than 0.7) compared to PC1 (around 0.2).

Table 4.2: Temperature Principal Component Pearson correlation coefficients between UDEL and CMIP5, CMIP5_SUBSET and CORDEX. Bold values show the modelled REOFs to compare with each observed REOF, and the red color shows the MME that performs best. Note that to enable direct comparison, CORDEX PC2 and PC3 have been switched

UDEL	CMIP5/CMIP5_SUBSET			CORDEX		
	PC1	PC2	PC3	PC1	PC2	PC3
PC1	**0.28/0.23**	0.26/0.24	0.27/0.21	**0.24**	0.24	0.22
PC2	0.68/0.62	**0.68/0.64**	0.69/0.64	0.58	**0.60**	0.60
PC3	0.74/0.74	0.75/0.77	**0.75/0.76**	0.79	0.78	**0.79**

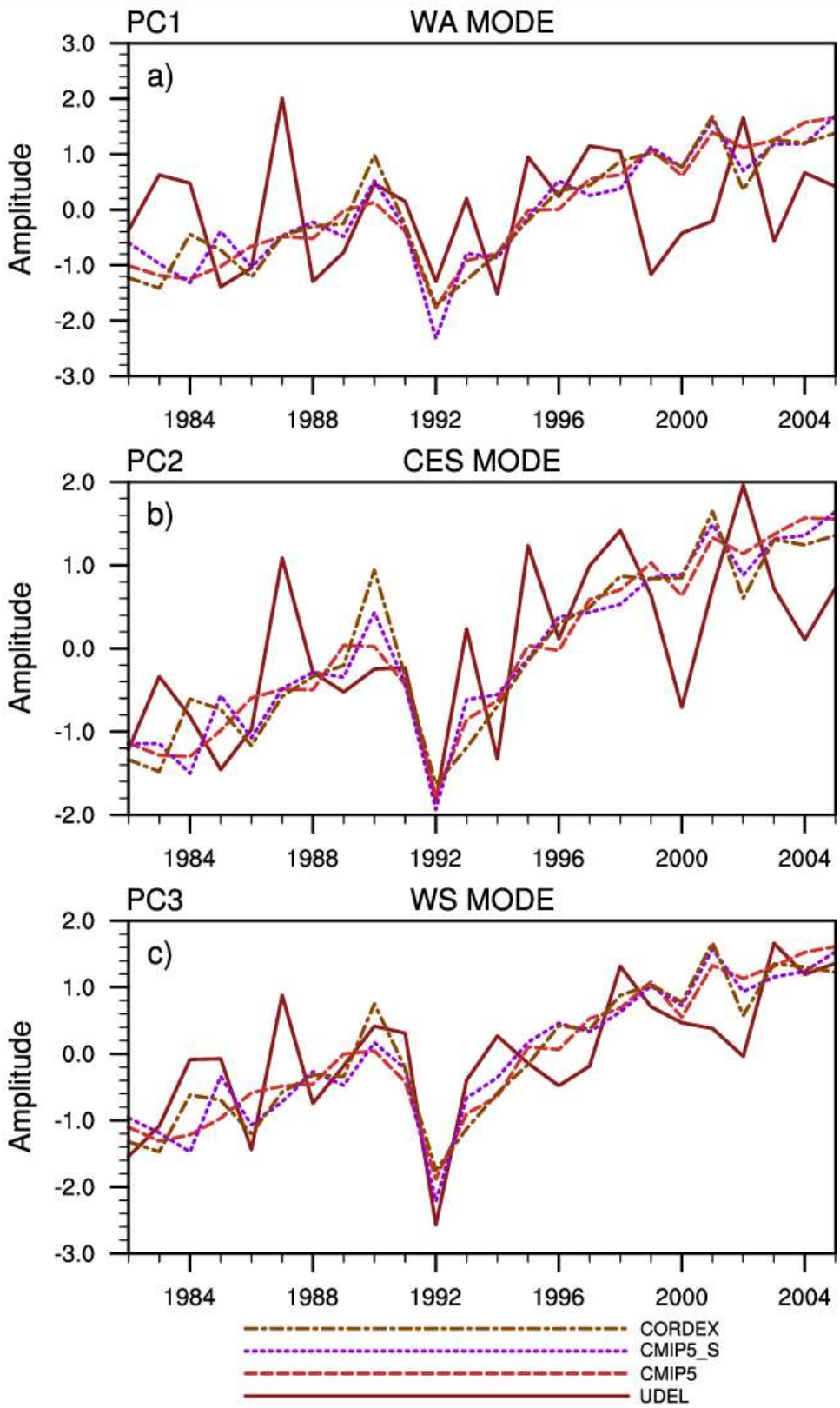

Figure 4.6 : The corresponding PCs of the first three modes of temperature REOFs for UDEL, CMIP5, CMIP5 SUBSET and CORDEX

Similar to the temperature REOF spatial patterns, the observed precipitation variability is characterized by the West African mode (i.e. REOF1; Figure 4.7a), the Central-Eastern Saharan mode (i.e. REOF2, Figure 4.7b), and the Western Saharan mode (i.e. REOF3, Figure 4.7c). The West African mode is mainly associated with widespread increase (decrease) of precipitation over West Africa during its positive (negative) phase with a weak decrease (increase) along the Gulf of Guinea. In addition, the Central-Eastern Sahara mode is characterized during its positive (negative) phase by dry (wet) anomalies along the Gulf of Guinea and wet (dry) anomalies over the Eastern Sahara..

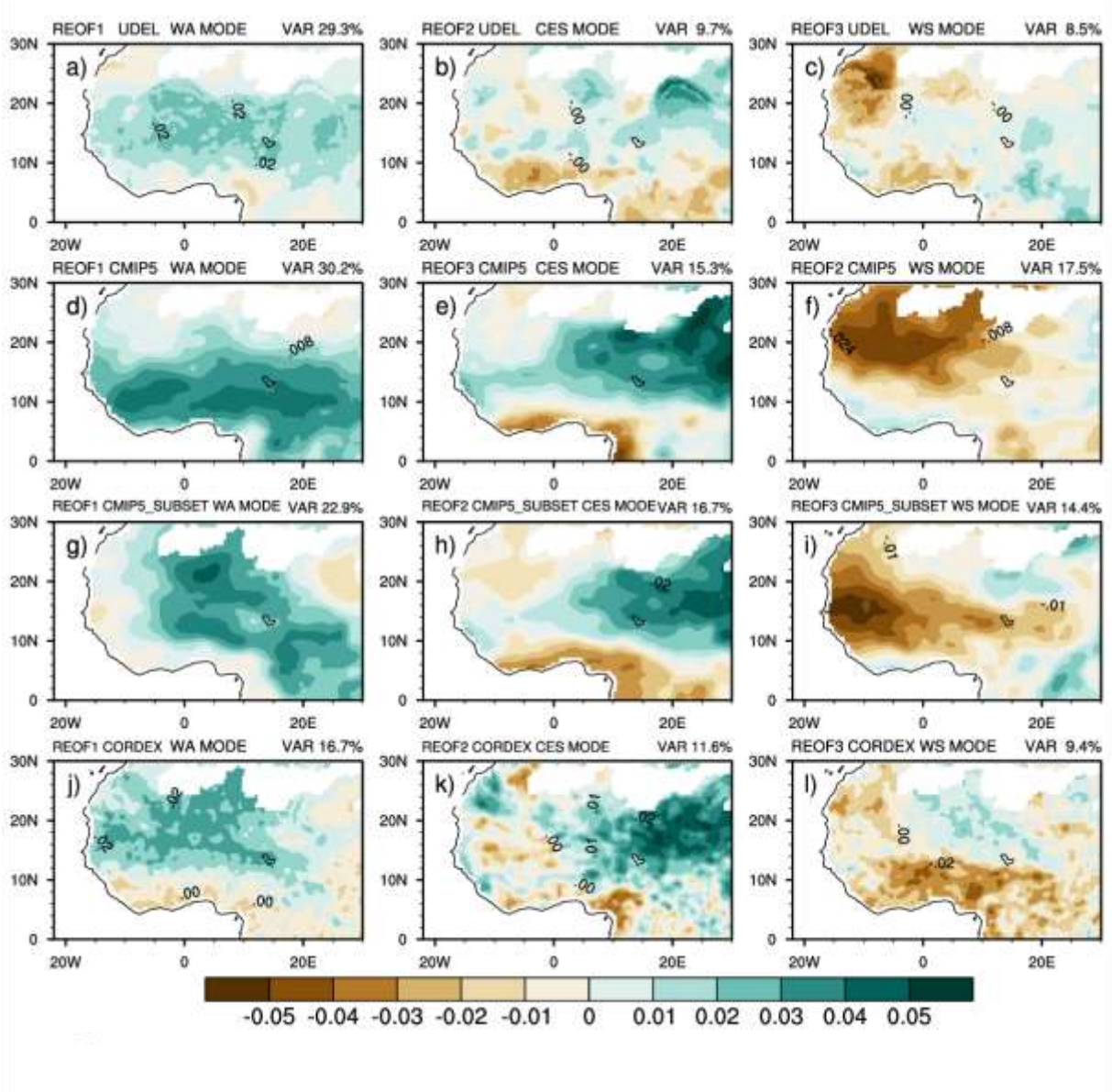

Figure 4.7 : REOFs of the first three modes for JJAS mean precipitation from UDEL (a, b, c), CMIP5 (d, e, f), CMIP5_SUBSET(g, h, i) and CORDEX (j, k, l). The percentage of variance explained by each mode is labeled

Finally, the Western Sahara mode describes a tripole in rainfall variability with strong negative (positive) anomalies along the Gulf of Guinea and western Sahara and weak positive (negative) anomalies in few areas of the Sahel during its positive phase. Altogether, these explain only 47.5% of the total variance.

Both the CMIP5_SUBSET and CORDEX MMEs roughly reproduce the different modes of precipitation variability over the region. However, CMIP5 misses the signal over the Gulf of Guinea for the West African mode, switches the Central-Eastern and the Sahara modes and reverses their signs. This suggests that CORDEX captures better the occurrence of the different modes of variability. To enable a direct comparison, the CMIP5 last two modes are switched and their signs reversed. In this case, both the CMIP5 and CMIP5_SUBSET simulate larger positive anomalies in each mode compared to the observations during their positive phase, thus exhibiting a substantial wet bias. CORDEX shows magnitudes and spatial distributions more in line with observations. The explained variance by CMIP5 is around 63% of the total variance, that of CMIP5_SUBSET 54% while for CORDEX it does not exceed 38%. This indicates that CORDEX simulates more precipitation fine-scale patterns compared to both CMIP5 and CMIP5_SUBSET. Spatial correlation coefficients between the observed and simulated West African mode are 0.36 for CMIP5, 0.31 for CMIP5_SUBSET and 0.41 for CORDEX, highlighting the improvement achieved with the higher resolution RCM MME. However, for the Central-Eastern and Western Sahara modes, CORDEX mostly follows CMIP5_SUBSET with lower correlation coefficients (Table 4.3).

Table 4.3: Precipitation Rotated EOFs pattern correlation coefficients between UDEL and CMIP5, CMIP5_SUBSET and CORDEX. Bold values show the modelled REOFs to compare with each observed REOF, and the red color show the MME that performs best. Note that to enable direct comparison, CMIP5 REOF2 and REOF3 have been switched and multiplied by (-1)

UDEL	CMIP5/CMIP5_SUBSET			CORDEX		
	REOF1	REOF2	REOF3	REOF1	REOF2	REOF3
REOF1	**0.36/0.31**	0.54/0.57	-0.08/-0.34	**0.41**	0.35	0.20
REOF2	-0.32/-0.05	**0.62**/**0.59**	-0.12/-0.01	0.29	**0.50**	0.36
REOF3	0.36/0.28	0.32/0.33	**0.43**/**0.31**	-0.16	0.25	**0.12**

Analysis of the observed PCs (i.e. Figure 4.8) reveals strong temporal variability in all modes with an evident and slow increasing trend in West African mode. This latter illustrates the precipitation recovery that occurred in recent decades over West Africa (Mohino *et al,.* 2011; Ibrahim *et al.,* 2014; Sylla *et al.*, 2016a). The MMEs simulate similar variability than observed for all modes but with significantly low correlation coefficient (Table 4.4). This can be expected in view of the fact that, as mentioned, the models do not use any assimilation of observed data for the simulated period. However, they produce a slow positive trend in the West African mode, perhaps suggesting that anthropogenic aerosols and greenhouse gases might have played a significant role in the precipitation recovery over West Africa (Ackerley *et al.,* 2011; Dong *et al.,* 2014)

Table 4.4: Precipitation Principal Component correlation coefficients between UDEL and CMIP5, CMIP5_SUBSET and CORDEX. Bold values show the modelled REOFs to compare with each observed REOF, and the red colour show the MME that performs best. Note that to enable direct comparison, CMIP5 PC2 and PC3 have been switched and multiplied by (-1)

UDEL	CMIP5/CMIP5_SUBSET			CORDEX		
	PC1	PC2	PC3	PC1	PC2	PC3
PC1	**0.21/-0.04**	0.46/0.14	0.06/-0.33	**-0.15**	0.05	-0.21
PC2	0.30/0.38	**0.31/0.30**	-0.04/-0.21	0.32	**0.30**	-0.39
PC3	-0.19/-0.33	0.13/-0.11	**0.12/0.08**	-0.26	-0.20	**0.25**

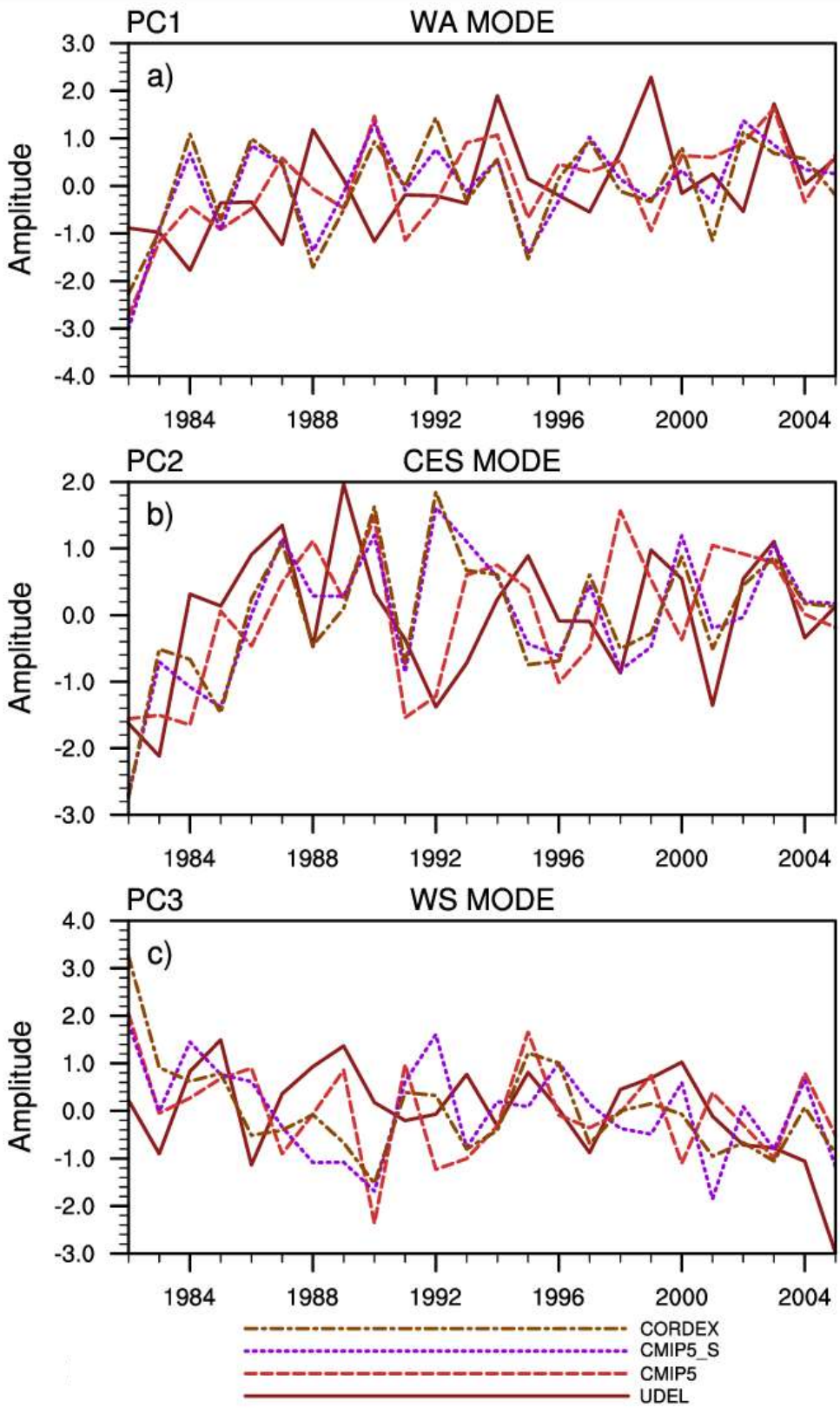

Figure 4.8 : The corresponding PCs of the first three modes of precipitation REOFs for UDEL, CMIP5, CMIP5_SUBSET and CORDEX

4.2 Bayesian assessment of CMIP5 and CORDEX simulations of historical summer precipitation variabilities over Sahel and Guinean Coast

4.2.1 Bayesian assessment of CMIP5 and CORDEX simulations of historical summer precipitation variabilities over Sahel

The joint distribution of the population mean and variance derived from Monte Carlo Sample over the Sahel region for precipitation are shown in Figure 4.9. The UDEL distribution, on top left is taken as reference with a mean of 5.80 mm/day and variance of 0.81.CMIP5 distribution top right is off compared to UDEL in terms of simulating the mean value. The CORDEX shows good approximation to the mean of UDEL whereas CMIP5_subset and CMIP5 approximate more closely the variance.

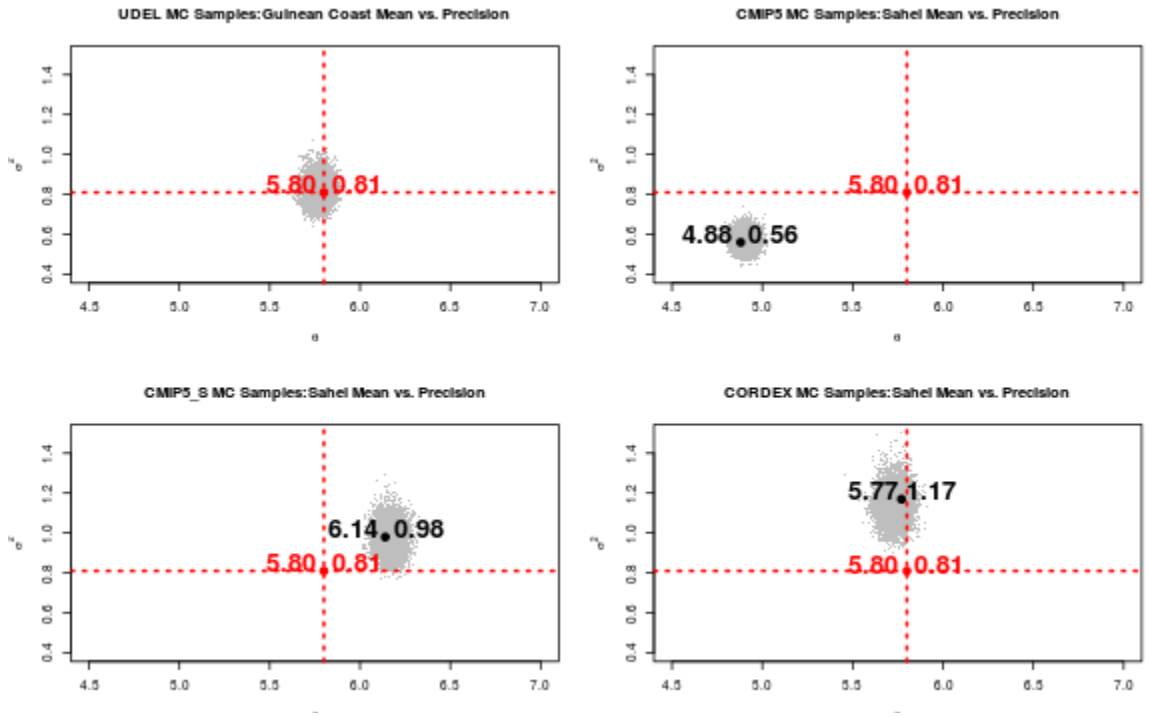

Figure 4.9: Monte Carlo sampling from the joint distribution of the population mean (θ) and the variance (σ^2) over the Sahel domain for UDEL a) and for CMIP5 b), CMIP5_SUBSET c) and CORDEX c) . The values in black show the mean value of the population mean (left side) and the population variance (left side). The mean value of θ and σ^2 for UDEL and are indicated in red. Precipitation given in mm/day.

Figure 4.10 shows the marginal distribution of mean from Monte Carlo sampling. The red line shows the mean value of the marginal distribution for UDEL and the blue line indicate a 95% quantile-based posterior bound. The posterior bounds of CMIP5 and CMIP5 Subset do not contain the mean value of UDEL. CORDEX shows a closer overlap with UDEL data meaning that CORDEX is approximating the mean more realistically over the Sahel .

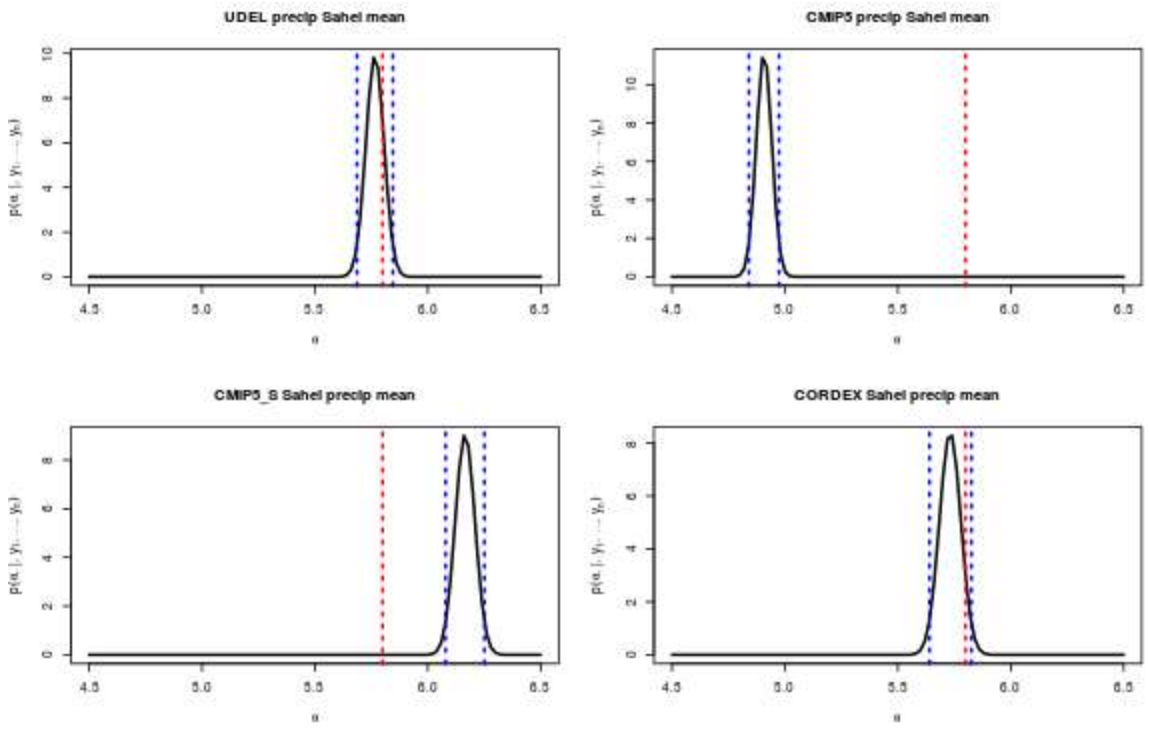

Figure 4.10: Monte Carlo samples from the marginal distribution of θ for UDEL a), CMIP5 b), CMIP5_S c) and CORDEX d) over the Sahel region. The blue vertical line give a 95% quantile-based posterior bound. In red, the mean value of UDEL posterior marginal distribution precipitation in mm/day.

The marginal distribution of UDEL variance is approximate more closely by CMIP5_subset as shown in Figure 4.11. However CMIP5 and CORDEX posterior bounds do not contain the mean value of UDEL variance.

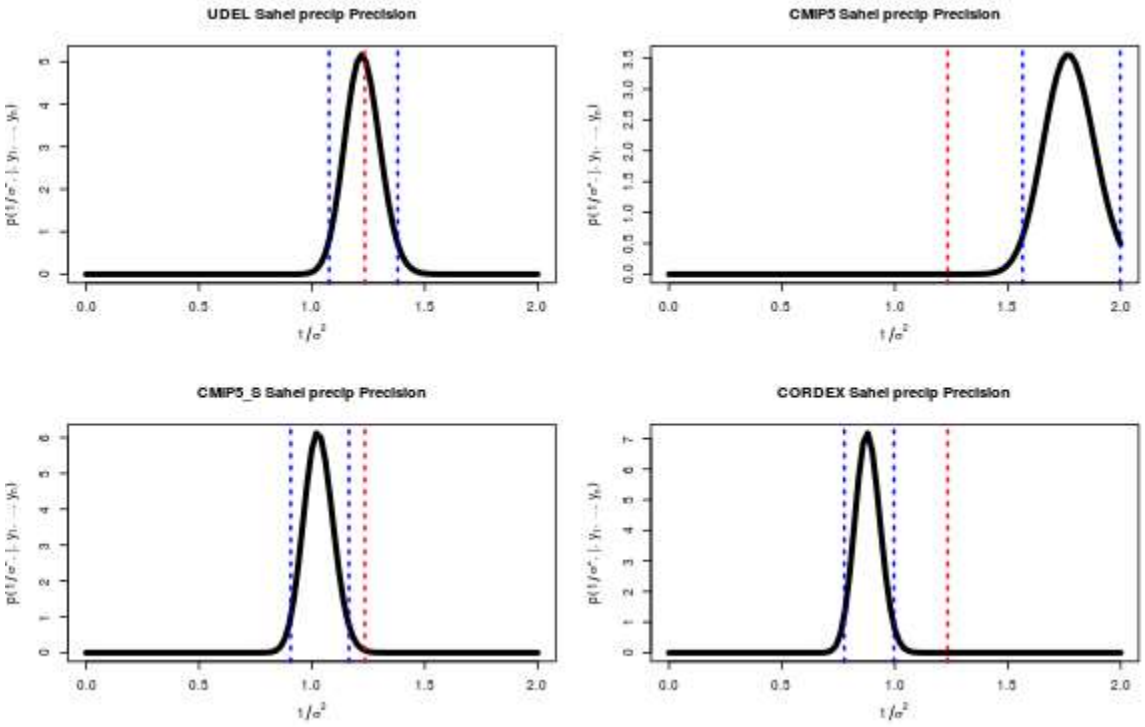

Figure 4.11: The same figure as Figure 4.10, but for the precision

4.2.2 Bayesian assessment of CMIP5 and CORDEX simulations of historical summer precipitation variabilities over Guinean Coast

Over Guinean Coast Figure 4.12 is showing Monte Carlo samples from the joint distribution of the population mean and variance from UDEL, CMIP5, CMIP5_Subset and CORDEX precipitation. CORDEX seems to approximate more realistically the mean and the variance closer to the UDEL ones.

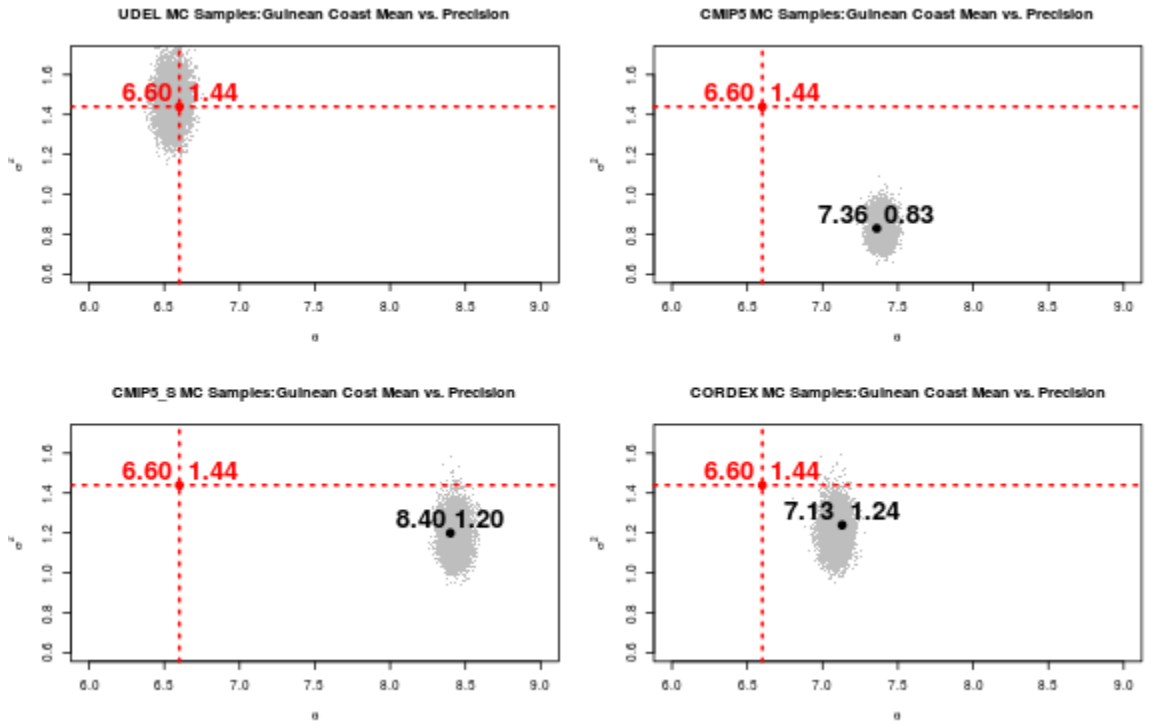

Figure 4.12 : Monte Carlo sampling from the joint distribution of the population mean (θ) and the variance (σ^2) over the Guinean Coast for UDEL a) and for CMIP5 b), CMIP5_SUBSET c) and CORDEX c). The values in black show the mean value of the population mean (left side) and the population variance (left side). The mean value of θ and σ^2 for UDEL and are indicated in red. Precipitation given in mm/day.

Figure 4.13 still illustrate that over the Guinean Coast with UDEL as a reference there is a considerable bias reduction with CORDEX simulation of precipitation compare to CMIP5_subset and CMIP5 even though CORDEX 95% quantile-based posterior bound fails to overlap with UDEL mean.

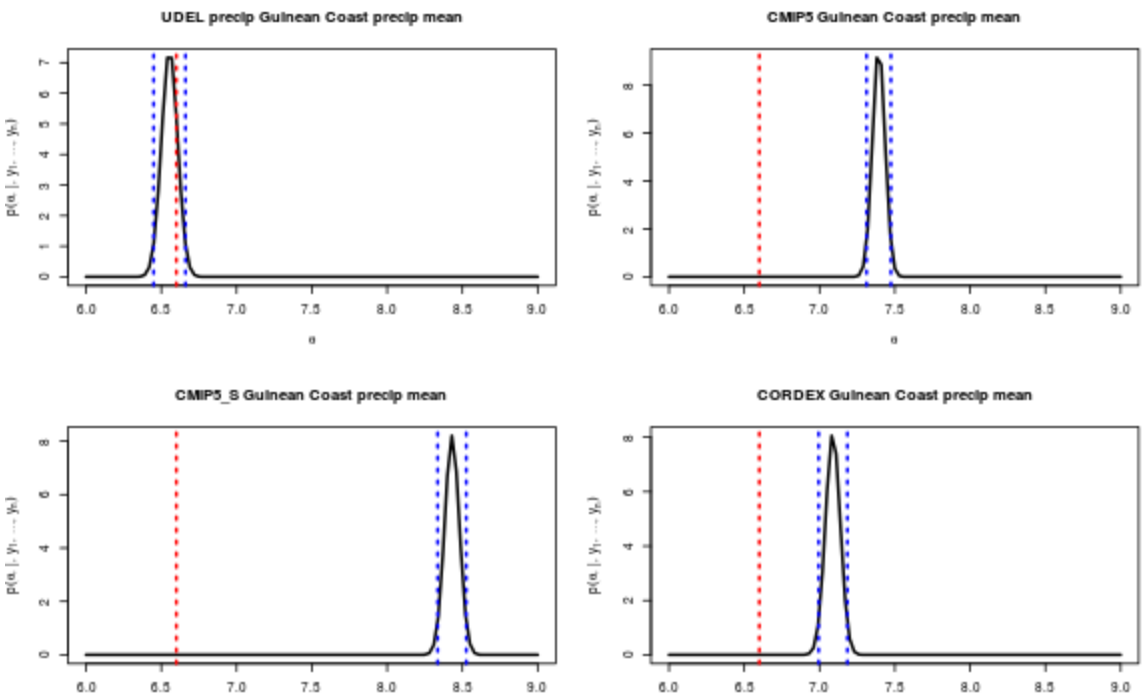

Figure 4.13: CMIP5 b), CMIP5_S c) and CORDEX d) over the Guinean Coast region. The blue vertical line give a 95% quantile-based posterior bound. In red, the mean value of UDEL posterior marginal distribution precipitation in mm/day

The marginal distribution of UDEL precipitation variance (Figure 4.14) is approximated more closely by CORDEX and CMIP5_subset. The added value from downscaling precipitation was not that much over Guinean coast in terms of variance.

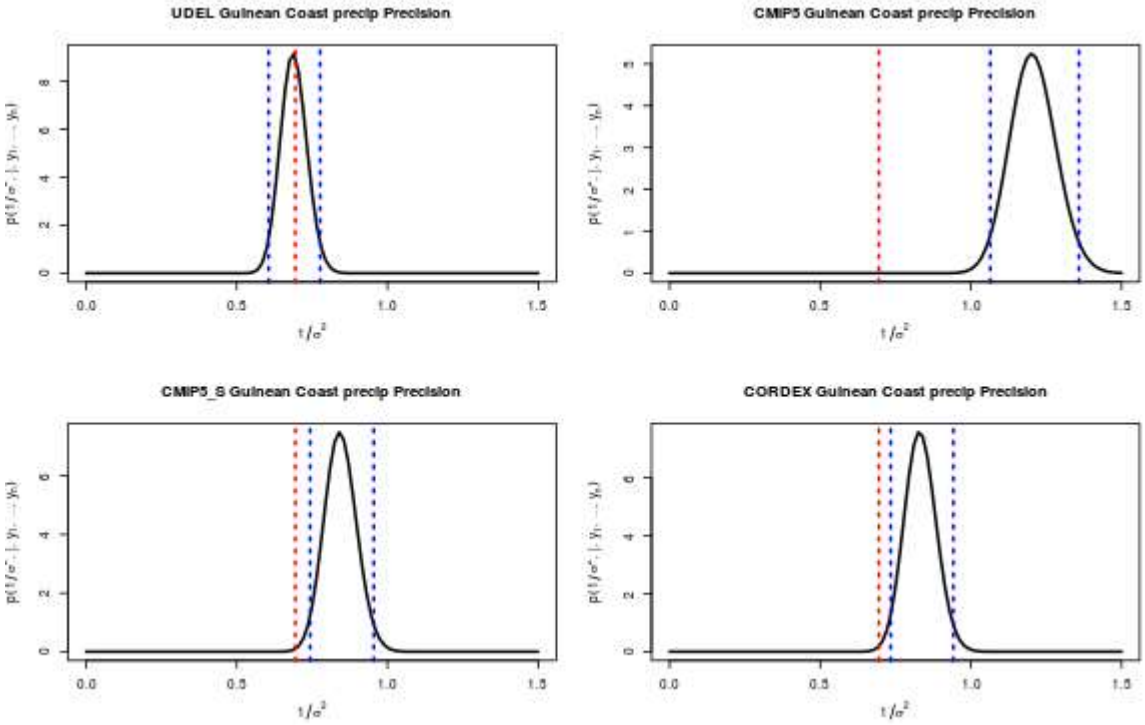

Figure 4.14 : The same figure as Figure 4.13, but for the precision

4.3 Temperature and precipitation change over West Africa: spatial and Bayesian analysis of CMIP5 and CORDEX MMEs simulation

4.3.1 Temperature and precipitation change over West Africa: spatial analysis of CMIP5 and CORDEX MMEs simulation

Temperature projection over West Africa for the late 21st century (2070-2099) from CMIP5 and CORDEX under RCP45 and RCP85 scenarios (Figure 4.15) range between 2^{o}C and 6^{o}C above the 1976-2005 baseline. For both scenarios the seasonal (JJAS) multi model mean temperature change follows a pattern of larger change in magnitude in northern part and mainly over land. Over the whole West African domain at least 80% of the models contributing to the different multi model ensemble (CMIP5, CMIP5_Subset and CORDEX) agreed on sign change. The warmest part is located over the Sahara (above 16^{o} latitude) under the RCP85 scenario(Figure 4.15,b),d),f)). This warning trend is consistent with the last IPCC report (IPCC,2014).

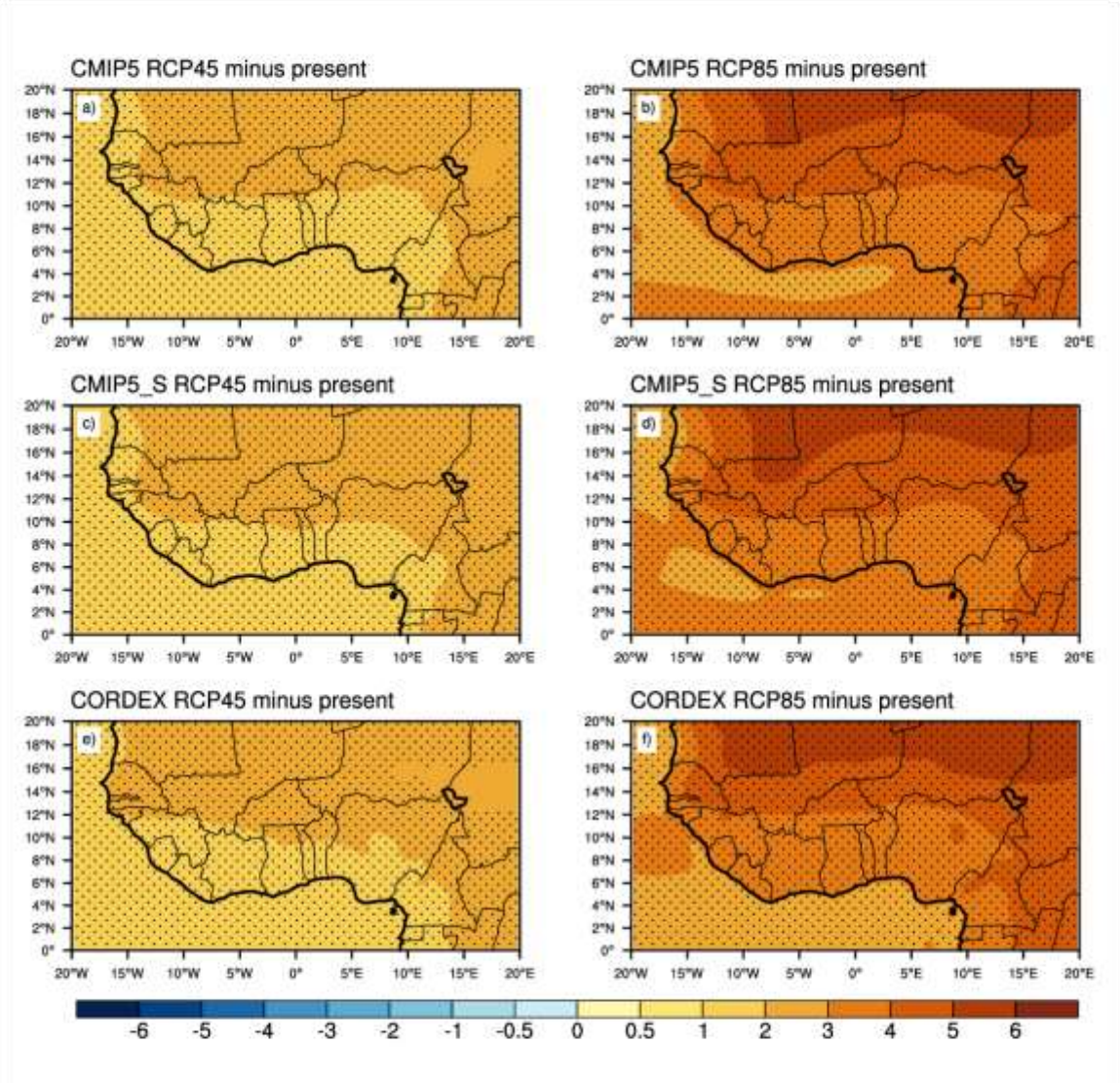

Figure 4.15: Multi-model mean of 2070-2099 seasonal average (JJAS) temperature change relative to the period of 1976-2005 for RCP45 (left panel) and RCP85 (right panel) for CMIP5 , CMIP5 subset and CORDEX. Stippling denote regions where 80 % percent of the model agree on change sign.

For precipitation, The last IPCC report highlight the inability of CMIP3 and CMIP5 to resolve the convective rainfall over West Africa (Roehrig *et al.,* 2013) and therefore the precipitation projection over West Africa had a low medium confidence (IPCC,2014). Through the CORDEX program (Giorgi *et al.,* 2009, Jones *et al.,* 2011) a relatively large number of Regional Climate Model simulation were made available over West Africa and it will give more robustness of the precipitation projection change over the region (IPCC,2014). Precipitation projection for the period 2071-2099 relative to 1976-2005 under the two scenarios for CMIP5, CMIP5_Subset and CORDEX multi model ensemble are shown in Figure 4.16(a)-(f). Figure 4.16 (e)-(f) shows an increasing trend of the rainfall up to 60 % over the Gulf of Guinea and eastern Sahel. There is a decreasing trend up to 40 % over Western Sahel (Senegal and Mauritania). And mainly over those regions at least 80 % of models contributing to the ensemble mean agreed on sign change. For the two scenarios downscaling was able to reverse the sign of change over the southern part of the Atlantic Ocean. Some part of Burkina Faso, Nigeria and Mali remains uncertain in terms of precipitation change and the downscaling didn't improved much this configuration.

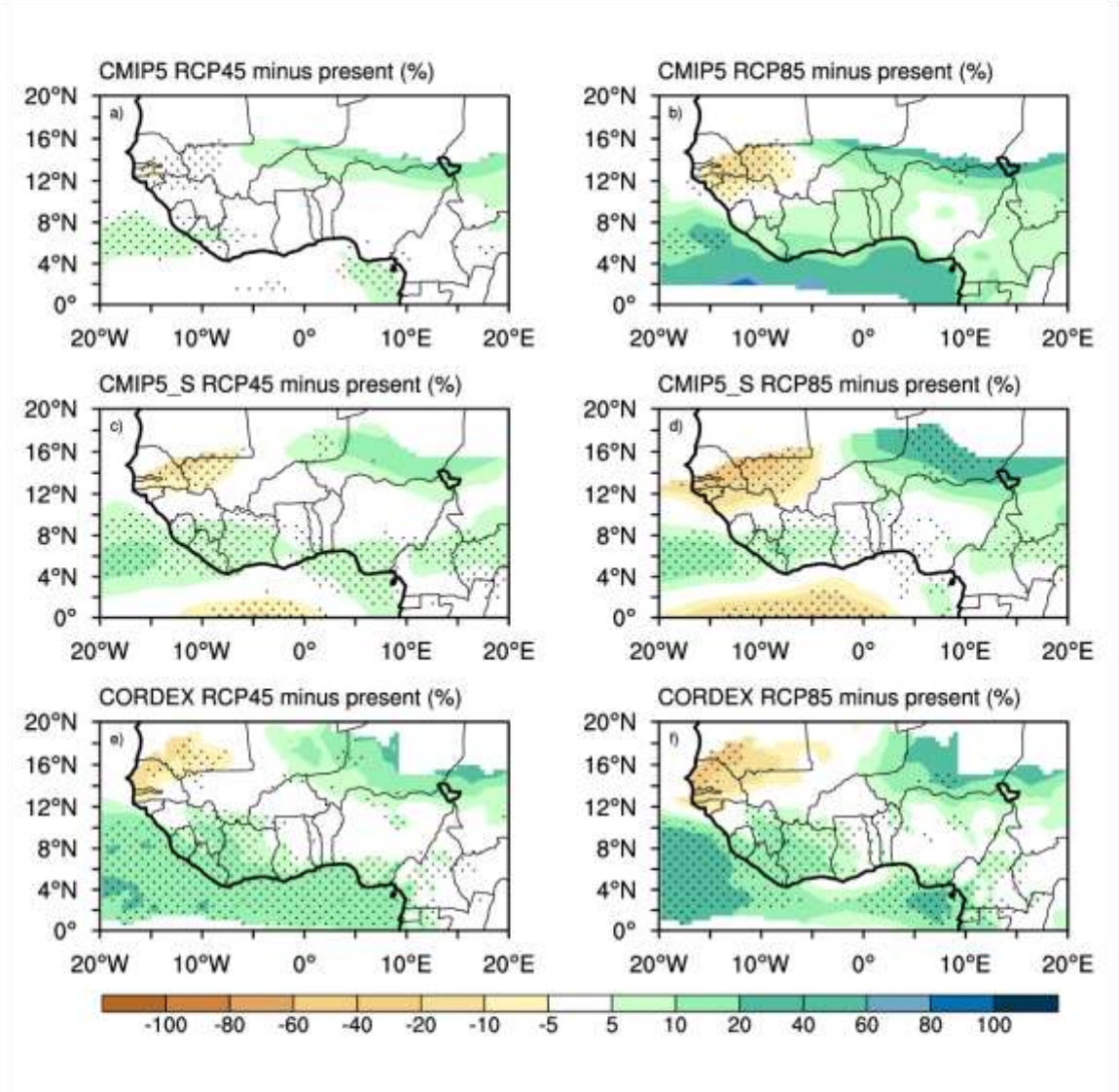

Figure 4.16: Multi-model mean of 2070-2099 seasonal average (JJAS) precipitation change relative to the period of 1976-2005 for RCP45 (left panel) and RCP85 (right panel) for CMIP5 , CMIP5 subset and CORDEX. Stippling denote regions where 80 % percent of the model agree on change sign

Figure 4.17 (a)-(f) adopted from Sylla *et al.* (2015), shows multi-model ensemble from CMIP5, CMIP5_subset and CORDEX long-term time series of seasonal (June-September) mean temperature anomalies with the range of possible values over the Sahel and the Gulf of Guinea during the historical (1976-2005) and the future (2006-2100) periods and for both RCP8.5 and RCP4.5 (Moss *et al.*, 2010). The reference period used to calculate seasonal mean anomalies was 1976-2005. Over the Sahel and the Gulf of Guinea, The three CMIP5, CMIP5_subset and CORDEX time series show a significant warming since 1996 and this warming will be amplified in future climate (2006-2100) under the high level Green House Gases (GHG) forcing scenario (RCP8.5) and a mid-level one (RCP4.5). The mid-level GHG forcing scenario produces lesser warming (less than 2^{o}C over the Sahel and Gulf of Guinea regions and for the three multi model ensemble) while the high level forcing leads to a greater warming (4^{o}C over the Guinean Coast and 5^{o}C over the Sahel). Therefore, temperature increases over the region with the new set of data made available from CORDEX program will range by the end of 21st Century from 1.5 ^{o}C to 5.0 ^{o}C, with the Sahel experiencing more warming.

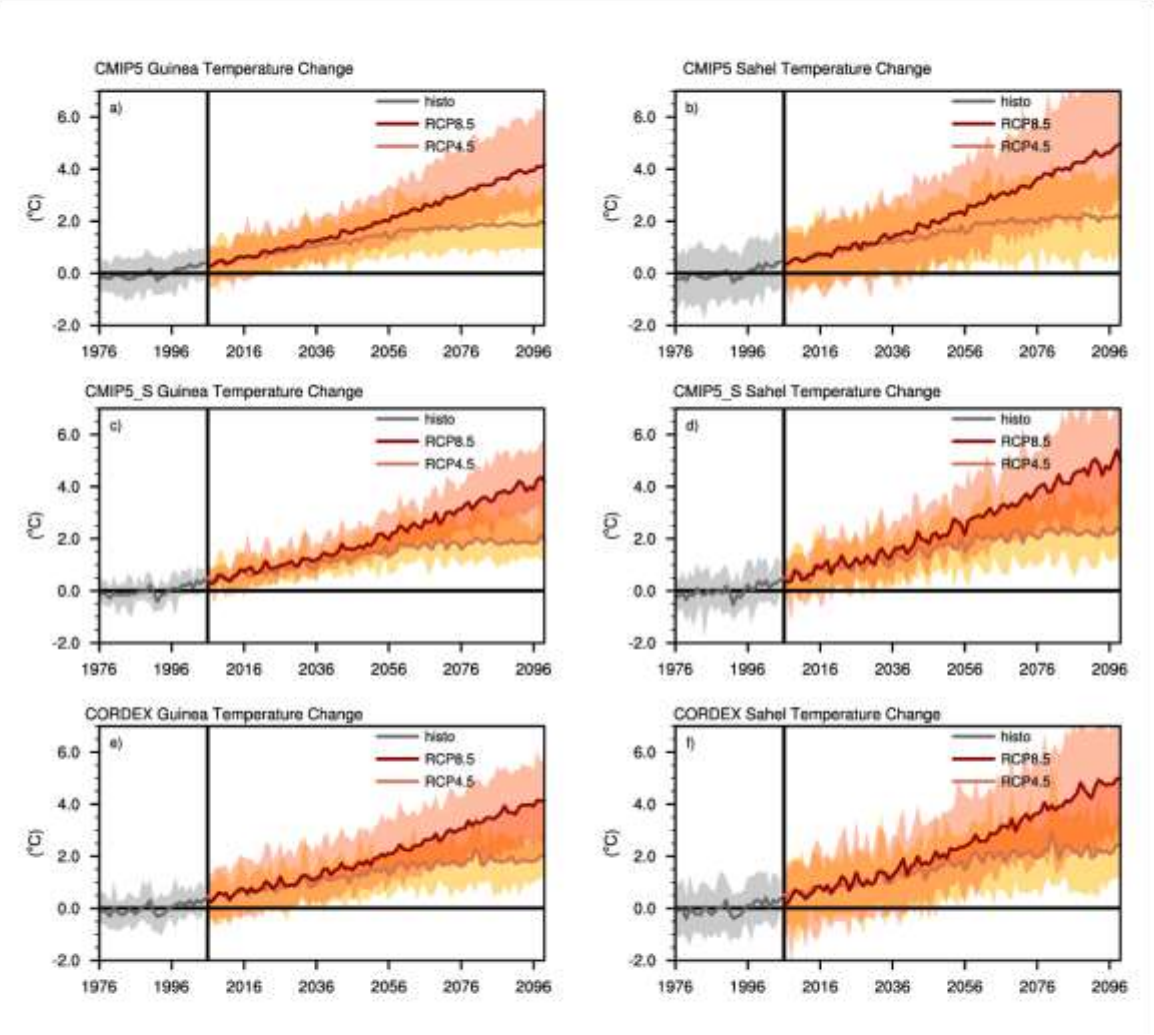

Figure 4.17: Long-term time series (1976-2099) of mean temperature (left panels) anomalies for the Guinean Coast (left panels) and the Sahel (right panels) and for both RCP4.5 and RCP8.5 based on multimodel of CMIP5 , CMIP5 Subset and CORDEX simulations. The anomalies are calculated with respect to the seasonal mean of the period 1976-2005. The shaded areas denote ensemble maxima and minima. Adopted from Sylla *et al. (*2015)

For the mean precipitation in Fig19 (a)-(f), the anomalies from the CMIP5 and CMIP5_subset multi model time series show a lesser evident trend but increased variability with larger amplitudes oscillating between -10% and 10% while the CORDEX multi model time series show a clear increasing trend up to 10 % for the two scenarios over the Sahel and the Gulf of Guinea. But the precipitation changes still spans both negative and positive values (between -40% to 80%). This means that uncertainties still remain in regional precipitation climate change projections consistent with IPCC (2014). As the scenario forcing increases (i.e. as the time frame increase), the range of uncertainty gradually increases and the Sahel shows the largest range. This suggests that the various RCMs produce substantial different responses to a same forcing and probably because of the models differences in the way they simulate the interactions of deep convection with the West African Monsoon features (Roehrig *et al.,* 2013; Sylla *et al*., 2013a).

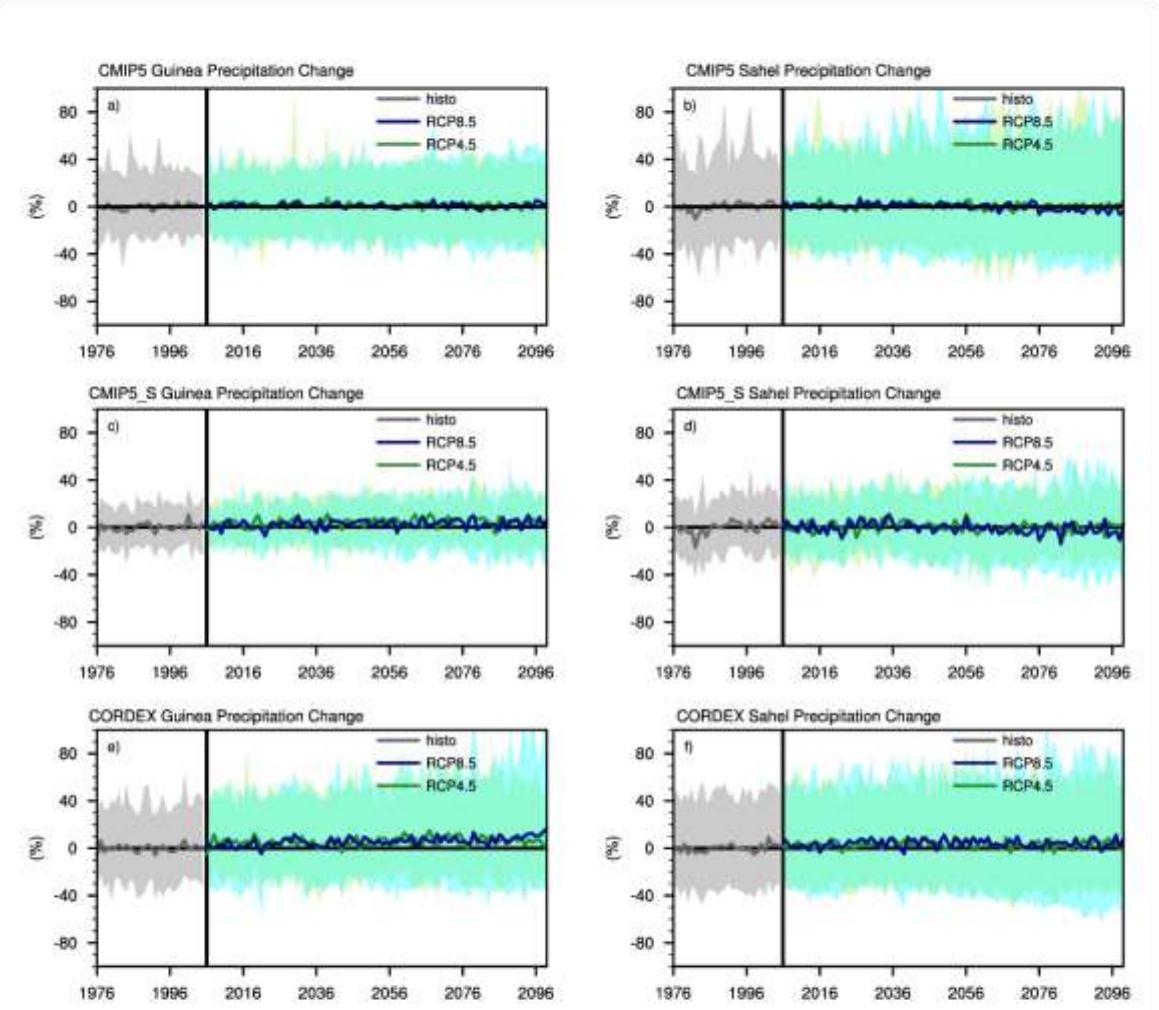

Figure 4.18 : Long-term time series (1976-2099) of mean precipitation (left panels) anomalies for the Guinean Coast (left panels) and the Sahel (right panels) and for both RCP4.5 and RCP8.5 based on multimodel of CMIP5 , CMIP5 Subset and CORDEX simulations. The anomalies are calculated with respect to the seasonal mean of the period 1976-2005. The shaded areas denote ensemble maxima and minima. Adopted from Sylla *et al.* (2015)

4.3.2 Temperature and precipitation change over West Africa: Bayesian analysis of CMIP5 and CORDEX MMEs simulation

Figure 4.19 shows the posterior distribution of temperature change $\Delta T = \nu - \mu$ over the Guinean Coast under RCP45 and RCP85 for JJAS season. Individual model response is plotted along the x axis to assess the measure of convergence for each model and find out those behaving like outliers and those reinforcing each other by projecting the same temperature change. Models having small bias receive large weight and the PDF is drawn where the model perform well with the two criteria (bias and convergence). The shape of the PDF may be unimodal (where models agree and outliers are down weighted due to large bias) or multimodal (where models disagree and cannot be discounted based on theirs bias). CMIP5_S models under RCP85 has a lot of uncertainties showing more bias and less agreement among models but the CORDEX seems to dramatically reduced those uncertainties.

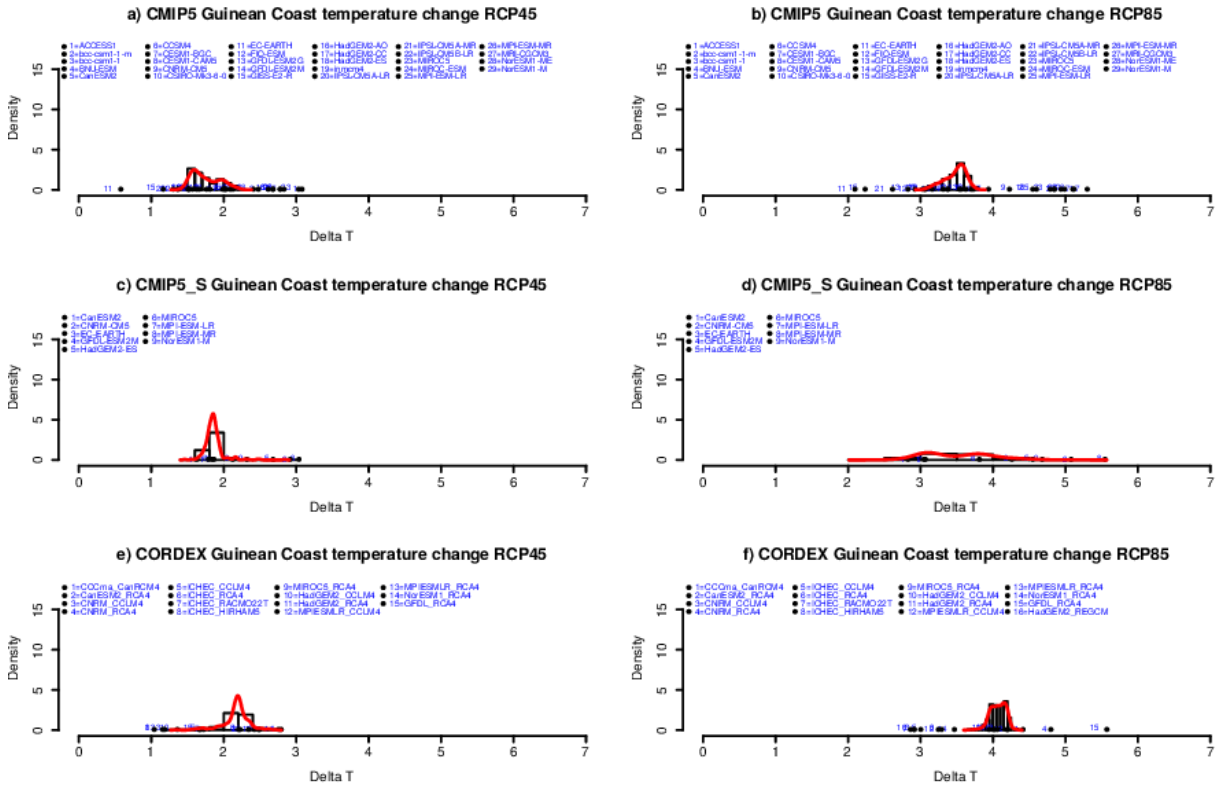

Figure 4.19: Posterior distribution of over the Guinean coast for CMIP5, CMIP5_subset and CORDEX under the RCP45 (a,c,e) and RCP85(b,d,f) scenario for JJAS season. The points along the base of the densities mark the model (GCM/RCM) temperature change predictions

Over the Sahel (Figure 4.20), only CORDEX under RCP45 scenario shows more agreement and less bias. CMIP5 and CMIP_S shows multi modal PDF pointing out some uncertainties and less agreement among models over the Sahel region. Under RCP85 CMIP5, CMIP5_S and CORDEX have unimodal PDF depicting less uncertainties with CMIP5 showing more outliers.

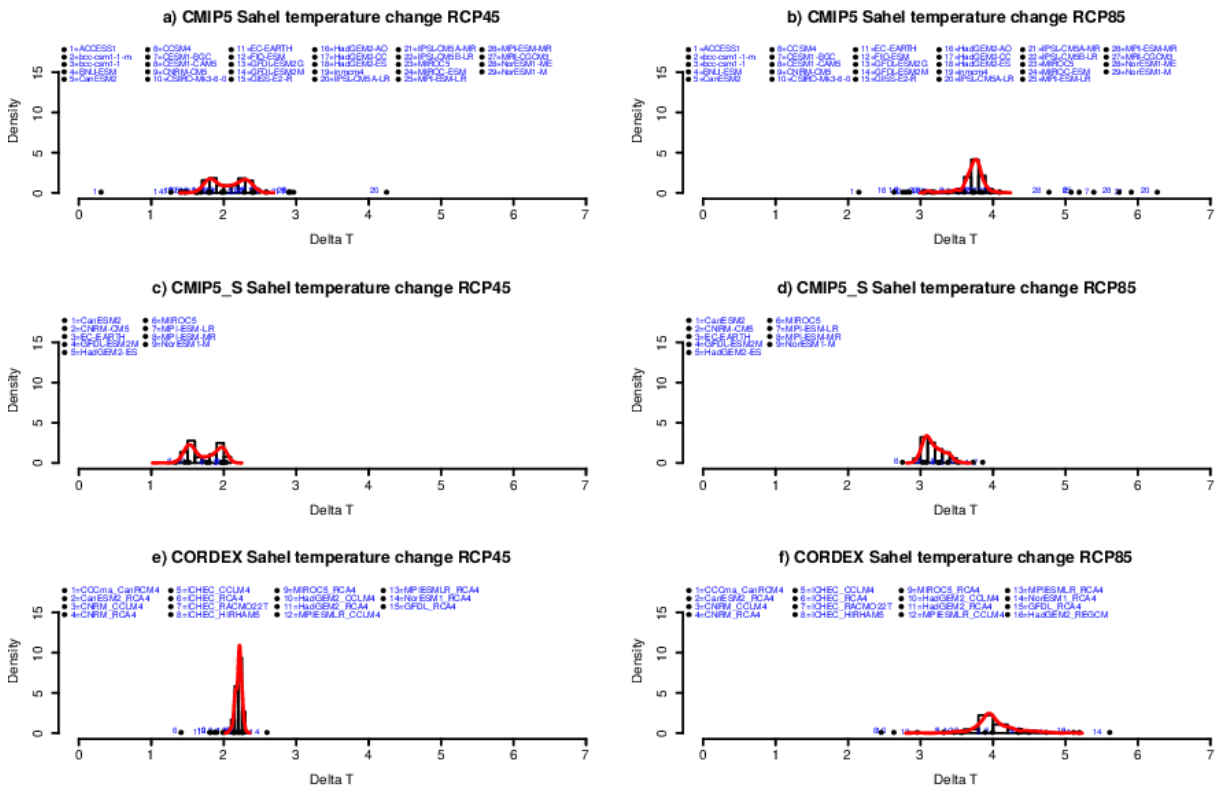

Figure 4.20: Posterior distribution of over the Sahel for CMIP5, CMIP5_subset and CORDEX under the RCP45 (a,c,e) and RCP85(b,d,f) scenario for JJAS season. The points along the base of the densities mark the model (GCM/RCM) temperature change predictions

For precipitation change over the Guinean Coast under RCP85 and RCP45 (Figure 4.21) uncertainties still remain in CORDEX model (following the CMIP5_S) with an increasing precipitation trend for the late century. The different scenarios seem to not have much impact on precipitation. There is no significant difference on precipitation change between RCP45 and RCP85.

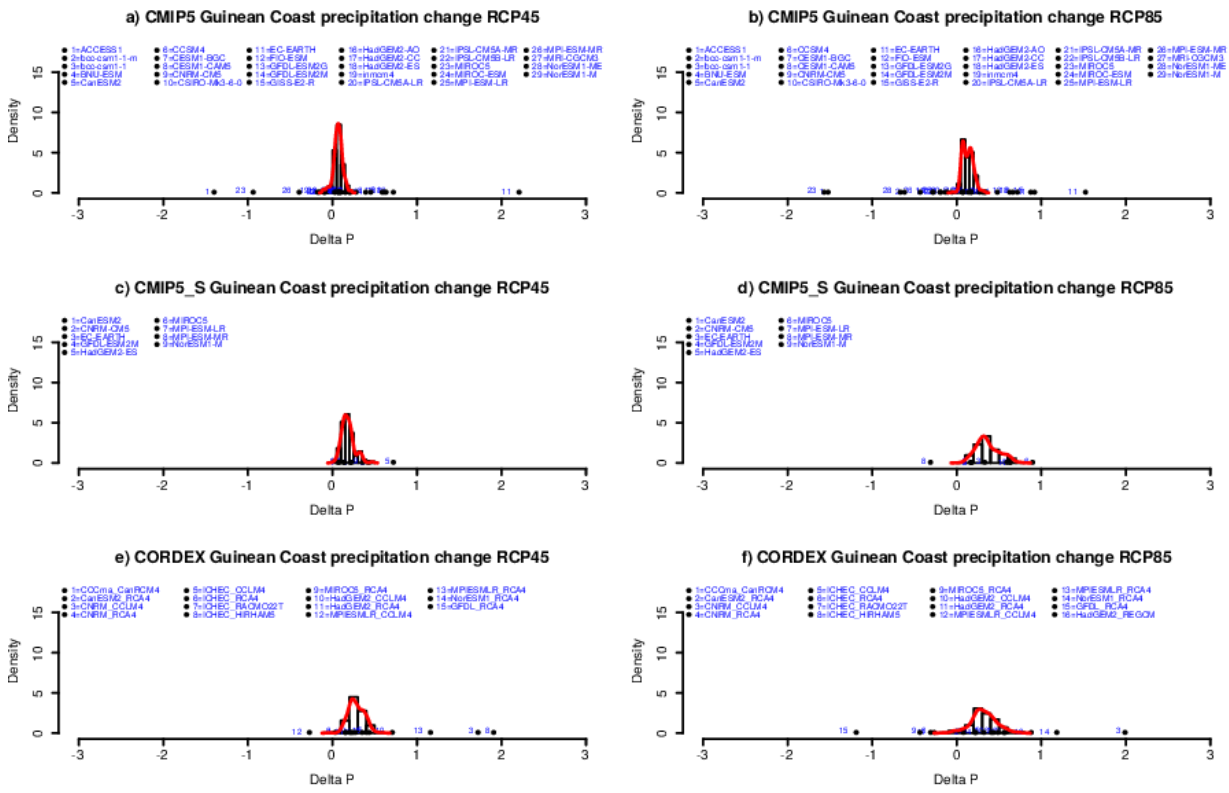

Figure 4.21: Posterior distribution of over the Guinean coast for CMIP5, CMIP5_subset and CORDEX under the RCP45 (a,c,e) and RCP85(b,d,f) scenario for JJAS season. The points along the base of the densities mark the model (GCM/RCM) temperature change predictions

Over the Sahel CMIP5 (Figure 4.22) models show more agreement on sign change (close to zero) compare to CMIP_S and CORDEX which show a change between 0 to 1 mm/day under the two scenarios with some outliers due to bias in present climate simulation and divergence from the future climate mean . CORDEX has a wide PDF curve under RCP45 and RCP85 scenario showing the persistence of uncertainties.

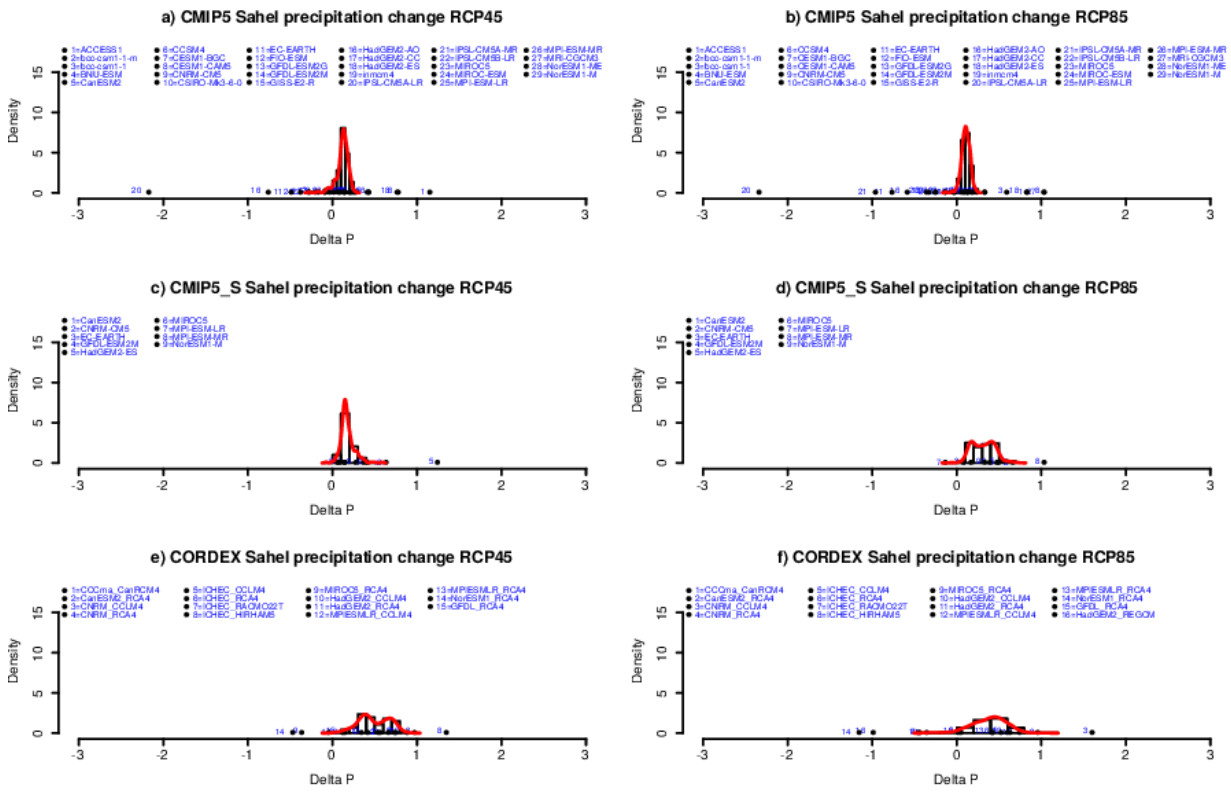

Figure 4.22: Posterior distribution of over the Sahel for CMIP5, CMIP5_subset and CORDEX under the RCP45 (a,c,e) and RCP85(b,d,f) scenario for JJAS season. The points along the base of the densities mark the model (GCM/RCM) temperature change predictions

Figure 4.23 shows boxplots of the posterior PDFs of temperature change under RCP45 and RCP85 scenario for CMIP5, CMIP5_Subset and CORDEX over Sahel and Guinean Coast for JJAS season. A pair of boxplots is shown for each region, the left represent the RCP45 and the right the RCP85.While CMIP5 is showing less variability (IQR) across the two regions, CMIP5_Subset and CORDEX show a significant shift in the PDFs range highlighting presence of biases in the present climate simulation and some degree of uncertainties in the future climate . However from CMIP5_Subset to CORDEX there is a significant reduction of uncertainty and more agreement among the models over the Guinea Coast for the RCP85 scenario and over the Sahel for RCP45. The IQR varies between 1^{o}C to 3^{o}C for the three models over the two regions under RCP45 and 2^{o}C to 5^{o}C under RCP85. The warming trend is certain over the two regions with different magnitudes.

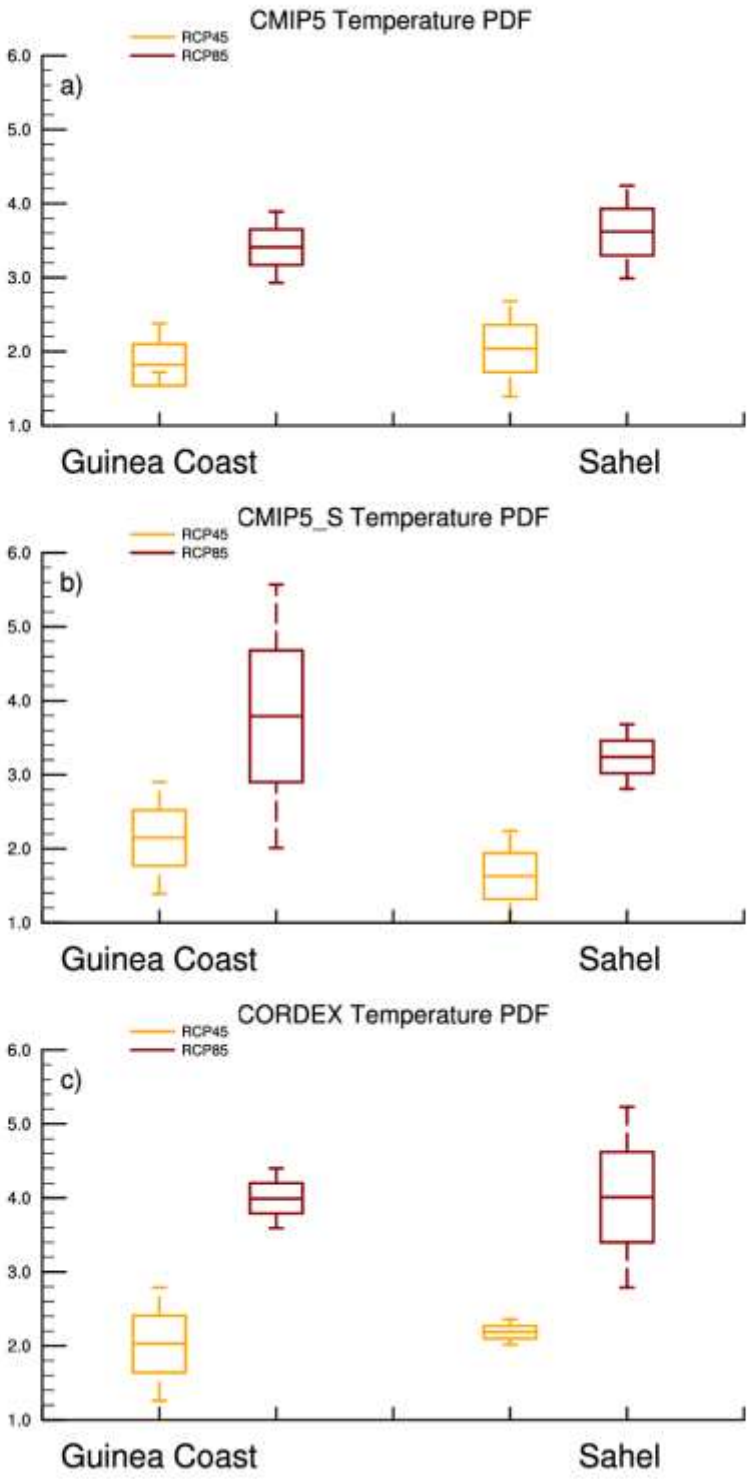

Figure 4.23: Posterior distribution of delta T in form of boxplot over Guinean Coast and the Sahel for CMIP5 (a), CMIP5_subset (b) and CORDEX(c) under the RCP45 and RCP85 scenario for JJAS season.

For precipitation boxplot of posterior PDFs of change under RCP45 and RCP85 scenario in Figure 4.24, CMIP5 is showing positive and negative change around the zero line over the two regions with less spread, meaning that, from CMIP5 GCMs a clear picture of precipitation change in terms of sign cannot be drawn. In CMIP5_S and CORDEX positive change are more prevalent than the negative one for the two scenarios (RCP45 and RCP85) over the two regions. However CORDEX is showing more spread under RCP85 scenario over the Sahel, still indicating some degree of uncertainty.

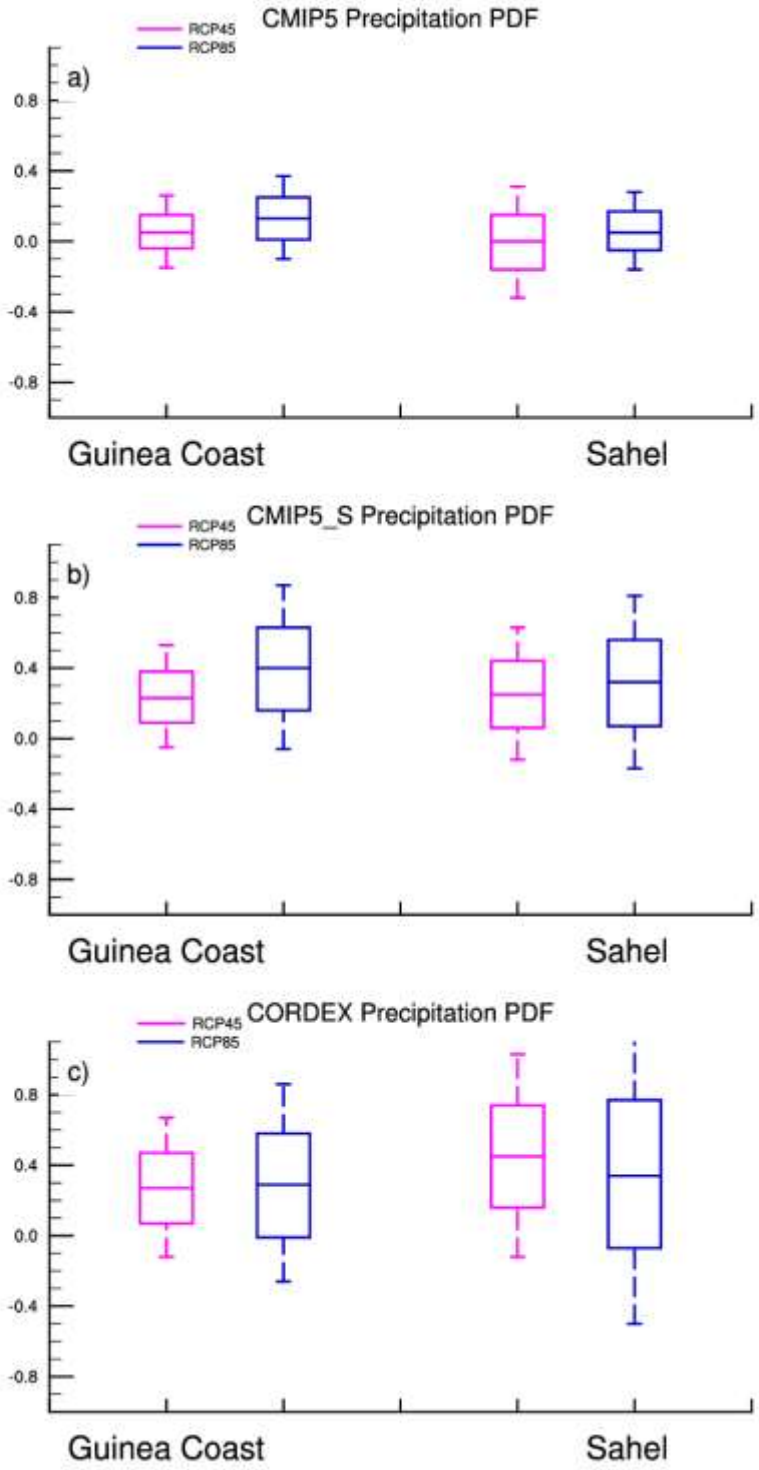

Figure 4.24: Posterior distribution of delta P in form of boxplot over Guinean Coast and the Sahel for CMIP5 (a), CMIP5_subset (b) and CORDEX(c) under the RCP45 and RCP85 scenario for JJAS season

4.4 Partitioning uncertainty in temperature and precipitation projections

Previous section shows that uncertainties still remain in climate projection over West Africa and there is need to separate and quantify those sources of uncertainties in order to get a reliable future climate projection for appropriate adaptation and mitigation strategies. We choose to analyze the last three decade of the 21st century (2070-2099) relative to the present day period (1976-2005) where the signal of change is expected to be stronger both for temperature and precipitation. Internal variability and inter-model variability will be investigated to constitute the total uncertainty since the scenario uncertainty cannot be covered due to the lack of data for the other two scenarios RCP2.6 and RCP6.0. In the following section, we will focused on temperature and precipitation internal and inter model variability patterns over West Africa , give light on how the new generation of model has improved the climate projection information over the region and derive the signal to noise ratio to appreciate the robustness of the climate change information.

4.4.1 Partitioning uncertainty in temperature projections

Figure 4.25 shows temperature Internal Variability (IV) for 2070-2079 JJAS season under RCP45 (a,c,e) and RCP85 (b,d,f) scenario for CMIP5, CMIP5_S and CORDEX MMEs. Based on the method of Hawkins and Sutton (2009), IV is assumed to be constant over the 21st Century. Over West Africa IV is mainly lower than 0.5 ^{o}C under the two scenarios for CMIP5, CMIP5_S and CORDEX. Maximum IV values are located in the highest latitudes and some part of Atlantic Ocean.

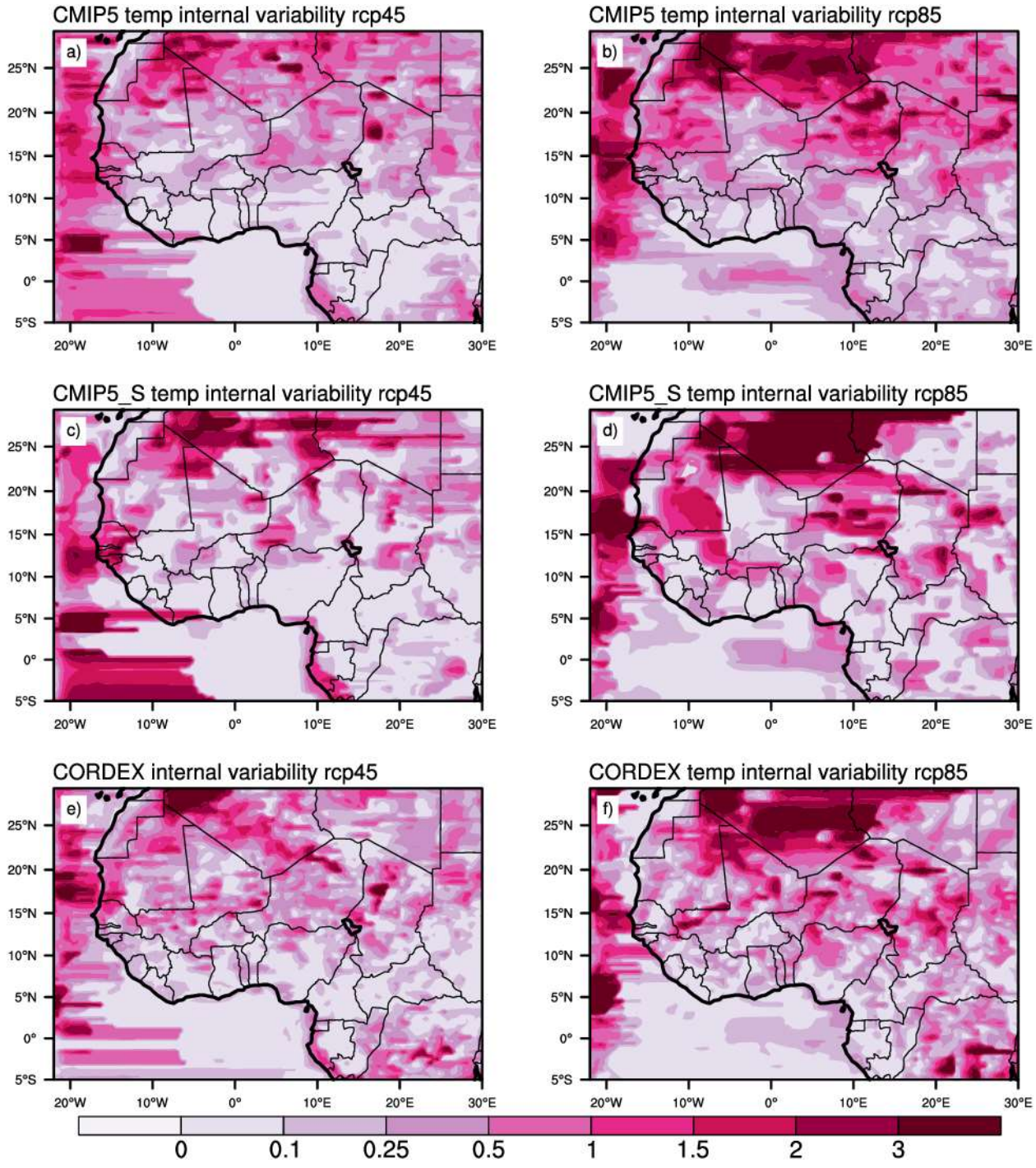

Figure 4.25: Internal variability of 2070-2099 JJAS mean temperature (oC) for CMIP5, CMIP5 subset and CORDEX for RCP45 (a,c,e) and RCP85(b,d,f) scenario

Figure 4.26 shows temperature Inter Model Variability (IMV) for 2070-2079 JJAS season under RCP45 (a,c,e) and RCP85 (b,d,f) scenario for CMIP5, CMIP5_S and CORDEX MMEs. The lowest values are located over the West African Domain and part of the Gulf of Guinea the highest value are located in the Northern part and some part of the Atlantic Ocean . The spatial patterns of IMV and IV are similar.

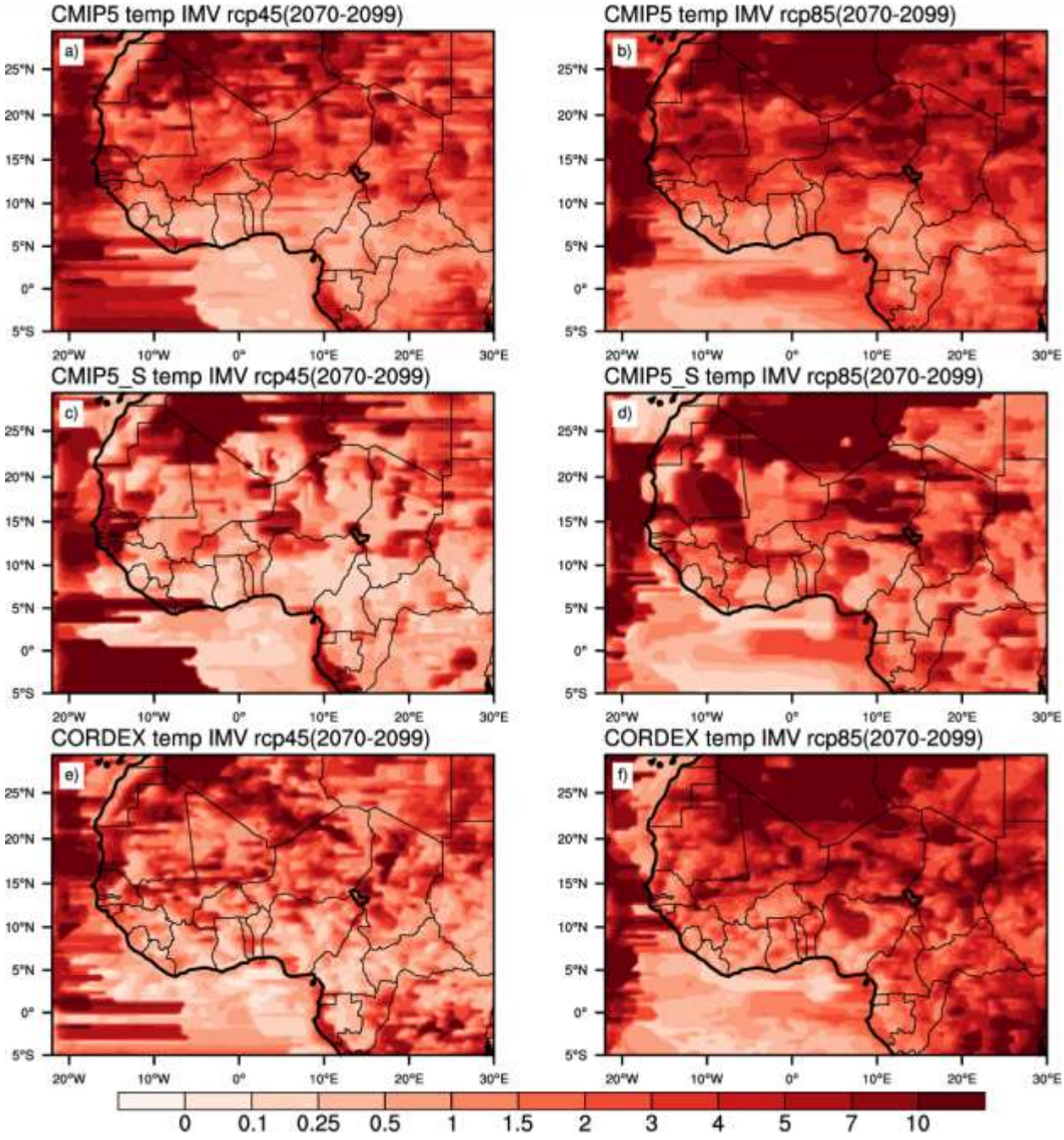

Figure 4.26: Inter Model Variability of 2070-2099 JJAS mean temperature (oC) for CMIP5, CMIP5 subset and CORDEX for RCP45 (a,c,e) and RCP85(b,d,f) scenario

Figures 4.27 and 4.28 are showing respectively the Ratio for internal variability (CMIP5 or CCMIP_S) over (CORDEX) and Inter Model variability for 1970-2099 JJAS mean temperature for RCP45 and RCP85 scenario. The regions where the new generation of model (CORDEX) show an improvement (reduction of IV/IMV) compare to CMIP5 and CMIP5_S are marked with dots. We found that under the two scenarios CORDEX MMEs (the new generation of models) have an added value compare to the driving GCMs (CMIP_S) and CMIP5 MMEs by reducing the spread over the West African region . At the end of 21st century, for the last three decade (2070-2099) IMV is the dominant source of uncertainties and is explaining up to 90 % of total uncertainty and IV explaining only 10 % . This finding is consistent with the finding of Blaquez *et al.* (2013) who analyze the uncertainties in future climate over South America with CMIP3 and CMIP5 GCMs.

Hawkins and Sutton, (2009) and Yip *et al. (*2011), found that after year 2050 the scenario uncertainty dominate the total uncertainty but in our study we did not consider the scenario uncertainty because the data we were able to get were the radiative forcing of 4.5 and 8.5. So considering scenario uncertainty may not cover the full range of uncertainties (2.6 and 6.0 forcing).

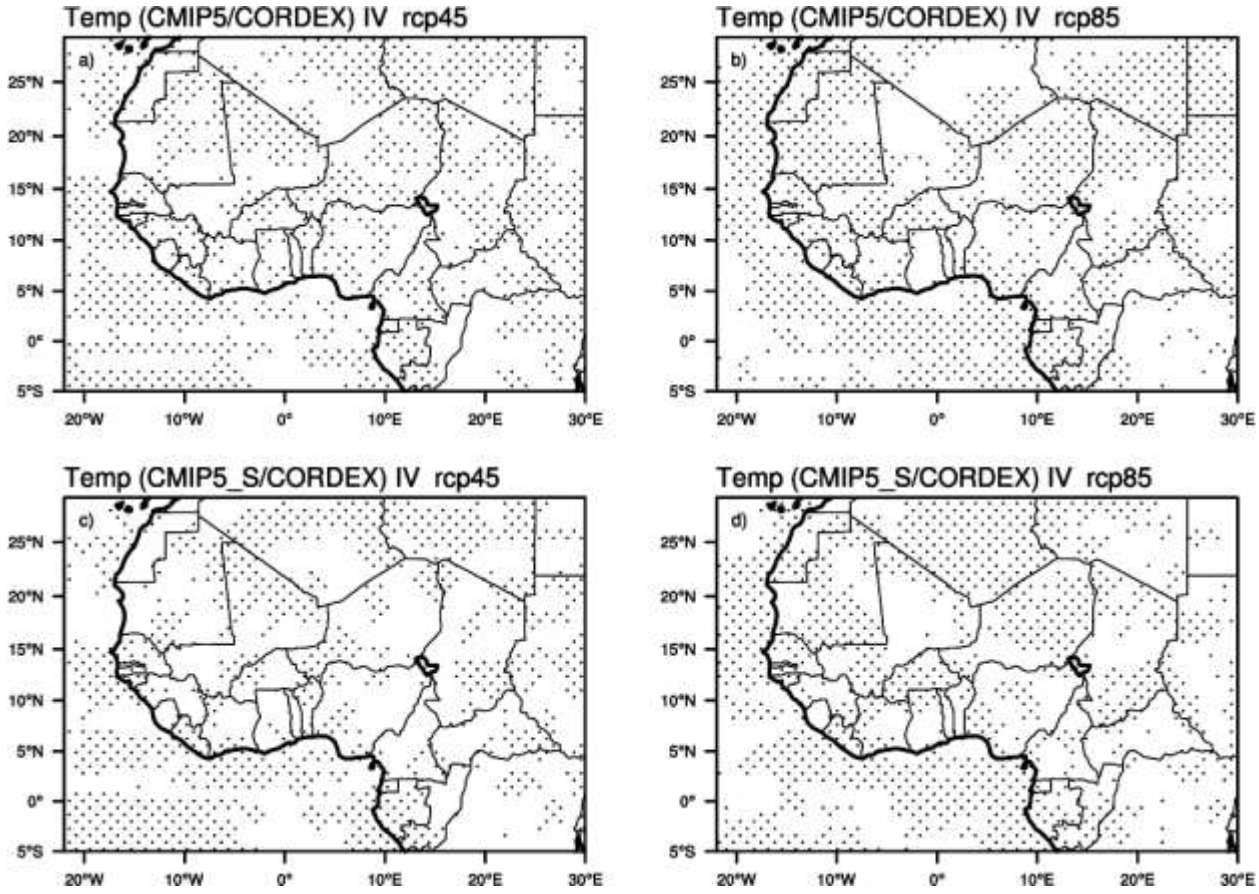

Figure 4.27: Ratio for internal variability (CMIP5 or CCMIP_S variability /CORDEX variability) for 1970-2099 JJAS mean temperature for RCP45 and RCP85 scenario

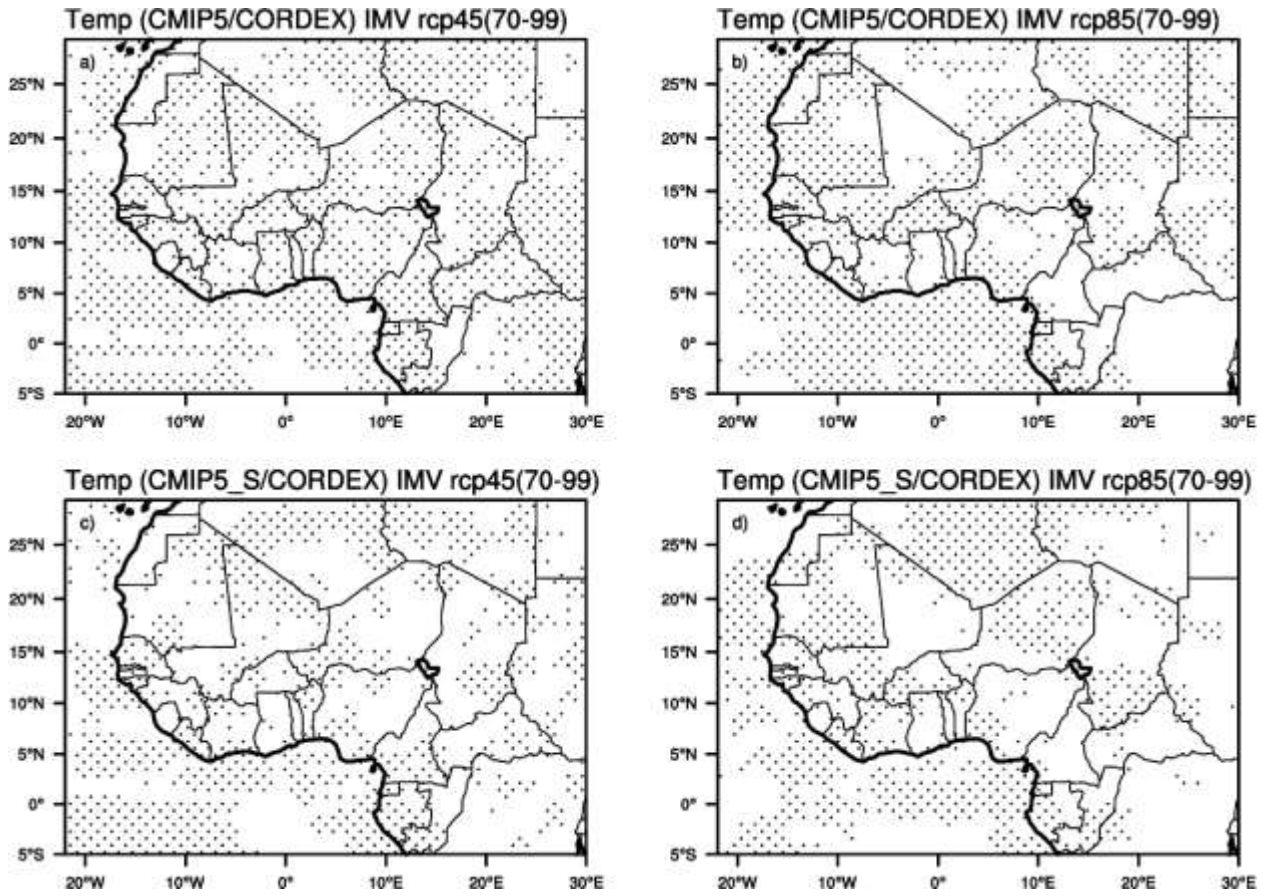

Figure 4.28: Ratio for inter model variability (CMIP5 or CCMIP_S variability /CORDEX variability) for 1970-2099 JJAS mean temperature for RCP45 and RCP85 scenario

Figure 4.29 shows the Signal to Noise Ratio (SNR) for the three MMEs . SNR is a measure of the robustness of climate change information taking into account uncertainties associated (Yip *et al.*, 2011). Region of high uncertainties (high values of IMV and IV) will have a low SNR. Region where the climate change signal dominate the noise is characterized by SNR>1. For temperature under the two scenarios, the change is robust over most of West African countries with more spatial details and improved SNR with CORDEX MMEs compare to CMIP5 and CMIP5_S MMEs. The warming trend over the region is consistent with the previous studies showing that there is more confidence (more robustness) about the temperature projection change (Tebadi *et al.* (2005), Hawkins and Sutton, 2009) over the region with less uncertainties in regional and Global models compare to precipitation.

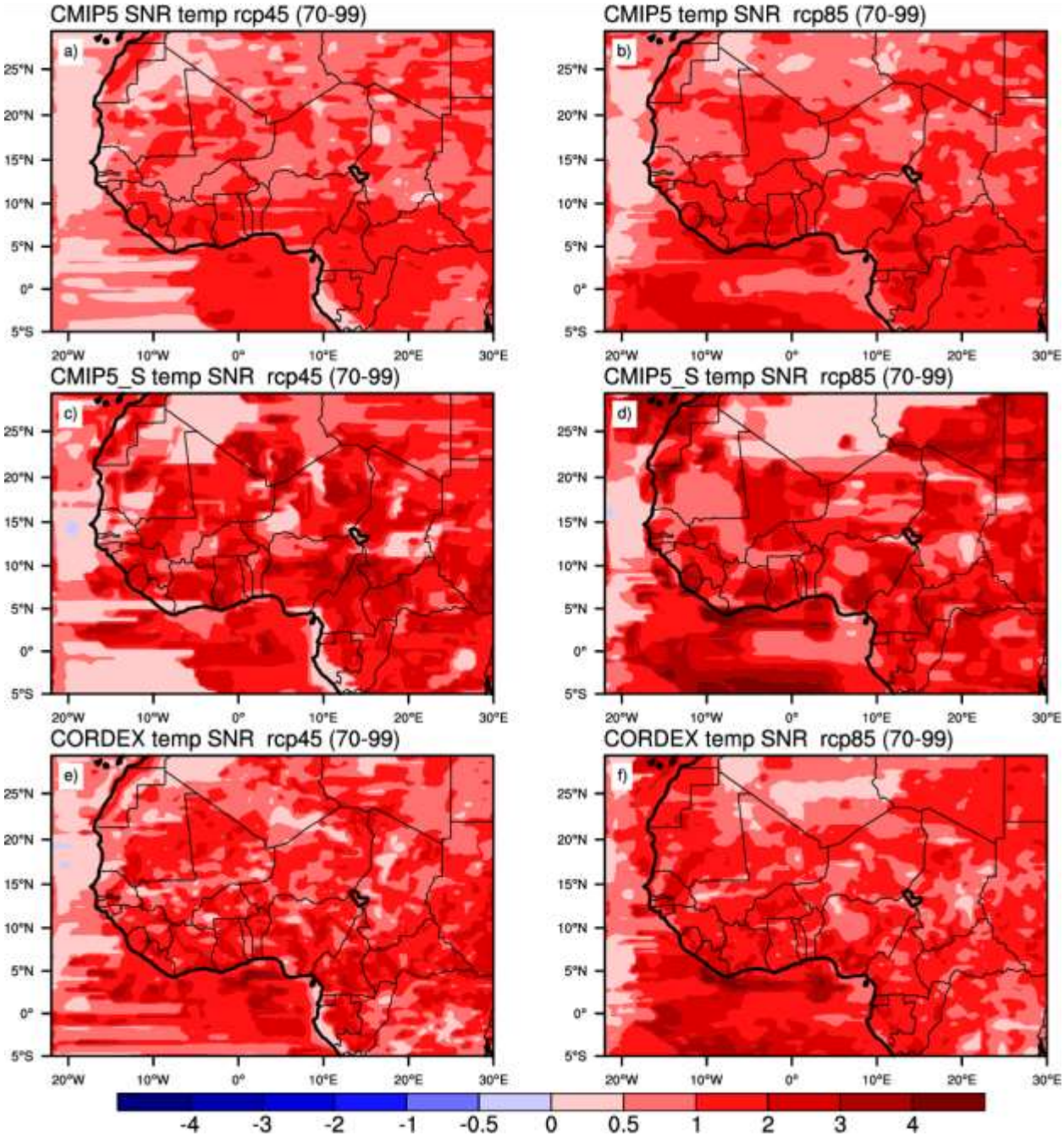

Figure 4.29: Signal to Noise ratio for 1970-2099 JJAS mean temperature (oC) for CMIP5, CMIP5 subset and CORDEX for RCP45 (a,c,e) and RCP85(b,d,f) scenario

4.4.2 Partitioning uncertainty in precipitation projections

Figure 4.30 shows precipitation Internal Variability (IV) (which had been assumed to be constant in time during the 21st century) for 2070-2079 JJAS season under RCP45 (a,c,e) and RCP85 (b,d,f) scenario for CMIP5, CMIP5_S and CORDEX MMEs. Variability peaks in CMIP5, CMIP5_S and CORDEX (>3mm/day) are located over the coastal area (Gulf of Guinea) and regions of high altitudes. CORDEX is showing more spatial details due to resolution and reduction of internal variability compare to CMIP_S.

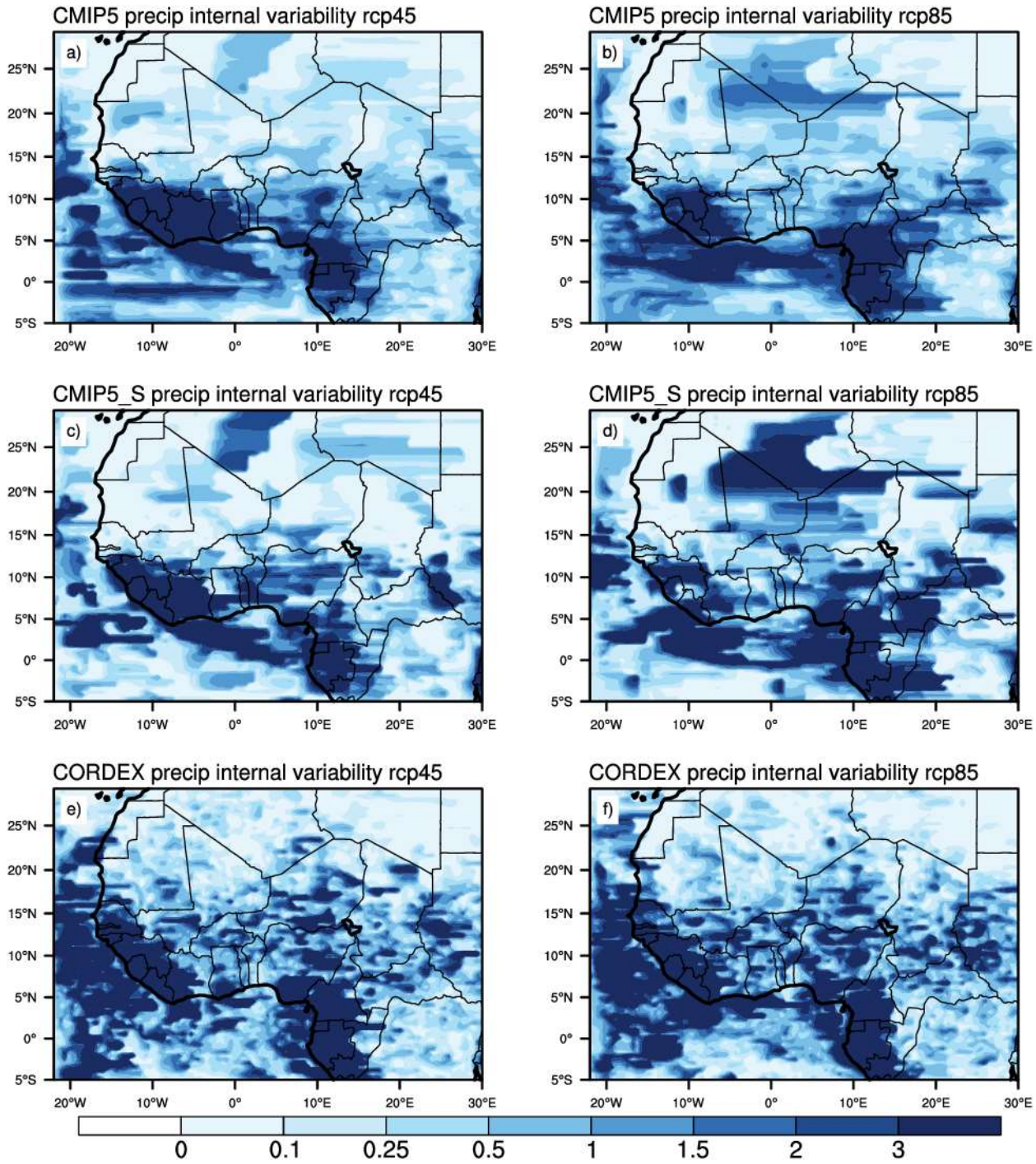

Figure 4.30: Internal variability of 2070-2099 JJAS mean precipitation (mm/day) for CMIP5, CMIP5 subset and CORDEX for RCP45 (a,c,e) and RCP85(b,d,f) scenario

Figure 4.31 shows precipitation Inter Model Variability (IMV) for 2070-2079 JJAS season under RCP45 (a,c,e) and RCP85 (b,d,f) scenario for CMIP5, CMIP5_S and CORDEX MMEs. The highest values are located over the coastal regions. However CORDEX is showing more variability over the Atlantic Ocean compare to CMIP5_S under the RCP45 scenario.

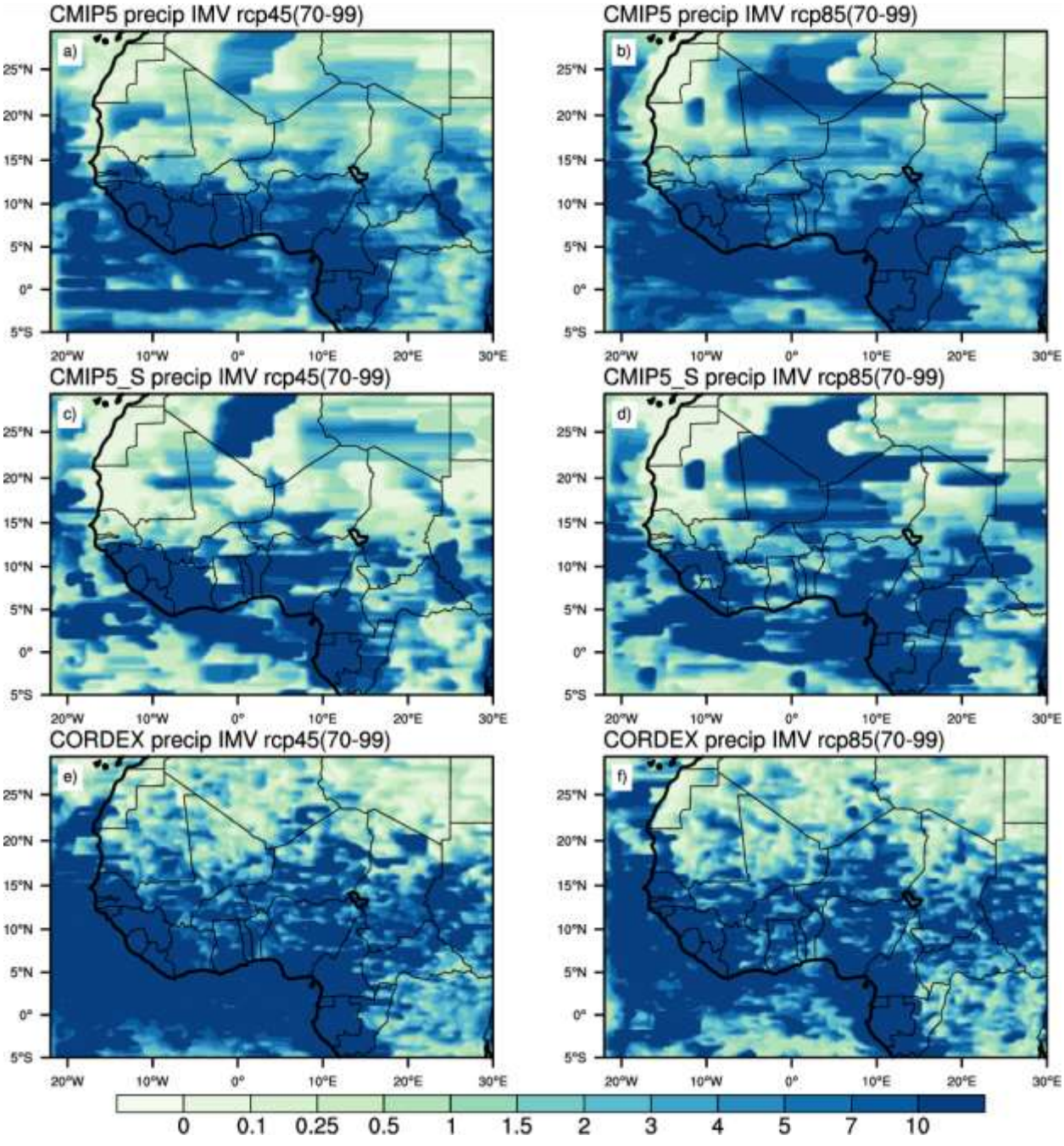

Figure 4.31: Inter model variability of 2070-2099 JJAS mean precipitation (mm/day) for CMIP5, CMIP5 subset and CORDEX for RCP45 (a,c,e) and RCP85(b,d,f) scenario

Figure 4.32 and 4.33 are showing respectively the Ratio for internal variability and Inter Model variability (CMIP5 or CCMIP_S) over (CORDEX) for 1970-2099 JJAS mean precipitation for RCP45 and RCP85 scenario. We notice that for the two scenarios the IV and IMV were reduced over Cote d'ivoire, Ghana, Benin and Nigeria.

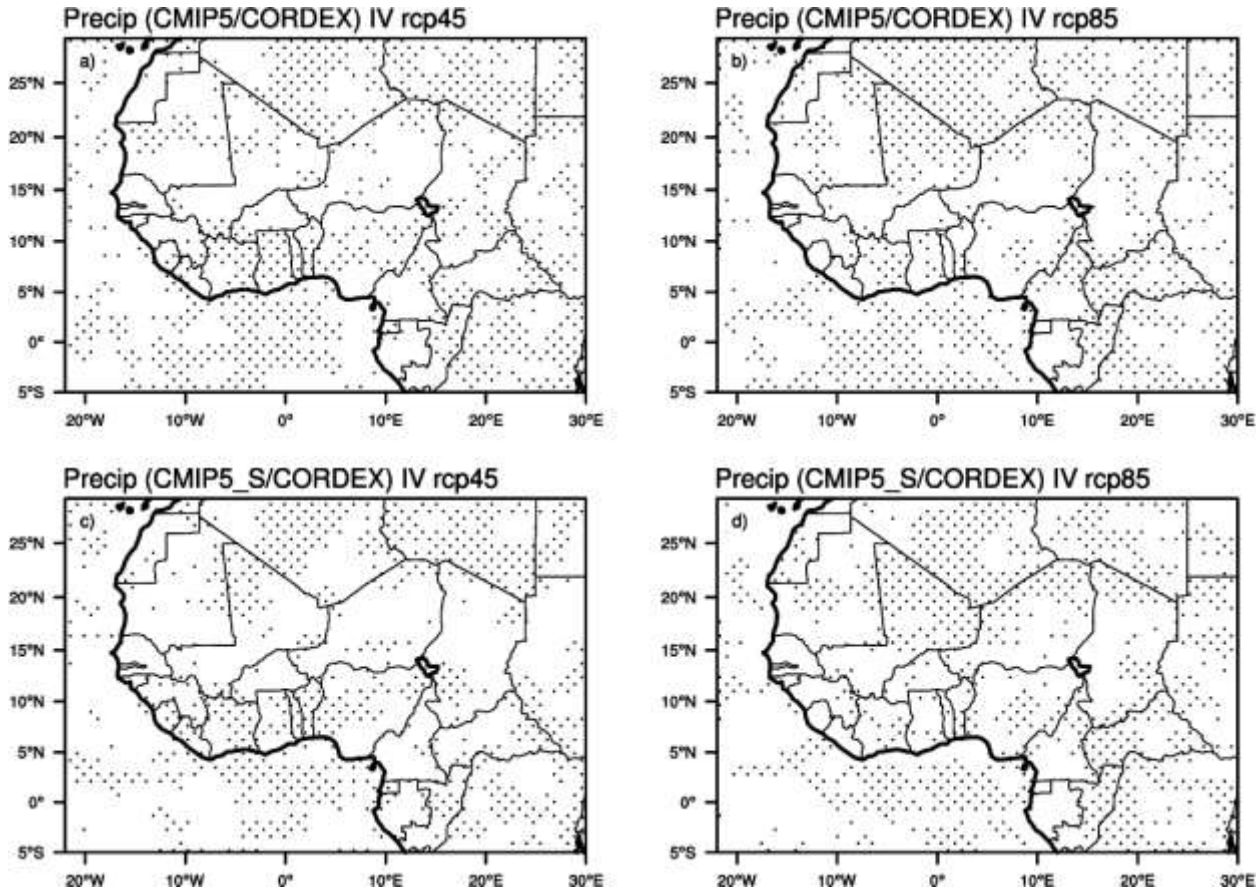

Figure 4.32: Ratio for internal variability (CMIP5 or CCMIP_S variability /CORDEX variability) for 1970-2099 JJAS mean precipitation for RCP45 and RCP85 scenario

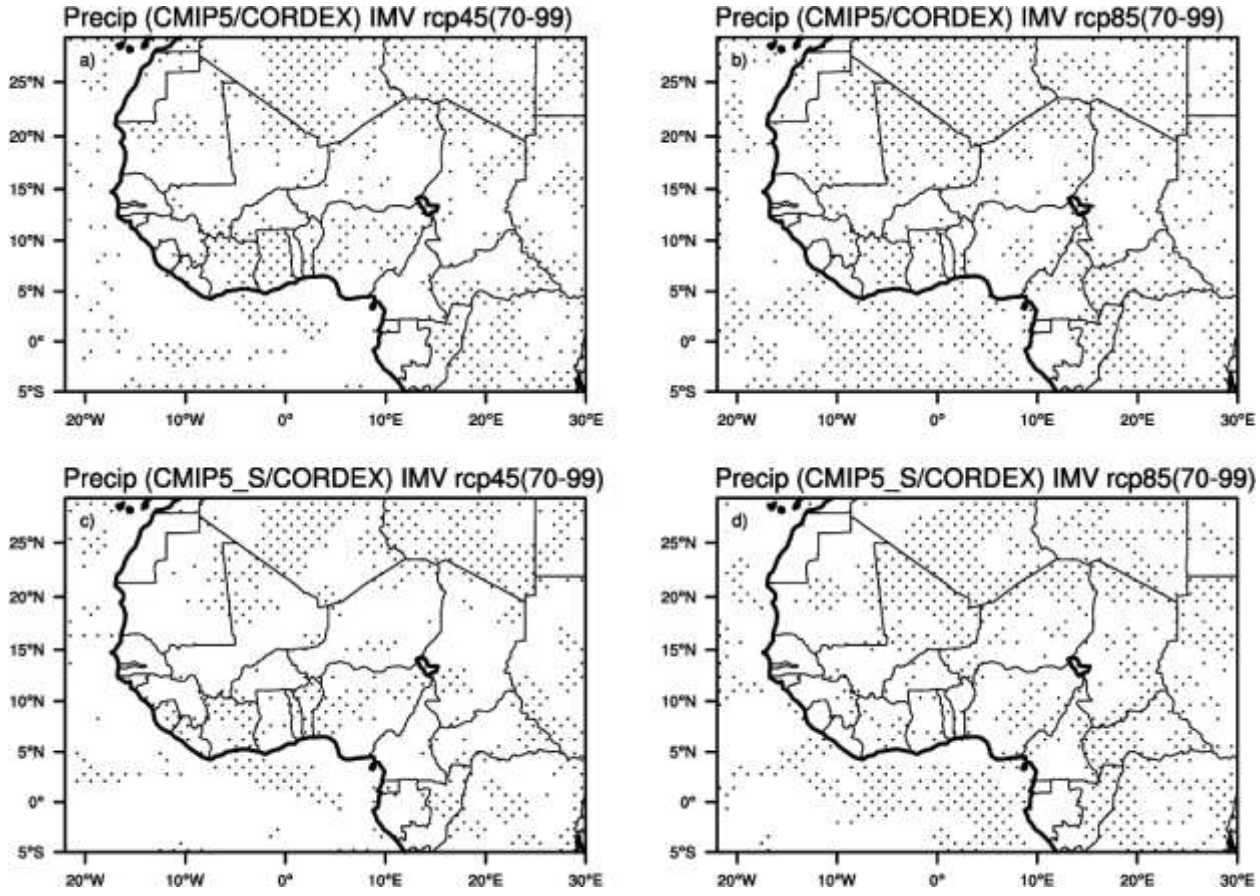

Figure 4.33: Ratio for inter model variability (CMIP5 or CCMIP_S variability /CORDEX variability) for 1970-2099 JJAS mean precipitation for RCP45 and RCP85 scenario

The reliability of the precipitation projection is explored in CMIP5, CMIP5_S and CORDEX MMEs. Figure 4.34 is showing the signal to noise ratio for 1970-2099 JJAS mean precipitation under the two scenarios RCP45 and RCP85. Only CORDEX under RCP45 has a signal to noise ratio greater than one over West Africa (between 5^{o} to 15^{o} N). It is showing an increasing trend of precipitation over the whole West African region (positive SNR). In CMIP5, CMIP5_S and CORDEX under RCP85, the noise dominate the signal.

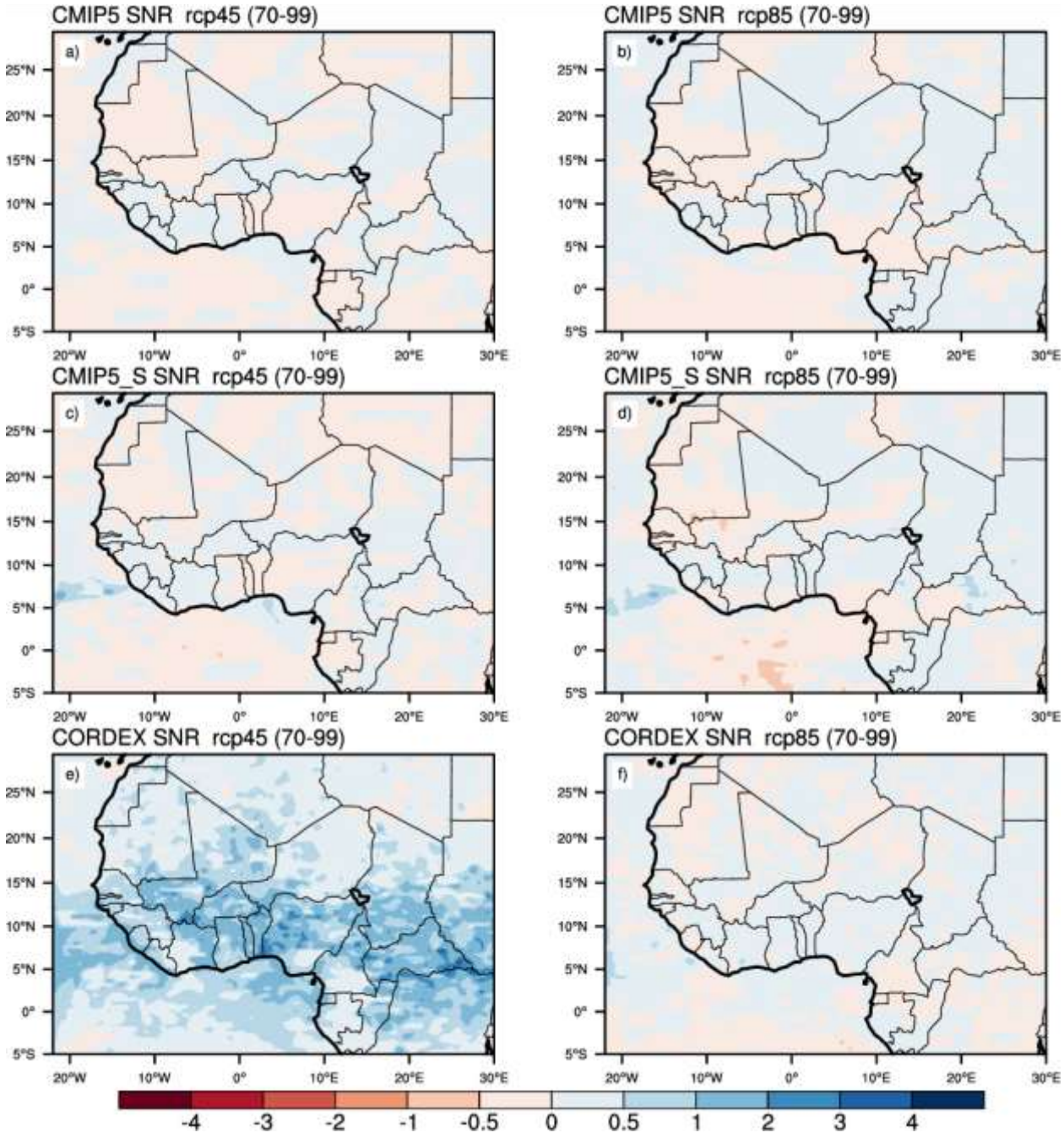

Figure 4.34: Signal to Noise ratio for 1970-2099 JJAS mean precipitation (mm/day) for CMIP5, CMIP5 subset and CORDEX for RCP45 (a,c,e) and RCP85(b,d,f) scenario

CHAPTER 5

. CONCLUSION AND RECOMEMMENDATIONS

An assessment of multimodel ensembles constructed from the CMIP5 and CMIP5_SUBSET GCMs, and CORDEX RCMs during the present-day (1982-2005) is first carried out for the West African region. The focus of the analysis is on temperature and precipitation inter-model and spatio-temporal variability. In addition, the origin of the biases in the RCM MME and the extent to which CORDEX adds useful detail to CMIP5 is also discussed.

We find that CORDEX exhibits larger cold temperature biases compared to CMIP5 and CMIP5_SUBSET, suggesting that these are mostly due to the RCM internal physics. Conversely, compared to the CMIP5 GCMs, for precipitation the RCM MME simulates a better spatial distribution, lower bias and more fine-scale details associated with the location of local complex topography and steep landuse gradients. A separation of the CORDEX ensemble into an ensemble inducing simulations with one RCM driven by multiple GCMs and multiple RCMs driven by one GCM shows that the internal model physics is more important than the boundary forcing in determining the model performance and inter-model spread.

The spatio-temporal variability is assessed with the use of Rotated Empirical Orthogonal Function (REOF) analysis. All the MMEs capture with different magnitudes the spatial distribution of the first mode of temperature and precipitation REOF characterizing the recent temperature increase and precipitation recovery over West Africa, with CORDEX providing the highest Pattern Correlation Coefficient. For the PCs of all modes CORDEX mostly follows the CMIP5_SUBSET, with little improvement compared to CMIP5.

Overall, it is evident that the different MMEs exhibit different level of bias and a pronounced intermodel and inter-ensemble variability. We found that, especially for precipitation, CORDEX is able to improve upon the performance of the CMIP5 models and the subset of driving GCMs, although this is not the case for temperature.

We further use a Bayesian approach to show how CORDEX MMEs is improving precipitation simulation compared to CMIP5 and CMIP5_Subset. The increased horizontal resolution is able to approximate the mean and the variance more closely to the observation over Sahel and the Guinean Coast.

For the future climate 2070-2099 we have applied the Bayesian model of Tebaldi et al.,2005 to the three sets of models (CMIP5, CMIP5_Subset and CORDEX) and derived PDFs of temperature and precipitation change for two sub region (Sahel and Guinea Coast). Two criteria of model evaluation were used: the Bias and Convergence. For temperature change over the Guinean Coast, CMIP5_S models under RCP85 has a lot of uncertainties showing more bias and less agreement among models but the CORDEX seems to dramatically reduced those uncertainties. Over the Sahel, only CORDEX under RCP45 scenario shows more agreement and less bias. CMIP5 and CMIP_S shows multi modal PDF pointing out some uncertainties and less agreement among models. Under RCP85 CMIP5, CMIP5_S and CORDEX have unimodal PDF depicting less uncertainties with CMIP5 showing more outliers.

For precipitation change over the Guinean Coast under RCP8.5 and RCP4.5, uncertainties still remain in CORDEX model (following the CMIP5_S) with an increasing precipitation trend for the late century. There is no significant difference on precipitation change between RCP45 and RCP85. Over the Sahel CMIP5 models show more agreement on sign change (close to zero) compare to CMIP_S and CORDEX which show a change between 0 to 1 mm/day under the two scenarios with some outliers due to bias in present climate simulation and divergence from the future climate mean . CORDEX has a wide PDF curve under RCP45 and RCP85 scenario showing the persistence of uncertainties.

The sources of uncertainty in climate projection from CMIP5, CMIP5_Subset and CORDEX were also examined. The source of uncertainty due to internal and inter-model variability were analyzed for temperature and precipitation.

For temperature over West Africa Internal Variability is mainly lower than 0.5 ^{o}C under the two scenarios for CMIP5, CMIP5_S and CORDEX. Maximum IV values are located in the highest latitudes (>15^{o} N) and some part of Atlantic Ocean. . The spatial patterns of the Inter Model Variability is similar to the Internal IV.

The ratio of (internal or inter-model) variability was used to compare CORDEX, CMIP5 and CMIP5_Subset. Under the two scenarios (RCP45and RCP85) CORDEX MMEs (the new generation of models) have an added value compare to the driving GCMs (CMIP_S) and CMIP5 MMEs by reducing the spread over the West African region . At the end of 21st century, for the last three decade (2070-2099) IMV is the dominant source of uncertainties and is explaining up to 90 % of total uncertainty and IV explaining only 10 %.

The Signal to Noise ratio is a measure of the robustness of climate change information taking into account uncertainties associated. Region where the climate change signal dominate the noise is characterized by SNR>1. For temperature under the two scenarios, the change is robust over most of West African countries with more spatial details and improved SNR with CORDEX MMEs compare to CMIP5 and CMIP5_S MMEs.

For precipitation, Internal Variability peaks in CMIP5, CMIP5_S and CORDEX (>3mm/day) and Inter Model Variability are located over the coastal area (Gulf of Guinea) and regions of high altitudes. CORDEX is showing more spatial details due to resolution and reduction of internal variability compare to CMIP_S. Considering the Ratio for internal variability and Inter Model variability for the two scenarios, the IV and IMV were reduced over Cote d'ivoire, Ghana, Benin and Nigeria. Only CORDEX under RCP45 has a signal to noise ratio greater than one over West Africa (between 5^{o} to 15^{o} N) with an increasing trend of precipitation over the whole West African region (positive SNR). In CMIP5, CMIP5_S and CORDEX under RCP85, the noise dominates the signal.

Clearly an assessment of climate change information over West African region needs to rely on the careful evaluation and compounded information deriving from multiple sources. This highlights the importance of large model ensembles and carefully designed MME approaches for the provision of useful climate information in impact and adaptation studies.

REFERENCES

Abiodun, B.J., Pal, J.S., Gutowski, W.J., Adedoyin, A. (2008). Simulation of West African monsoon using RegCM3 Part II: impacts of deforestation and desertification. Theoretical and Applied Climatology, 93(3–4):245–261. DOI:10.1007/s00704-007-0333-1

Abiodun, B. J., Kamoru, A. L., Ayobami, T. S., Abayomi, A. A. (2013). Potential influences of global warming on future climate and extreme events in Nigeria. Regional Environmental Change 13:477–491. DOI: 10.1007/s10113-012-0381-7

Ackerley D, Booth BBB, Knight SHE, Highwood EJ, Frame DJ, Allen MR, Rowell DP. 2011. Sensitivity of twentieth-century Sahel rainfall to sulfate aerosol and CO(2) forcing. Journal of Climate 24: 4999–5014. DOI: http://dx.doi.org/10.1175/JCLI-D-11-00019.1

Afiesimama, E., Pal, J.S., Abiodun, B.J., Gutowski, W.J., Adedoyin, A. (2006). Simulation of West African monsoon using the RegCM3. Part I: model validation and interannual variability. Theoretical and Applied Climatology,86(1–4):23–37. DOI:10.1007/s00704-005-0202-8

Akinsanola,A.A., Ogunjobi, K.O. Gbode,I.E. and Ajayi, V.O. (2015). Assessing the Capabilities of Three Regional Climate Models over CORDEX Africa in Simulating West African Summer Monsoon Precipitation," Advances in Meteorology, vol. 2015, Article ID 935431, 13 pages, 2015. DOI:10.1155/2015/935431

Annan, J., and Hargreaves,J. (2011). Understanding the CMIP3 multimodel ensemble. Journal of Climate, 24, 4529–4538. DOI:10.1175/2011JCLI3873.1.

Biasutti, M. (2013). Forced Sahel rainfall trends in the CMIP5 archive. Journal of Geophysical Research: Atmospheres, 118:1613–1623. DOI:10.1002/jgrd.50206

Bellenger, H., Guilyardi, E., Leloup, J., Lengaigne, M. and Vialard, J. (2014). ENSO representation in climate models: from CMIP3 to CMIP5. Climate Dynamics, 42:1999-2018. DOI: 10.1007/s00382-013-1783-z

Blázquez, J., Nuñez,M.N. (2013). Analysis of uncertainties in future climate projections for South America: comparison of WCRP-CMIP3 and WCRP-CMIP5 models. Climate Dynamics, 41(3):1039-1056. DOI: 10.1007/s00382-012-1489-7.

Boko, M., Niang, I., Nyong, A., Vogel, C., Githeko, A., Medany, M., Osman-Elasha, B., Tabo, R. and Yanda, P. (2007). Africa Climate Change 2007: Impacts, Adaptation and Vulnerability.Contribution of Working Group II to the Fourth Assessment Report of the Intergovernmental Panel on Climate Change,Parry, M. L., Canziani, O. F., Palutikof, J. P., van der Linden, P. J. and Hanson, C. E. (eds). Cambridge University Press.Cambridge UK. pp. 433 – 467.

Buontempo, C., Mathison, C., Jones, R., Williams, K., Wang, C., McSweeney, C. (2014). An

ensemble climate projection for Africa. Climate Dynamics, 44(7):2097-2118. DOI: 10.1007/s00382-014-2286-2

Deser C, Phillips AS, Alexander MA (2010) Twentieth century tropical sea surface temperature trends revisited. Geophysical Resources Letter, 37:L10701. DOI:10.1029/2010GL043321

Cook, K.H., Vizy, E.K. (2015). Detection and analysis of an amplified warming of the Sahara Desert. Journal of Climate. DOI: http://dx.doi.org/10.1175/JCLI-D-14-00230.1

Cox, P., and Stephenson, D. (2007) A changing climate for prediction.

Science, 317, 207–208, DOI:10.1126/science.1145956

Crétat, J., Vizy, E.K., Cook, K.H. (2013). How well are daily intense rainfall events captured

By current climate models over Africa? Climate Dynamics,42:2691. DOI:10.1007/s00382-013-1796-7

Christensen, J.H., Christensen, O.B. (2007) .A summary of the PRUDENCE model projections of changes in European climate by the end of this century. Climate Change. DOI:10. 1007/s10584-006-9210-7

Diallo, I., Sylla, M.B., Giorgi, F., Gaye, A.T. and Camara, M. (2012). Multi-model GCM-RCM ensemble based projections of temperature and precipitation over West Africa for the early 21st century. International Journal of Geophysics, Article ID 972896. DOI:10.1155/2012/972896

Diallo I, Bain C, Gaye A, Moufouma-Okia W, Niang C, Dieng M, Graham R (2014) Simulation of the West African monsoon onset using the HadGEM3-RA regional climate model. Climate Dynamics, 43:575–594. DOI: 10.1007/s00382-014-2219-0

Di Luca, A., de Elıa, R., Laprise, R. (2012). Potential for added value in precipitation simulated by highresolution nested Regional Climate Models and observations. Climate Dynamics, 38:1229–1247.DOI: http://dx.doi.org/10.1007/s00382-011-1068-3

Dong, B., Sutton, R.T., Highwood, E., Wilcox, L. (2014). The impacts of European and Asian anthropogenic sulfur dioxide emissions on Sahel rainfall. Journal of Climate, 27: 7000–7017. DOI: htp://dx.doi.org/10.1175/JCLI-D-13-00769.1

Dosio, A., Panitz, H.J., Schubert-Frisius, M., Lüthi, D. (2015).Dynamical downscaling of CMIP5 global circulation models over CORDEX-Africa with COSMO-CLM: evaluation over the present climate and analysis of the added value. Climate Dynamics, 44: 2637–2661. DOI:10.1007/s00382-014-2262-x

Dosio, A., Panitz, H. J. (2016).Climate change projections for CORDEX-Africa with COSMO-CLM regional climate model and differences with the driving global climate models. Climate Dynamics, 46: 1599-1625. DOI:10.1007/s00382-015-2664-4

Druyan, L.M., Feng, J., Cook, K.H., Xue, Y., Fulakeza, M., Hagos, S.M., Konaré, A., Moufouma-Okia, W., Rowell, D.P., Vizy, E.K., Ibrah, S.S. (2010). The WAMME

regional model intercomparison study. Climate Dynamics, 35(1):175–192. DOI:10.1007/s00382-009-0676-7

Druyan, L., and Fulakeza, M. (2015). Downscaling GISS ModelE boreal summer climate over Africa. Climate Dynamics, early on-line. DOI:10.1007/s00382-015-2880-y.

Gbobaniyi. E., Sarr, A., Sylla, M.B., Diallo, I., Lennard, C., Dosio, A., Dhiédiou, A., Kamga, A., Klutse, N.A.B., Hewitson, B., Nikulin, G., Lamptey, B. (2014) .Climatology, annual cycle and interannual variability of precipitation and temperature in CORDEX simulations over West Africa. International Journal of Climatology, 34(7): 2241–2257. DOI:10.1002/joc.3834

Gaetani, M., Fontaine, B., Roucou, P., Baldi, M. (2010). Influence of the Mediterranean Sea on the West African monsoon: intraseasonal variability in numerical simulations Journal of Geophysical Resources, 115:D24115. DOI:10.1029/2010jd014436

Gallée, H., Moufouma Okia, W., Bechtold,P., Brasseur, O. Dupays,I., Marbaix,P. Messager, C. Ramel,R., and Lebel T. (2004). A high resolution simulation of a West African rainy season using a regional climate model. Journal of Geophysical Resources,109 , D05108, DOI:10.1029/2003JD004020

Giorgi, F., and Mearns L. O. (1999). Introduction to special section: Regional climate modeling revisited. Journal of Geophysical Research, 104(6): 6335-6352. DOI: 10.1029/98JD02072

Giorgi, F., Mearns, L.O. (2002). Calculation of average, uncertainty range, and reliability of regional climate changes from AOGCM simulations via the 'reliability ensemble averaging' (REA) method. Journal of Climate 15:1141–115. DOI: http://dx.doi.org/10.1175/1520-0442(2002)015<1141:COAURA>2.0.CO;2

Giorgi,F., Mearns, L.O. (2003). Probability of regional climate change based on the reliability ensemble averaging (REA) method . Geophysical Research Letters, 30 (12) (2003), pp. 1629–1632. DOI: http://dx.doi.org/10.1029/2003GL017130, 2003

Giorgi, F., Bi, X. (2009) Time of emergence (TOE) of GHG-forced precipitation change hot-spots. Geophysical Resources Letter, 36:L06709. DOI:10.1029/2009GL037593

Giorgi, F., Jones, C. and Asrar, G. (2009). Addressing climate information needs at the regional level: the CORDEX framework. World Meteorology Organ Bulletin 58(3):175-183.

Giorgi ,F., Coppola, E., Raffaele, F., Diro, G., Fuentes-Franco, R., Giuliani, G., Mamgain, A., Llopart, M., Mariotti, L., Torma, C. (2014) . Changes in extremes and hydroclimatic regimes in the CREMA ensemble projections. Climate Change, 125:39–51. DOI:10.1007/s10584-014-1117-0

Hannachi, A., Jolliffe, I.T., Stephenson D.B.(2007). Empirical orthogonal functions and related techniques in atmospheric science: a review . International Journal of Climatology, 27 (9) : 1119–1152. DOI: 10.1002/joc.1499

Harris, I., Jones, P.D., Osborn, T.J., Lister, D.H .(2014). Updated high-resolution grids of monthly climatic observations - the CRU TS3.10 Dataset. International Journal of

Climatology, 34: 623-642. DOI: 10.1002/joc.3711

Hawkins, E., and Sutton, R., (2009). The potential to narrow uncertainty in regional climate predictions. Bulletin of American Meteorological Society,90, 1095–1107, doi:10.1175/2009BAMS2607.1

Hawkins, E., and Sutton R. (2011). The potential to narrow uncertainty in projections of regional precipitation change, Climate Dynamics., 37, 407–418.DOI:10.1007/s00382-010-0810-6.

Hernández-Díaz L., Laprise,R., Sushama, L., Martynov,A., Winger, K., and Dugas, B.(2013). Climate simulation over CORDEX Africa domain using the fifth-generation Canadian Regional Climate Model (CRCM5). Climate Dynamics,40,1415–1433. DOI: 10.1007/s00382-012-1387-z

Huffman, G.J., Adler, R.F., Morrissey, M.M., Bolvin, D.T., Curtis, S., Joyce, R., McGavock, B. and Susskind, J. (2001). Global Precipitation at One-Degree Daily Resolution from Multisatellite Observations. Journal of Hydrometeorology, 2:36–50.DOI: http://dx.doi.org/10.1175/1525-7541(2001)002<0036:GPAODD>2.0.CO;2

Hulme, M., Doherty, R.M., Ngara, T., New, M.G. and Lister, D. (2001). African climate change: 1900–2100.Climate Research, 17:145-168. DOI:10.3354/cr017145

Ibrahim, B., Karambiri, H., Polcher, J., Yacouba, H., Ribstein, P. (2014). Changes in rainfall regime over Burkina Faso under the climate change conditions simulated by 5 regional climate models. Climate Dynamics, 42, 1363–1381. DOI 10.1007/s00382-013-1837-2

IPCC AR4 WG2 (2007), Parry, M.L., Canziani, O.F., Palutikof, J.P., van der Linden, P.J., Hanson, C.E., eds., Climate Change (2007). Impacts, Adaptation and Vulnerability, Contribution of Working Group II to the Fourth Assessment Report of the Intergovernmental Panel on Climate Change, Cambridge University Press, ISBN 978-0-521-88010-7 (pb: 978-0-521-70597-4).

IPCC (2014). Climate Change 2014: Synthesis Report. Contribution of Working Groups I, II and III to the Fifth Assessment Report of the Intergovernmental Panel on Climate Change [Core Writing Team, R.K. Pachauri and L.A. Meyer (eds.)]. IPCC, Geneva, Switzerland, 151 pp.

James, S.R., Stephan, L., Clothilde, L., Didier, P. M., Terence J. O. and Naomi, O. (2014). Well estimated global surface warming in climate projections selected for ENSO phase. Nature Climate Change, 4:835–840. DOI:10.1038/nclimate2310

Jenkins, G.S., Kamga, A., Garba, A., Diedhiou, A., Morris, V. and Joseph, E. (2002). Investigating the West African Climate System Using Global/Regional Climate Models. Bulletin of American Meteorological Society, 83: 583–595. DOI: http://dx.oi.org/10.1175/1520-0477

Jenkins, G. S., Gaye,A.T. and Sylla,B.(2005). Late 20th century attribution of drying trends in the Sahel from the Regional Climate Model (RegCM3), Geophysical Resources. Letter., 32,L22705. DOI:10.1029/2005GL024225

Jones, C., Giorgi, F., Asrar, G. (2011). The Coordinated Regional Downscaling Experiment:

CORDEX An international downscaling link to CMIP5. CLIVAR Exchanges 56(16):34-40

Kamga, A. F. and Buscarlet, E. (2006). Simulation du climat de l'Afrique de l'Ouest à l'aide d'un modèle climatique régional. La Météorologie , 52:28-37.

Kang, S.M., Deser, C., Polvani, L.M. (2013). Uncertainty in climate change projections of the Hadley Circulation: The role of internal variability. Journal of Climate, 26:7541–7554. DOI: 10.1175/JCLI-D-12-00788.1

Kim, J. , Duane, E., Waliser, Mattmann, C.A.,Goodale, C.E., Hart, A.F., Zimdars, P.A., Crichton, D.J., Jones, C., Nikulin, G.,Hewitson, B., Jack, C., Lennard, C., Favre, A. (2013). Evaluation of the CORDEX-Africa multi-RCM hindcast:systematic model errors. Climate Dynamics, 42(5):1189-1202. DOI:10.1007/s00382-013-1751-7

Klutse, N.A.B., Sylla, M.B., Diallo, I., Sarr, A., Dosio, A., Diedhiou, A., Kamga, A., Lamptey, B., Ali, A., Gbobaniyi, E.O., Owusu, K., Lennard, C., Hewitson, B., Nikulin, G., Panitz, H.J., Büchner, M. (2015). Daily Characteristics of West African Monsoon Rainfall in CORDEX Regional Climate Models. Theoretical and Applied Climatology,1-18. DOI: 10.1007/s00704-014-1352-3

Knutti, R., and Sedláček J.(2013), Robustness and uncertainties in the new CMIP5 climate model projections,Nat. Clim. Change ,3, 369–373,doi:10.1038/nclimate1716.

Legates, D.R., Willmott, C.J. (1990). Mean seasonal and spatial variability in gauge-corrected, global precipitation. International Journal of Climatology, 10(2): 111-127. doi:10.1002/joc.3370100202

Li, J.L., Waliser, F.D.E., Stephens, G., Lee, S., L'Ecuyer, T., Kato, S., Loeb, N., and Ma, H.Y. (2013).Characterizing and understanding radiation budget biases in CMIP3/CMIP5 GCMs, contemporary GCM, and reanalysis. Journal of Geophysical Research: Atmosphere, 118(15):8166–8184. DOI:10.1002/jgrd.50378.

Lian T. and Chen D. (2012). An Evaluation of Rotated EOF Analysis and Its Application to Tropical Pacific SST Variability. Journal of Climate., 25:5361–5373. DOI:10.1175/JCLI-D-11- 00663.1

Lorenz, E. N.(1956). Empirical orthogonal functions and statistical weather prediction. Technical report, Department of Meteorology, MIT, science Report 1.

Mariotti, L., Coppola, E., Sylla, M. B, Giorgi, F. and Piani, C. (2011). Regional climate model simulation of projected 21st century climate change over an all-Africa domain: Comparison analysis of nested and driving model results. Journal of Geophysical Research, 116,D15111. DOI: 10.1029/2010JD015068

Meehl, G.A., Boer, G.J., Covey, C., Latif, M. and Stouffer R.J. (2000). The Coupled Model Intercomparison Project (CMIP). Bulletin of American Meteorological Society, 81: 313-318.DOI:http://dx.doi.org/10.1175/1520-0477

Meehl, G.A. , Covey, C., Taylor, E.K., Delworth, T., Stouffer, J.R., Latif, M., McAvaney, B., Mitchell, F.B.J. (2007). The WCRP CMIP3 multimodel dataset: a new era in climate change research. Bulletin of American Meteorological Society , 88(9) :1383–1394. DOI: http://dx.doi.org/10.1175/BAMS-88-9-1383

Mesquita, M.B., Adlandsvik, B., Bruye re, C., and Sandvik, A.D.(2012) Bayesian assessment of horizontal resolution in a nested-domain wrf simulation. 13th WRF Users' Workshop, Boulder,CO,URL https://www.regonline.com/AttendeeDocuments/1077122/43357632/43357632_1045166.pdf.

Mohino, E., Janicot, S., Bader, J. (2011). Sahel rainfall and decadal to multi-decadal sea surface temperature variability. Climate Dynamics, 37(3):419–440. DOI: 10.1007/s00382-010-0867-2

Moss, R.H., Edmonds, J.A., Hibbard, K.A., Manning, M.R., Rose, S.K., van Vuuren D.P., Carter, T.R., Emori, S., Kainuma, M., Kram, T. Meehl,G.A., Mitchell,J.F.B, Nakicenovic,N.,Riahi, K., Smith,S.J., Stouffer,R.J., Thomson,A.M., Weyant, J.P., Wilbanks, T.J. (2010). The next generation of scenarios for climate change research and assessment. Nature, 463:747–756. DOI:10.1038/nature08823

Nicholson, S.E. (2009) A revised picture of the structure of the "monsoon" and land ITCZ over West Africa. Climate Dynamics 32(7):1155–1171.DOI 10.1007/s00382-008-0514-3

Nikulin, G., Jones, C., Giorgi, F., Asrar, G., Büchner, M., Cerezo-Mota, R., Christensen, O.B., Déqué, M., Fernandez, J., Hänsler, A., van Meijgaard, E., Samuelsson, P., Sylla, M.B., Sushama, L. (2012). Precipitation Climatology in an Ensemble of CORDEX-Africa Regional Climate Simulations. Journal of Climate, 25: 6057-6078.DOI: http://dx.doi.org/10.1175/JCLI-D-11-00375.1

Paeth, H., Born, K., Podzun, R. and Jacob D. (2005). Regional dynamical downscaling over West Africa: model evaluation and comparison of wet and dry years. Meteorologische Zeitschrif 14(3):349-367.DOI: 10.1127/0941-2948/2005/0038

Paeth, H., and Thamm, H. (2007). Regional modelling of future African climate north of 15°S including greenhouse warming and land degrada-tion, Climate Change, 83 , 401 –427, DOI:10.1007/s10584-006-9235-y

Paeth, H., Hall, N.M.J., Gaertner, M.A., Alonso, M.D., Moumouni, S., Polcher, J., Ruti, P.M., Fink, A.H., Gosset, M., Lebel, T., Gaye, A.T., Rowell, D.P., Moufouma-Okia, W., Jacob, D., Rockel, B., Giorgi, F., Rummukainen, M. (2011). Progress in regional downscaling of West African precipitation. Atmospheric Science Letter 12(1):75-82. DOI:10.1002/asl.306

Palmer, T. N., Alessandri, A., Andersen, U., Cantelaube, P., Davey, M., Délécluse, P., Déqué, M., Díez, E., Doblas-Reyes, F.J., Feddersen, H., Graham, R., Gualdi, S., Guérémy, J.-F., Hagedorn, R., Hoshen, M., Keenlyside, N., Latif, M., Lazar, A., Maisonnave, E., Marletto, V., Morse, A. P., Orfila, B., Rogel, P., Terres, J.-M. and Thomson M. C. (2004). Development of a European multi-model ensemble system for seasonal to interannual prediction (DEMETER). Bulletin of American Meteorological Society, 85:853–872. DOI:10.1175/BAMS-85-6-853

Panitz, H.J., Dosio, A., Büchner, M., Lüthi, D., Keuler, K. (2013). COSMO-CLM (CCLM) Climate Simulations over CORDEX Africa Domain: Analysis of the ERA-Interim Driven Simulations at 0.44° and 0.22° Resolution. Climate Dynamics, 42(11):3015-3038.DOI: 10.1007/s00382-013-1834-5

Parry, M.L., Canziani, O.F., Palutikof, J., Van der Linden, P., Hanson, C.E. (2007). Climate Change 2007: Impacts Adaptation and Vulnerability: Contribution of Working Group II to the Fourth Assessment Report of the Intergovernmental Panel on Climate Change. Cambridge Univ Press, Cambridge, UK, 976 pp

Panitz, H.J., Dosio, A., Büchner, M., Lüthi, D., Keuler, K. (2014). COSMOCLM (CCLM) climate simulations over CORDEX-Africa domain: analysis of the ERA-Interim driven simulations at 0.44 and 0.22 resolution. Climate Dynamics, 42(11–12):3015–3038. DOI:10.1007/s00382-013-1834-5

Paxian, A., Sein, D., Panitz, H.J., Warscher, M., Breil, M., Engel, T., Tödter, J., Krause, A., Cabos Narvaez,W.D., Fink, A.H., Ahrens, B., Kunstmann, H., Jacob, D., Paeth H. (2016). Bias reduction in decadal predictions of West African monsoon rainfall using regional climate models. Journal of Geophysical Resources Atmosphere, 121 ,1715 1735, DOI:10.1002/2015JD024143

Rodríguez-Fonseca, Mohino, B.E., Mechoso, C.R., Caminade, C., Biasutti, M., Gaetani, M., Garcia-Serrano, J., Vizy, E.K., Cook, K., Xue, Y., Polo, I., Losada, T., Druyan, L., Fontaine, B., Bader, J., Doblas-Reyes, F.J., Goddard, L., Janicot, S., Arribas, A., Lau, W., Colman, A., Vellinga, M., Rowell, D.P., Kucharski, F. and Voldoire, A. (2015) .Variability and predictability of West African droughts: A review of the role of sea surface temperature anomalies. Journal of Climate, 28(10): 4034-4060. DOI:10.1175/JCLI-D-14-00130.1.

Roehrig, R., Bouniol, D., Guichard, F., Hourdin, F. and Redelsperger, J.L. (2013). The present and future of the West African monsoon: a process-oriented assessment of CMIP5 simulations along the AMMA transect. Journal of Climate, 26:6471–6505. DOI: 10.1175/JCLI-D-12-00505.1

Stephenson, D. B., C. A. S. Coelho, F. J. Doblas-Reyes, and M. Balmaseda, (2005). Forecast assimilation: A unified frame-work for the combination of multi-model weather and climate predictions.Tellus,57A,253–264

Sylla, M. B., Gaye, A. T., Pal, J. S., Jenkins, G. S., and Bi., X. Q. (2009). High resolution simulations of West Africa climate using Regional Climate Model (RegCM3) with different lateral boundary conditions. Theoretical and Applied Climatology, 98 (3-4):293-314. DOI:s00704-009-0110-4

Sylla, M.B., Dell'Aquila, A., Ruti, P.M., Giorgi, F. (2010a). Simulation of the Intraseasonal and the Interannual Variability of Rainfall over West Africa with a Regional Climate Model (RegCM3) during the Monsoon Period. International Journal of Climatology, 30(12):1865–1883. DOI:10.1002/joc.2029

Sylla, M.B., Coppola, E., Mariotti, L., Giorgi, F. and Ruti, P.M. , Dell'Aquila, A., Bi, X. (2010b). Multiyear simulation of the African climate using a regional climate model (RegCM3) with the high resolution ERA-interim reanalysis. Climate Dynamics, 35:231-247. DOI:s00382-009-0613-9

Sylla, M.B., Gaye, A.T., Jenkins, G.S. (2012). On the fine-scale topography regulating changes in atmospheric hydrological cycle and extreme rainfall over West Africa in a Regional Climate Model projections. International Journal of Geophysics, Article ID 981649. DOI: 10.1155/2012/981649

Sylla, M.B., Diallo, I., and Pal, J.S. (2013a). West African Monsoon in State-of-the-Science Regional Climate Models, Climate Variability - Regional and Thematic Patterns, Dr. Aondover Tarhule (Ed.), ISBN: 978-953-51-1187-0, InTech,. DOI: 10.5772/55140

Sylla, M.B., Giorgi, F., Coppola, E. and Mariotti, L. (2013b). Uncertainties in daily rainfall over Africa: assessment of observation products and evaluation of a regional climate model simulation. International Journal of Climatology, 33: 1805-1817. DOI: 10.1002/joc.3551

Sylla, M.B., Giorgi, F., Pal, J.S., Gibba, P., Kebe, I., Nikiema, M. (2015) Projected Changes in the Annual Cycle of High Intensity Precipitation Events over West Africa for the Late 21st Century. Journal of Climate, 28: 6475-6488. DOI: 10.1175/JCLI-D-14-00854.1

Sylla, M.B., Elguindi, N., Giorgi, F., Wisser, D. (2016a). Projected Robust Shift in Climatic Zones over West Africa in Response to Anthropogenic Climate Change for the Late 21st Century. Climatic Change, In press. DOI: 10.1007/s10584-015-1522-z

Sylla, M.B., Nikiema, P.M., Gibba, P., Kebe, I., Klutse, N.A.B. (2016b). Climate Change in West Africa: Recent Trends and Future Projections. In Dr. Hesselberg and Dr. Yaro (Ed): Adaptation to climate change and variability in rural West Africa. Springer, In Press

Taylor, K.E., Stouffer, R.J., Meehl, G.A. (2012). An Overview of CMIP5 and the Experiment Design. Bulletin of American Meteorological Society, 93:485– 498. DOI: http://dx.doi.org/10.1175/BAMS-D-11-00094.1

Tebaldi, C.,Mearns , L., Nychka, D., Smith, R., (2004). Regional probabilities of precipitation change: a Bayesian analysis of multimodel simulations. Geophysical. Resources, Lett. 31, L24213. doi:10.1029/2004GL021276.

Tebaldi, C., Smith, R., Nychka, D., Mearns, L., (2005). Quantifying uncertainty in projections of regional climate change: a Bayesian approach to the analysis of multi-model ensembles. Journal of Climate, 18, 1524–1540. DOI:10.1175/JCLI3363.1.

Tebaldi, C., Knutti, R. (2007). The use of the multi-model ensemble in probabilistic climate projections. Philosophical Transactions of the Royal Society A, 365:2053–2075. DOI: 10.1098/rsta.2007.2076

Xu, Y., Xuejie, G., Giorgi, F. (2010). Upgrades to the reliability ensemble averaging method for producing probabilistic climate change projections. Climate Ressources,41:61–81. DOI:10.3354/cr00835

Yip S., Ferro, C.A.T., Stephenson, D.B., Hawkins, E. (2011). A simple, coherent framework for partitioning uncertainty in climate predictions. Journal of Climate,24:4634–4643. DOI: http://dx.doi.org/10.1175/2011JCLI4085.1